University of Nevada, Reno

Multi-Transceiver Free-Space-Optical Structures for Mobile Ad-Hoc Networks

A dissertation submitted in partial fulfillment of the

requirements for the degree of Doctor of Philosophy in

Computer Science and Engineering

by

Mehmet Bilgi

Dr. Murat Yuksel
Dissertation Advisor

December, 2010

University of Nevada, Reno
Statewide • Worldwide

THE GRADUATE SCHOOL

We recommend that the dissertation
prepared under our supervision by

MEHMET BILGI

entitled

Multi-Transceiver Free-Space-Optical Structures for Mobile Ad-Hoc Networks

be accepted in partial fulfillment of the
requirements for the degree of

DOCTOR OF PHILOSOPHY

Murat Yuksel, Ph.D., Advisor

George Bebis, Ph.D., Committee Member

Monica Nicolescu, Ph.D., Committee Member

Mehmet H. Gunes, Ph.D., Committee Member

M. Sami Fadali, Ph.D., Graduate School Representative

Marsha H. Read, Ph. D., Associate Dean, Graduate School

December, 2010

Multi-Transceiver Free-Space-Optical Structures for Mobile Ad-Hoc Networks

Mehmet Bilgi

University of Nevada, Reno, 2010

Advisor: Murat Yuksel

Abstract

Radio frequency-based communication has been the dominant way of wireless networking throughout the last two decades. Although new medium access control (MAC) technologies have been adapted to provide better per-node throughput, we have arrived to a point where the frequency spectrum saturates because of the overwhelmingly high data load caused by ever-increasing usage of multimedia content. To remedy this problem of diminishing end-to-end per-node throughput, we propose a novel "optical antenna" model that is tessellated with multiple free-space-optical (FSO) transmitter and receiver (transceiver) pairs that exploit spatial reuse of the shared medium and are capable of handling extremely high data rates using optical modulation techniques. However, because of the highly directional nature of FSO transceivers, nodes face a serious issue to communicate reliably: line-of-sight (LOS) alignment.

First, we propose four different types of FSO antennas, each with a number of optical transceivers. Then, we present an auto-alignment protocol to opportunistically

probe and detect available links to neighbors in a mobile setting. Later, we present the propagation model of optical communication for a single link and required simulation extensions to realistically simulate networks of multi-transceiver FSO nodes. Next, we present a set of simulation results that demonstrate the characteristics of an optical wireless link. We evaluate the performance of different node designs under a number of system parameters such as: different environment settings (indoor and outdoor), mobility, visibility, and node density. After this base set of simulations, we identify the major problem with networks of mobile FSO nodes with highly directional multiple transceivers: *intermittent connectivity*. To remedy this issue, we propose two different buffering schemes: node-wide buffering and per-flow buffering. We, then, present the results of major simulation settings using the two buffering mechanisms. We conclude that such buffering mechanisms are vital for the realization of free-space-optical mobile ad-hoc networks. We also investigate other possible ways to use this directional nature of FSO transceivers and consider efficient relative localization of nodes on a 3 dimensional terrain. Later, we focus on a prototype implementation of such a multi-element FSO antenna and auto-alignment protocol and demonstrate that the proposed system is implementable using off-the-shelf components. We conclude by providing results of various mobility experiments using our prototype.

İsm-i Vedûd içün:

Verily, those who believe and work deeds of righteousness,
the Most Beneficent will bestow love into their hearts.

Acknowledgments

I would like to thank my advisor, Dr. Murat Yuksel, for his never ending and nurturing support and leniency even during my extended periods of unproductiveness. His patience made this dissertation possible. I sincerely want to demonstrate a similar guidance to my own students one day. I am well aware that I took a lot of his time and caused a large number of headaches. For that, my deepest thanks go to my advisor.

I also would like to thank my lab mates for their close friendship and encouraging discussions, starting with Omer Kilavuz. I will never forget the dust that came out of that tiny room when the two of us were given the task of "establishing" the network lab. Moreover, I would like to thank Abdullah Sevincer, my collaborator on the FSO project, for putting up with me and for being so approachable during all the technical discussions we had. I would also like to thank Tarik Karaoglu for being such a humble figure during my graduate study even though I had my most thought provoking discussions with him on a vast spectrum of topics from migrating geese to the types of calendars we had been using. My sincere thanks go to all the members of the Computer Networking Lab for creating such a warm environment.

Moreover, I would like to thank my committee members Dr. Monica Nicolescu, Dr. Mehmet H. Gunes, Dr. George Bebis, and Dr. M. Sami Fadali for their valuable comments. I know that they spent a considerable amount of time reviewing my write up and I appreciate their time very much.

I would like to thank NSF, DARPA, and UNR boards for their continued financial support. I also would like to thank American Government for providing such a well-established system in which one can dream and pursue the means to realize his dream.

Finally, I would like to thank my family. They supported me in my ambition of coming to US without questioning any of the decisions I made throughout this process. They were always unconditional in extending their trust and belief in me. I only hope to be capable of showing such an unprecedented amount of forgiveness and compassion to my own children.

Mehmet Bilgi

University of Nevada, Reno

December 2010

Contents

Abstract **i**

Acknowledgments **iv**

List of Tables **x**

List of Figures **xi**

Chapter 1 Introduction **1**

1.1 Contributions 6

1.2 Dissertation Organization 6

Chapter 2 Literature Survey **9**

2.1 High-speed FSO Communications 14

2.1.1 Terrestrial Last Mile and Indoor Applications 15

2.1.2 Hybrid (FSO and RF) Applications 18

2.1.3 Free-Space-Optical Interconnects 21

2.2 Mobile Free-Space-Optical Communications 24

2.3 Effects of Directional Communication on Higher Layers 25

2.4 Localization in MANETs 29

2.4.1 Range-Only Techniques 29
2.4.2 Orientation-Only Techniques 31
2.4.3 Hybrid Techniques 31
2.5 Buffer Allocation and Management in Multi-Element Structures . . . 34
2.6 Summary 37

Chapter 3 Packet-Based Simulation for Multi-Transceiver Optical Communication 38

3.1 FSO Propagation Model 38
3.1.1 Geometrical Loss 39
3.1.2 Atmospheric Loss 39
3.2 NS-2 Simulation Models for Multi-Element FSO Structures 41
3.2.1 Interface Alignment Implementation in NS-2 41
3.2.2 Alignment Scenarios and Mobile Node Design 45
3.2.3 Auto-Alignment Circuitry 46
3.3 Validation Simulations 47
3.3.1 Effect of Separation 48
3.3.2 Effect of Visibility 49
3.3.3 Effect of Noise and Interference 51
3.4 Summary 51

Chapter 4 Effects of Multi-Element FSO Structures on Higher Layers 54

4.1 Simulation Environment Setup 55
4.2 Visibility 58
4.3 Divergence Angle 58
4.4 Mobility 58

4.5 Node Density 60
4.6 Re-alignment Timer 62
4.7 Obstacle Scenarios in Lounge and City Environments 64
4.8 Summary 66

Chapter 5 Buffering Techniques for Multi-Element Communication Structures 68

5.1 Node-Wide Buffering 69
5.2 Per-Flow Buffering 71
5.3 Buffering Performance Results 73
5.4 Summary 79

Chapter 6 Localization for FSO-MANETs 83

6.1 System Model 90
6.2 Heuristics 93
6.2.1 Stale Info Gets Forgotten 93
6.2.2 The Lower Rank Preference 95
6.2.3 Angular Prioritization 96
6.3 Performance Evaluation 96
6.3.1 Comparison of Heuristics 97
6.3.2 Node Density 97
6.3.3 Anchor Density 98
6.3.4 Divergence Angle 98
6.3.5 Message Overhead and Localization Extent 98
6.4 Summary 99

Chapter 7 Prototype Implementation and Experiments **100**

7.1 Prototype Blueprints 102

7.1.1 Transceiver Circuit 103

7.1.2 Controller Circuit 104

7.1.3 Alignment Protocol 106

7.2 Experiments 107

7.2.1 Proof-of-Concept Experiments 107

7.3 Summary 114

Chapter 8 Conclusions **115**

8.1 Future Work 117

Bibliography **119**

List of Tables

3.1 Table of default values common to each simulation set in our experiments. 48

4.1 Table of default parameter values common to each simulation set in our experiments. 56

5.1 Abbreviations for quantities of buffering components. 72

5.2 Complexity of each major step in buffering. 72

List of Figures

1.1 Radio frequency spectrum usage. 2
1.2 Multi-element antenna design tessellated with transceivers. 3

2.1 The expected roadmap of wireless technologies in 10 years. [86] 11
2.2 Basic architecture of the broadband access network [11] 15
2.3 Indoor FSO communication system sketch. [31] 16
2.4 Proposed use case for the indoor FSO system. [31] 17
2.5 Throughput vs. range for FSO, UWB, and 802.11a technologies. Mobile robot with FSO/RF capabilities. [33] 20
2.6 FSO interconnect and active alignment demonstration [35] 22
2.7 Multi-Hop RTS [27] 28

3.1 Light intensity profile of an optical beam. 40
3.2 Internal design of a wireless node in NS-2. [5] 42
3.3 Multi-element antenna design in 2D view and sample alignment table kept in interface 7 of node A. 44
3.4 Sample alignment scenario for two mobile nodes. 46
3.5 Received power in the field of view of a 1 rad light source. 49
3.6 Received power between 90 and 100 meter ranges. 50

3.7 Probability of error increases as a receiver is moved away from the transmitter. 50
3.8 Percentage of successfully delivered packets decreases as the receiver is moved away from the light source. Used transport agent is UDP. . . . 51
3.9 Probability of error decreases as the visibility in the medium is increased. Percentage of delivered packets follows a similar but coarser grained behavior. 52
3.10 Theoretical error probability and simulated packet error increase as the noise is increased. 52

4.1 FSO node structure with a separate stack for each optical transceiver. 55
4.2 Visibility Effect. 57
4.3 Divergence Angle Effect. 57
4.4 Mobility Effect. 59
4.5 Network-wide throughput. 59
4.6 Per-node throughput. 61
4.7 Enlarging Simulation Area. 61
4.8 Alignment timer effect. 63
4.9 Alignment timer effect in log-scale. 63
4.10 A dense lounge setting with multiple RF wireless devices to demonstrate the substantially decreasing per node throughput problem in RF. 64
4.11 A two story lounge with FSO nodes communicating with another back-end node in the second floor. 65

4.12 Throughput comparisons for in-door and out-door deployment of RF and FSO. 66

5.1 FSO node structure with a separate stack for each optical transceiver. 70
5.2 Mobility results for 4 transceiver node design. 73
5.3 Mobility results for 8 transceiver node design. 74
5.4 Mobility results for 16 transceiver node design. 74
5.5 Node density results in which the number of nodes are increased (4 transceivers). 76
5.6 Node density results showing per-node throughput (4 transceivers). . 76
5.7 Node density results in which the number of nodes are increased (8 transceivers) 77
5.8 Node density results showing per-node throughput (8 transceivers). . 77
5.9 Node density results for fixed power and enlarged area configuration. 78
5.10 Visibility simulations. 79

6.1 A third node triangulating using the advertised normals received from two other localized or GPS-enabled nodes. 85
6.2 A simplified triangulation in 2D using two GPS-enabled nodes and error in default LOS model. 86
6.3 Localization errors are being amplified during the simulation when two latest received information sets are used for triangulation. 87
6.4 GPS-enabled node effect on localization error. 88
6.5 GPS-enabled node effect on localization extent. 89
6.6 Localization extent with respect to message exchange for 200 nodes. . 89
6.7 Node density effect on localization error. 93

6.8 Node density effect on localization extent. 94

6.9 Divergence angle effect. 94

7.1 Picture of prototype optical antenna. 101

7.2 Default placement of alignment protocol in protocol stack. 101

7.3 Transceiver circuit front and rear view. 102

7.4 Controller circuit front and rear view. 104

7.5 State diagram of alignment algorithm. 105

7.6 Experiment setup: 3 laptops (collinear placement), each with a 3-transceiver optical antenna. 107

7.7 Throughput screen shots of a prototype experiment where transmitting node is mobile. Straight green lines show the drops due to the transmitting node's mobility. Red arrows indicate loss of alignment (and data) due to mobility. Once the mobile node returns to its place, data phase is restored and transmission continues. (Green spots show data loss) 108

7.8 Throughput behavior as baud rate varies. 109

7.9 Payload size effect on throughput. 110

7.10 Frame count effect on channel usage. 110

7.11 Distance effect on throughput. 112

List of Algorithms

5.1 Node-wide Buffering 81

5.2 Per-flow Buffering 82

6.1 Relative Localization 90

Chapter 1

Introduction

The capacity gap between radio frequency (RF) based wireless and optical fiber (wired) network speeds remains huge because of the limited availability of the RF spectrum [32]. Though efforts for an all-optical Internet [6, 49, 69, 83, 85, 98] will likely provide cost-effective solutions to the last-mile problem within the *wireline* context, high-speed Internet availability for mobile ad-hoc networks is still mainly driven by the RF spectrum saturation and spectral efficiency gains through innovative multi-hop techniques such as hierarchical cooperative MIMO (multiple-input multiple-output) antenna [79]. Alternative wireless technologies using the non-RF spectrum are highly needed (Figure 1.1). Free-Space-Optical wireless (FSO) provides angular diversity, spatial reuse, and high speed of optical modulation. However, FSO requires clear line-of-sight. FSO propagation is highly directional and this creates a challenge for mobile FSO deployments.

Free-space-optical transceivers are cheap (less than $1 per transceiver package), small ($\sim 1mm^2$), low weight (less than 1g), amenable to dense integration (1000+ transceivers possible in 1 sq ft), very long lived/reliable (10 years lifetime), consume

low power (100 microwatts for 10-100 Mbps), can be modulated at high speeds (1 GHz for LEDs/VCSELs and higher for lasers), offer highly directional beams for spatial reuse/security (1-10 microrad beam spread), and operate in large swathes of unlicensed spectrum amenable to wavelength-division multiplexing (infrared/visible) as depicted in Figure 1.1.

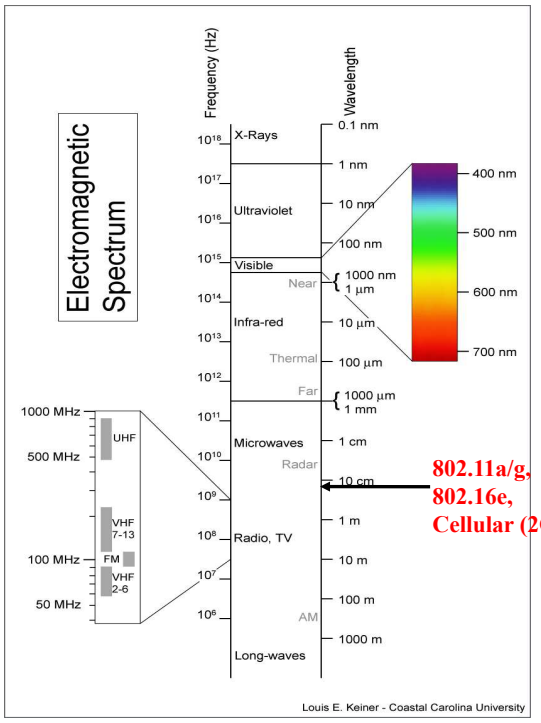

Figure 1.1: Radio frequency spectrum usage.

On the other hand, FSO requires clear line-of-sight (LOS), and LOS alignment between the transmitter and receiver for communication. FSO communication also suffers from beam spread with distance (tradeoff between per-channel bit-rate and power) and unreliability during bad weather (especially fog).

Mobile communication using FSO has been considered for indoor environments, within a single room, using diffuse optics technology [31, 46, 51]. Due to limited power of a single source that is being diffused to spread in all directions, these techniques are only suitable for small distances (typically tens of meters). FSO has received attention for high-altitudes as well, e.g., space communications [25] and building-top metro-area communications [2]. Various techniques have been developed for such fixed deployments of FSO to tolerate small vibrations [17, 18], swaying of the buildings, using

mechanical auto-tracking [15, 22, 72] or beam steering [95]; but, none of these techniques target mobility.

Similarly, for optical interconnects, auto-alignment or wavelength diversity techniques improve the misalignment tolerances in 2-dimensional arrays [37, 41, 48, 54, 80]. These techniques involve cumbersome and heavy mechanical tracking instruments. Moreover, they are designed to improve the tolerance to movement and vibration but not to handle mobility. Thus, mobile FSO communication has not been realized, particularly for ad hoc networking environments.

In this dissertation, we investigate and tackle challenges involved in realizing general purpose FSO mobile ad-hoc networks (FSO-MANETs). FSO-MANETs can be possible by means of "optical antennas", i.e., FSO spherical structures like the one shown in Figure 1.2. Such FSO spherical structures achieve *angular diversity* via spherical surface, *spatial reuse* via directionality of FSO signals, and are *multi-element* since they are covered with multiple transceivers (e.g., LED and photo-detector pairs).

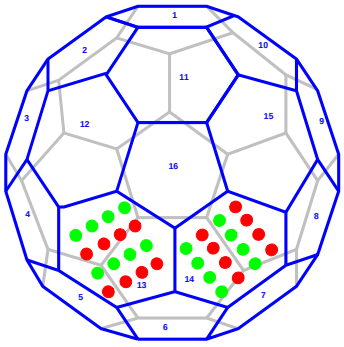

Figure 1.2: Multi-element antenna design tessellated with transceivers.

FSO suffers from its line of sight requirement when used in a mobile context RF achieves a relatively stable but lower line of throughput against increased mobility. We show that although the mobility of an FSO node causes its transceivers to loose their alignment with other transceivers in the network, it can re-gain it in a short amount of time. These events of frequent alignment and misalignment yield an "*intermittent connectivity pattern of free-space-optical structures*". We inspect the implications of this intermittent connectivity pattern on higher layers, especially on Transmit Control

Protocol (TCP).

To remedy this issue, we consider usage of buffering at layer 2 so that the intermittent connectivity becomes seamless to higher layers. We investigate two types of buffers: node-wide and per-flow. In the former type, packets of a misaligned neighbor are delivered to a node-wide buffer that is shared by all the transceivers of the node. In the latter case, there are dedicated buffers for each neighbor and in case of a misalignment, the packets are delivered to the appropriate buffer depending on the next hop. Each design responds differently to mobility and has trade-offs with memory usage. To point out the added value of buffers, we compare the buffering schemes against the cases without a buffer in extensive simulation experiments. Our investigation clearly shows that such buffering mechanism are critical for any multi-transceiver directional communication system and are not just required by FSO-MANETs.

Directionality of FSO communications can be used to achieve various higher layer goals. Localization of nodes has been an extremely helpful higher layer networking function and has attracted a lot of attention from the research community. For MANETs, the key issue regarding localization is to localize a node by using as few localized neighbors as possible. Traditional localization techniques require at least three localized neighbors since an accurate estimation of angle-of-arrival is not possible via RF signals. We explore the possibility of using the directionality of FSO-MANETS to solve the 3-D localization problem in ad-hoc networking environments. Range-based localization methods either require a higher node density (i.e., at least three other localized neighbors must exist) than required for assuring connectedness or a high-accuracy power-intensive ranging device, such as a sonar or laser range finder which exceeds the form factor and power capabilities of a typical ad-hoc node. Our approach

exploits the readily available directionality information provided by the physical layer using *optical wireless* and uses a limited number of GPS-enabled nodes, requiring a very low node density (2-connectedness, independent of the dimension of space) and no ranging technique. We investigate the extent and accuracy of localization with respect to varying node designs (e.g., increased number of transceivers with better directionality) and the density of GPS-enabled and ordinary nodes as well as messaging overhead per re-localization. We conclude that, although denser deployments are desirable for higher accuracy, our method still works well with sparse networks with little message overhead and small number of anchor nodes (as little as 2).

Finally, we present a prototype implementation of such multi-transceiver electronically steered communication structures. Our prototype uses a simple LOS detection and establishment protocol and assigns logical data streams to appropriate physical links. We show that by using multiple directional transceivers we can maintain optical wireless links with minimal disruptions that are caused by relative mobility of communicating nodes.

RF and FSO are in fact complementary to each other. In a hybrid environment, where nodes accommodate both RF and FSO capabilities and a suitable network stack that can take advantage of both technologies, RF can overcome FSO's coverage issues while FSO can meet the high-bandwidth requirements of the network. Hence, in this dissertation, we position our work not to replace RF, but to aid RF with high modulation speed and benefits of directionality.

1.1 Contributions

Contributions of this dissertation are two-fold: conclusions derived from extensive simulation studies and confirmation from a proof-of-concept prototype. On the simulation front, this dissertation builds upon the contributions of [99] in which the concept of spherical antenna was first revealed. Our contributions in this dissertation include:

- assessment of throughput characteristics of FSO-MANETs,
- diagnosis of intermittent connectivity through a comprehensive set of simulations,
- cross-layer buffering schemes to make the intermittent connectivity seamless to higher layers,
- optical-only 3-D localization techniques, and
- proof-of-concept prototype to demonstrate the effectiveness of our approach [1].

1.2 Dissertation Organization

This dissertation is organized as follows: Chapter 2 provides a summary of relevant major research efforts in the literature, their common use cases, problems, and solutions in those fields. We cover representative papers in the fields of terrestrial last mile and indoor applications where FSO has been popularly deployed. We cover hybrid applications of FSO and RF and also free-space-optical interconnects in the literature. Later, we cover how mobile FSO has been provisioned in the past and provide

[1] This contribution was achieved in collaboration with Mr. Abdullah Sevincer.

insight on how researchers coped with directionality and sectored communication instead of an omnidirectional one. We also provide a survey on localization techniques for MANETs: range-only, orientation-only, and hybrid techniques. Lastly, we cover cross-layer buffering usage in the literature. Although today's applications do not target solving the intermittent connectivity problem, we find similarities between buffer management methodologies.

Chapter 3 gives the details of FSO technology, propagation model of light in free-space and our NS-2 contributions. First, we provide details on the well-accepted FSO propagation model of optical radiation. Moreover, we present details of our NS-2 enhancements to realistically simulate an FSO link and network of multi-transceiver nodes. Lastly, we present our validation study of our simulation modules where we study important measures such as received power and bit error rate with respect to separation and visibility in the medium.

Chapter 4 covers our research on FSO's throughput potential in mobile ad-hoc scenarios. We present a thorough simulation study where we investigate the effect of mobility, visibility, divergence angle, and node density. We also provide two scenarios: indoor and outdoor settings, and compare the throughput results with RF-based equivalent network setups. Finally, we detail our discussion on impact of multi-element communication mechanisms on higher layers and conclude that cross-layer buffering mechanisms are necessary for the realization of highly mobile FSO nodes with large number of highly directional transceivers.

Chapter 5 presents our designs of cross-layer buffering mechanisms and provides results on how they affect the overall throughput of the network. We repeat the major simulation scenarios that we discuss in Chapter 4 and compare the buffering results with non-buffered results.

Chapter 6 extends the usage of FSO to the well-known localization problem and emphasizes the directionality benefits that are inherent to FSO by sketching a cross-layer design to abstract the directionality information and present it to upper layers. We provide a light-weight localization algorithm that does not need any additional extra hardware than the FSO hardware and requires a small number of anchor nodes that know their location initially.

Lastly, we back our multi-transceiver node design with a prototype. Chapter 7 provides details of our proof-of-concept prototype that can handle multiple simultaneous data streams targeted to different neighbors. We present a set of mobility experiments that conform to our conclusions from simulation studies. Finally, in Chapter 8, we conclude our work and provide our intuition about future directions.

Chapter 2

Literature Survey

This chapter reviews the literature related to our work with Free-Space-Optical MANETs, starting with a general introduction on bandwidth expectations of future applications. FSO MANET related work in the literature can be categorized into three main groups:

- high-speed FSO communications,
- mobile FSO communications,
- effects of FSO-like communications on higher layers of the networking stack.

The NSF Mobile Planning Group [86] expects significant qualitative changes to the Internet that will be driven by the rapid proliferation of mobile and wireless devices. They advocate that modifications or a complete redesign of the Internet will be needed to support applications and architectures that are fundamentally different in nature like mobile and wireless device users and sensor-based applications. Those applications will need new emerging wireless network technologies such as mobile terminals, ad-hoc routers and embedded sensors to better enable end-to-end service

abstractions and provide a more programmable environment for application development. They expect a diverse set of use case scenarios (Figure 2.1) that involve WiFi-hotspots, Infostations, mobile peer-to-peer, ad-hoc mesh networks for broadband access, vehicular networks, sensor networks and pervasive systems to drive the demand for design and implementation of new protocols that tightly integrates the mobile and stationary parts of the world.

The group argues that, after evaluating other viable solutions such as IP-overlays and extensions to IP, a "clean-slate" architecture (i.e., disruptive design) will be needed to meet the requirements of the aforementioned use cases, in which the number of mobile and wireless devices will reach billions (around 2 billion as of 2005). Additionally, they argue that there will be a dramatic need for change in experimental research of networking, not just in wireless/mobile context but also in the context of large-scale end-to-end system evaluation. Such testbeds should facilitate programmable protocols running on wireless and mobile nodes that are also connected to a programmable Internet backbone and will provide a viable judgment of different approaches.

The group introduces enhancements or replacement technologies for;

- Addressing and identity resolution for mobile nodes that change IP subnets without any application level challenges,
- Delay tolerant disconnected operations that enable new network services that caches commonly used data,
- Exploiting location awareness by using it as a routing mechanism and harnessing location-aware applications. The group gives suggestions on the representation of the location data, as latitude-longitude based (i.e., Universe Transverse Mer-

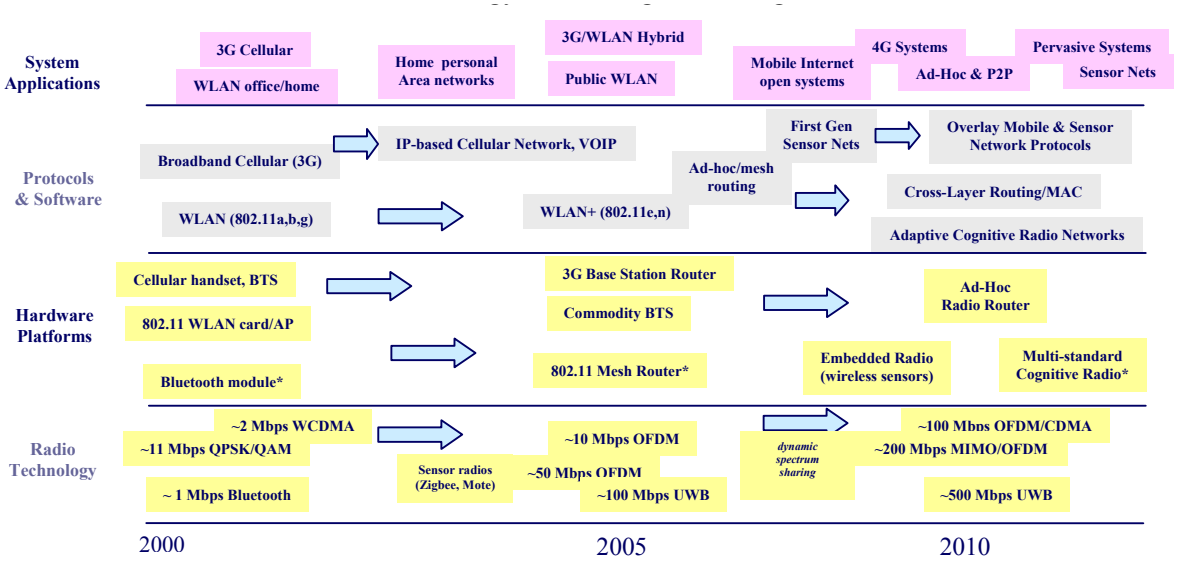

Figure 2.1: The expected roadmap of wireless technologies in 10 years. [86]

cator) representation.

- Security and privacy. Primarily, radio jamming, denial-of-service attacks and authentication of location data.

- Deployment of self-healing and self-configuring network architectures since the traditional commercial management boundaries will be more blurred. Authors expect to see new management instruments become available such as wireless channel characteristic assessment tools and tools that automatically extract MAC and routing level information. Decentralized management for remote monitoring will be applied for configuration and control of distributed and heterogeneous wireless networks.

- Cross-layer protocol support that exposes valuable information among multiple layers and new protocol stack designs.

- Cognitive radio networks that enable wireless devices to flexibly create many different kinds of communication links depending on required performance and spectrum/interference constraints.

The group strongly argues that the building blocks that will be deployed in future Internet should be widely tested in an "Experimental Infrastructure for Wireless Network Research". The wireless/sensor testbed should be integrated with a flexible wide-area network that can be used to study new architectures and protocols in an end-to-end fashion. For this experimental infrastructure, they give examples of open API radios, cognitive radios, and virtualization of wireless medium access control (MAC) for innovative usage in selecting a MAC protocol. They conclude that the future Internet will undergo a fundamental transformation over the next 10-15 years. Thus, a need to focus on central network architecture questions related to future mobile, wireless and sensor scenarios.

B. Metcalfe argues that all-optical networking infrastructure will become the dominant choice for service providers as new types of multimedia applications that require more and more bandwidth are seeing high demands from end users [67]. The article mentions Dr. David R. Hubert as one of the few people that influenced such a change by introducing 16-channel dense wave division multiplexing hardware to the market as early as 1992. While the Dot-Com era saw start-up companies that came up with ideas like deploying fiber optical cables through the sewer canals [40], the fact that fiber-to-home projects failed is apparent.

Japan is leading the way in deploying optical links at large scale [6]. There is only a handful of proprietary deployments in the US which include:

- FirstWorld started with a plan to provide fiber connectivity in Orange County, CA, but was unable to cover the whole area. The company has changed its

name to Vurado Holdings (2001) and was acquired by EarthLink in the same year.

- SpectraNet is close to total-coverage in Anaheim, CA.
- A Rye, Colorado community also has fiber deployed widely.
- Another fairly extensive fiber network providing high-speed Internet access as well as video broadcast is Intercable‘s system installed in Alexandria, VA.
- GST Telecom (Seattle, WA) is active in developing small, isolated high-speed fiber access, generally in planned communities
- Recently, the City of Palo Alto‘s public utilities department has started to offer fiber to its residents.

Since the article was written in 1998, most of the above companies have either closed down or have been acquired by other companies. However, this list demonstrates that there have been efforts to provide wired optical connectivity in the US, although they failed to reach *every* home or business.

What the companies saw while deploying the technology over a decade is that the expected quick integration and demand from small businesses and homes was not realistic. Customers were unwilling to pay the high initial cost of the technology. Researchers conclude that Internet Service Providers (ISPs) are laying fiber and will continue to do so gradually since the fiber is economically the most viable solution when evaluated based on the gained bandwidth against copper-based technologies. Authors also give examples of so-called Premium Internet Service Providers including Concentric Networks, Frontier GlobaLAN, AboveNet, Digital Island, and NaviSite, as they no longer adhere to the routing schemes of the public Internet. Instead, they

have established private paths for data that avoid the congested public access points, the network access points, and Internet exchange points, in favor of data exchanges at restricted access switches owned by the fiber providers.

Demand for high-speed communication has always existed, even increasingly with more bandwidth-intensive multimedia applications of today. This demand from the end-user, is only being suppressed by internet service providers by charging with exponentially increased rates and fees. Wired optical coverage is still far less widespread than basic telephone service because the initial cost to lay fiber optical cable is widely considered as *sunk cost*.

This section reviewed the efforts for laying fiber during the last decade and their relatively minimal success compared to copper-based technologies. These efforts stand as evidence of the requirement of high-speed demand, even 10 years ago, and the obstacle of initial sunk costs. As we indicated, the bottleneck in an end-to-end communication system is at the last mile. To remedy this long-experienced problem of low bandwidth, we advocate easily deployable (not buried), re-locatable optical systems that are comparable to fiber in terms of bandwidth. Such systems will be considered as a house-hold or business commodity, other than a sunk cost.

2.1 High-speed FSO Communications

Legacy optical wireless, also known as free-space-optical (FSO) wireless, communication technologies use high-powered lasers and expensive components to reach long distances. Thus, the main focus of the research has been on offering only a single primary beam (and some backup beams); or using expensive multi-laser systems to offer redundancy and some limited spatial reuse of the optical spectrum [22, 95].

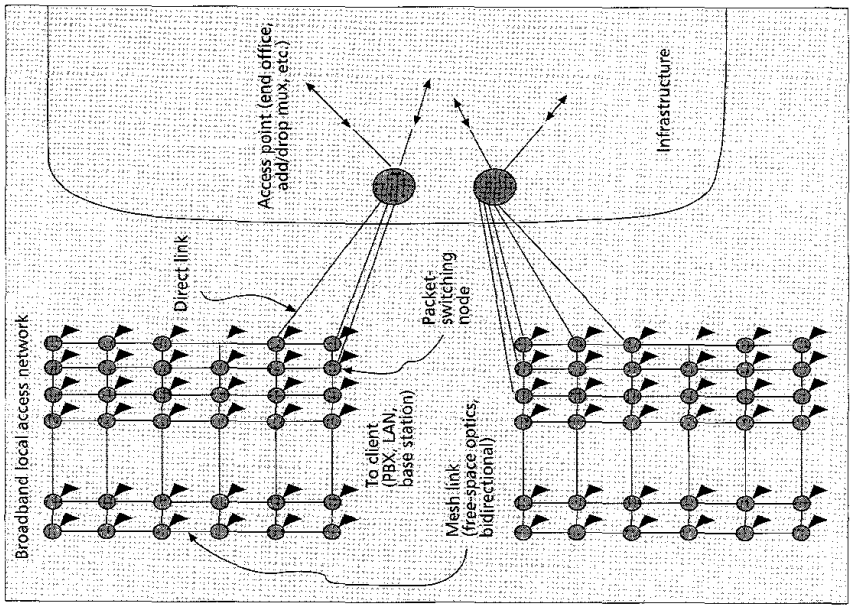

Figure 2.2: Basic architecture of the broadband access network [11]

The main target application of these FSO technologies has been to serve commercial point-to-point links (e.g., [2]) in terrestrial last mile applications and in infrared indoor LANs [11, 16, 46, 51, 91, 95] and interconnects [22, 23, 72]. Although cheaper devices such as LEDs and VCSELs have not been considered seriously for outdoor FSO in the past, recent work shows promising success in reaching longer distances by aggregation of multiple LEDs or VCSELs [1, 4].

2.1.1 Terrestrial Last Mile and Indoor Applications

Acampora *et al.* describe an approach to broadband wireless access using directional FSO links [11]. Key to this approach is its use of short, inexpensive, and extremely dependable focused free-space-optical links to interconnect densely deployed packet-switching nodes in a multihop mesh arrangement (Figure 2.2). Each node can then serve a client, which may consist of a building containing private branch exchanges

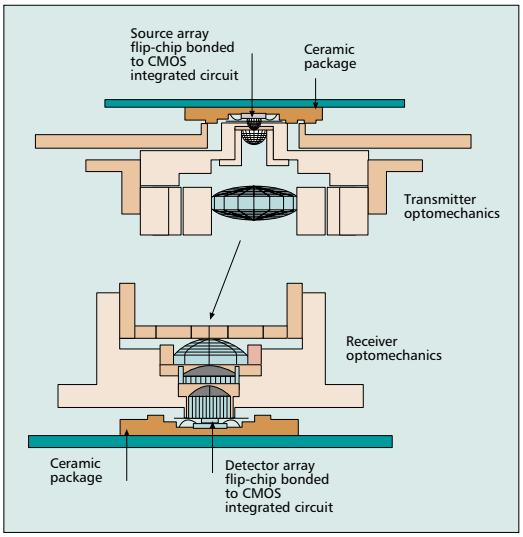

Figure 2.3: Indoor FSO communication system sketch. [31]

(PBXs) and LANs (for fixed-point semice), a picocellular base station (for wireless semice), or both. The great advantage of this approach is that very high access capacity can be economically and reliably delivered over a wide service area. Many clients can be served by a single access mesh which attaches to the infrastructure at a single access point. Acampora et al.'s work provides the most common use-case of FSO in today's applications; roof-top deployments through a high-powered laser components to reach long distances.

The authors of [35] examine possible performance improvements by changing receiver and transmitter hardware used in infrared wireless systems for short range indoor communication. Tweaked hardware includes: single-element receivers replaced by imaging receivers and diffuse transmitters replaced by multi-beam (quasi-diffuse) transmitters. Obtained power gain is from $13dB$ to $20dB$ while still meeting acceptable bit error rates of 10^{-9} with 95% probability. The authors encourage usage of quasi-diffuse (i.e., multiple beams) transmitters since they leverage Space Division

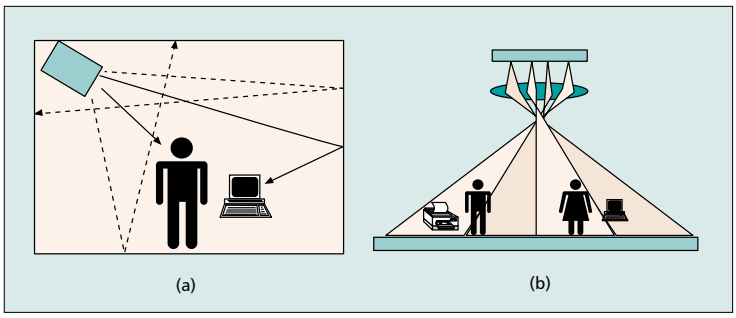

Figure 2.4: Proposed use case for the indoor FSO system. [31]

Multiple Access (SDMA).

O'Brien *et al.* provide an approach to fabricating optical wireless transceivers [31]. They use devices and components that are suitable for integration. The tracking transmitter and receiver components with diffuse transmitters and multi-cell photo-detectors have the potential for use in the wide range of network architectures. They fabricated and tested the multi-cell photo- detectors and diffuse transmitters, specifically seven transmitters and seven receivers operating at a wavelength of 980 nm and 1400 nm for eye-safety regulations. They designed transmitters and receivers to transmit 155 Mb/s data using Manchester Encoding. They compare optical access methods: a wide-angle high-power laser emitter scattering from the surfaces in the room to provide an optical ether or using directed line-of-sight paths between transmitter and receiver. In the first approach to transmitter design, although a wider coverage area is achieved, multiple paths between source and receiver cause dispersion of the channel and thus limit its bandwidth (Figures 2.1.1 and 2.1.1).They found that the second approach has spatial reuse and directionality advantages. Hence, it provides better data rates while not achieving a blanketing coverage. They conclude that directional optical communication will be dominant in the future beating

non-directional optics and radio frequency communication because of its promising bandwidth. They project to overcome the line-of-sight problems in the near future using high precision micro-lenses and highly sensitive arrays of optical detectors.

The last two papers [31,35] proposed to use relatively directional beams (quasi-diffuse) to take advantage of directionality. Due to the limited power of a single source that is being diffused to spread in all directions, these techniques are suitable for small distances (typically tens of meters); and they can't be considered for longer distances.

2.1.2 Hybrid (FSO and RF) Applications

With similar vision to ours, Yan *et al.* anticipate that RF-based MANETs are facing saturation in throughput due to high demands and that FSO is a complementary technology [96]. They introduce FSO capabilities to traditional RF-based MANETs. They advocate that pure-FSO MANET would be unrealistic because of the coverage and reachability issues caused by the extremely directional FSO beams. They conduct a search for commercially available hardware such as gimbals for steering the FSO beam. This is because the nature of the FSO technology that they target is fundamentally different than ours. The FSO beams that we advocate can potentially have a wide angle of transmission (divergence angle, θ), and dense packaging of such transceivers eliminates the need for complex mechanical steering methods. Our auto-alignment and tracking approach is fundamentally different in nature, which we will illustrate through specific circuitry later in Chapter 3. The authors conduct simulations of such hybrid networks in OPNET simulation environment. The number of nodes in the simulated network is far from being close to a realistic network; there are only 5 nodes, including a hub. Mobility pattern of nodes is predetermined and hard-coded. The average end-to-end delay that a packet experiences is 1.3 seconds,

which is unexpectedly high. Although the article starts with proposing simulation of hybrid nodes, it only simulates nodes that are FSO-capable; none of the 5 nodes has additional RF capabilities. This work stands out since it is the first attempt to simulate FSO with a reasonably realistic propagation model in free-space-optical communication literature.

The authors of [68] design a hybrid deployment of RF and FSO. FSO is mainly used as the high bandwidth backbone for the network. They focus on the "software" that controls the network: topology and diversity control software module, combined with hardware that handles pointing, acquisition and tracking. This software should be aware of actual and potential connectivity of the network and exploit this information to provide best connectivity available. Hence, the network is highly reconfigurable (i.e., self-configuring) leveraging an autonomous switching hardware between FSO and RF at the node level and pointing of FSO/RF aperture to re-establish an optimal network topology. Note that, since the described hardware (aperture) is shared by FSO and RF, the mentioned RF is *directional*, placing the reconfiguration software at a higher degree of importance. They evaluate the failure scenarios of FSO and/or RF links; failure of an FSO link can't be compensated only by RF because of the inherent bandwidth gap. Scenarios like this impose another set of requirements on the control software in terms of efficient routing. Those responsibilities of control software are mapped to appropriate layer/sublayers in the TCP/IP stack.

According to Derenick *et al.*, RF links serve as a low-bandwidth backup to the primary optical communication link [33]. Both technologies are considered as accommodating significant weaknesses and they are complementary and have the potential to address each other's limitations (Figure 2.5). The article criticizes the much anticipated ultra wideband (UWB) technology - with theoretical throughput

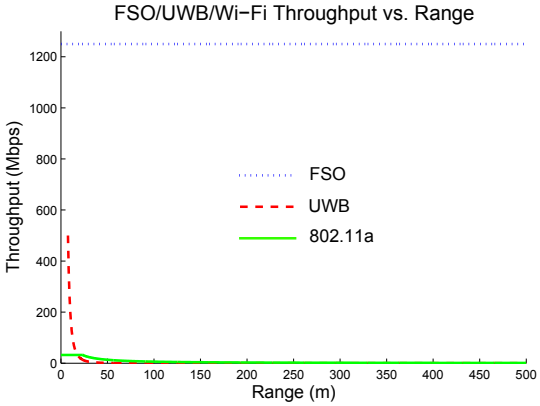

Figure 2.5: Throughput vs. range for FSO, UWB, and 802.11a technologies. Mobile robot with FSO/RF capabilities. [33]

of 100s of Mbps - dropping to levels lower than 802.11a at modest ranges (r $\geq$ 15m). Disaster relief applications are considered as the target application group. They also evaluate localization benefits of FSO. Mobile robots are selected as host to FSO and RF communication technologies. RF was seen performing unsatisfactory for surveillance video streaming task among robots, hence, FSO is used successfully for this bandwidth-intensive operation.

Additionally, the same authors designed a hierarchical link acquisition system for mobile robots to pair with each other in [34]. Alignment is aimed to work in three phases: coarse alignment using local sensors (robots are assumed to know each robot's objective position) and positioning systems like GPS, refinement of line-of-sight using a vision based robot detection, and finally precise FSO alignment. The authors focus on the first two, leaving the third step to internal FSO tracking/pointing system. The paper also discusses Hierarchical State Routing (HSR) algorithm in which hybrid nodes are more outstanding candidates of being a cluster head to establish a 2 or more tiered network architecture. The authors favor hybrid nodes, in this phase of node

head election, as they promise to relax bandwidth requirements of their cluster using high-throughput FSO antenna.

Wang and Abouzeid draw theoretical throughput scaling limits of hybrid FSO/RF deployments in which a subset of the nodes in the network are equipped with FSO transceivers [92]. In their work, they assume that all the nodes have RF transceivers and all the nodes are stationary. The stationarity assumption poses limitations on the applicability of their findings to real life mobile settings. We see that mobility decreases per-node throughput especially because our designs are pure FSO-based. However, their work is of significant importance since we both anticipate that a hybrid design will prevail to handle both high-connectivity in highly mobile environments and high throughput in stationary and moderately mobile settings. Including FSO while calculating theoretical throughput scaling limits of MANETs is very important to show the significance of FSO's contribution even though they only consider stationary settings.

2.1.3 Free-Space-Optical Interconnects

World-wide internet traffic experienced huge growth in past the few decades. This phenomenal growth created big demand for IP and ATM router and switch products with a throughput level of 1Tb/s and beyond. Free-space-optical communication systems provide an outstanding alternative to conventional cable based connections required in such large machines to connect frames and racks in big data centers. While optical data rates are quite attractive, there exist problems in such FSO systems deployed in computers:

1. vibration in the environment can easily cause misalignment,

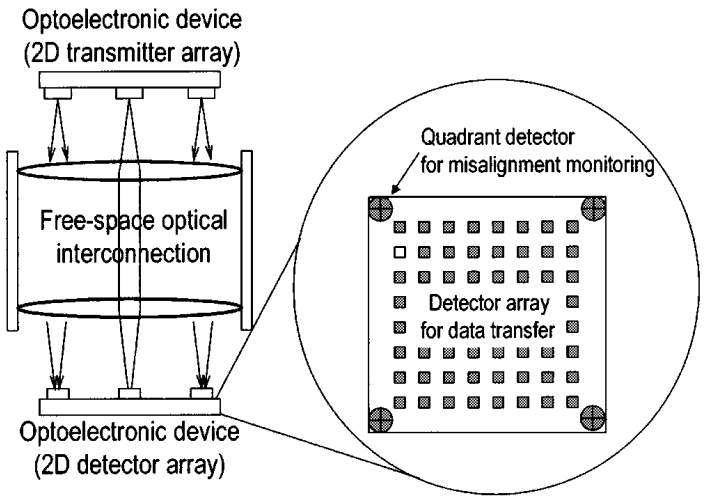

Figure 2.6: FSO interconnect and active alignment demonstration [35]

2. parallel deployments can experience cross-talk,

3. proposed solutions may need expensive mechanical instruments like highly precise steering devices.

In this section, we examine papers that investigate use of FSO technology in interconnects.

Naruse *et al.* investigate a real-time active alignment circuitry for short-distance FSO interconnects to compensate dynamical disturbances [72] (Figure 2.6). The proposed approach solves tight misalignments while preserving spatial density of optical channels. They implemented a piezoelectric microstage and a proportional-integral-derivative control scheme as an experimental system and 118Hz-demonstrations were done. In their design, the misalignment detector arrays play an important role, as they are placed at the peripherals of the parallel data transfer bus channels to detect lateral misalignment error. They, then, use the misalignment signal as a feedback signal for driving the actuator. They also conducted experiments to demonstrate the

effectiveness of active alignment, finding that the amplitude of vibration is $10\mu m$ under a 100 Hz mechanical vibration. With the active alignment, fluctuation of misalignment is reduced to $5\mu m$ which poses an attractive solution for misalignment problem in FSO interconnects.

In order to obtain high misalignment tolerances, Bisaillon *et al.* propose an active alignment scheme that uses a redundant set of optical links and active selection of the best link [22]. The authors previously attacked the same problem by placing a large area detector. Their new approach provides a more viable solution since it reduces cross talk between clusters in the case of parallel implementation of such FSO interconnects. Also, they expect better data rates because of the reduced area. They also provide an improved interconnect design to guarantee the efficient source-detector power coupling in desired misalignment tolerance window. They implemented a vertical-cavity surface-emitting laser (VCSEL) and photo-detector (PD) based bi-directional interconnect and examined ranges from 5cm to 25cm with $\pm$ 1mm lateral and $\pm$ 1° angular misalignment and obtained promising results.

Faulkner *et al.* designed a system that uses multi-element antennas to achieve better coverage in an indoor environment [37]. The authors conducted a demo system in a lab environment. They used arrays of laser transmitters and photodiode receivers, and beam-steering optical lenses in between the two. They investigated a solid-state tracking technique that basically selects the best receiver among the photodiodes according to its light intensity. The system is limited in coverage because of low receiver sensitivity and has laser eye-safety issues.

Similarly, Boisset *et al.* [23] designed an active alignment system for FSO interconnects that is based on a quadrant detector and Risley beam steerers. The detector can successfully detect the misalignment error between the center of a spot of light

and the center of quadrant detector. This information is then fed to an algorithm that calculates rotational displacement required for steerers at both sides. The authors conducted experiments that showed that the system is capable of establishing the alignment up to 160 μm of deviation of spot light. They uses highly sensitive instruments like step motors in Risley beam steerers which tend to be costly. They used a single beam that drops on a single photo detector, although the quadrant detector is able to provide the information about beam misalignment.

2.2 Mobile Free-Space-Optical Communications

The key limitation of FSO regarding *mobile* communications is the fact that *LOS alignment must be maintained* for communication to take place successfully. Since the optical beam is highly focused, it is not enough if LOS exists. The transmitter and receiver pair should be aligned and the alignment must be maintained to compensate for any sway or mobility in the mounting structures. Mobile communication using FSO is considered for indoor environments within a single room, using diffuse optics technology [23, 29, 31, 35, 36, 46, 51, 100], including multi-element transmitter and receiver based antennas. Due to the limited power of a single source diffused to spread in all directions, these techniques are suitable for small distances (typically 10s of meters) but not suitable for longer distances.

For outdoors, *fixed FSO communication* techniques have been studied to remedy small vibrations [17, 18] of the mounting platform. Swaying of the buildings have been handled using mechanical auto-tracking [15, 22, 72] or beam steering [97]. Additionally, interference [70] and noise [89] has been considered among possible challenges. LOS scanning, tracking and alignment have also been studied for years

in satellite FSO communications [38, 57]. Again, these works considered long-range links which utilize very narrow beamwidths (typically in the microradian range), and which typically use slow bulky beam-scanning devices such as gimballed telescopes driven by servo motors.

We propose to use electronic scanning/steering techniques by leveraging angular diversity of spherical structures covered with multiple transceivers. We studied such FSO spherical structures and built some of their elementary features such as re-alignment mechanism working at very short distances and very low speeds [13, 99]. These studies showed promising results and we plan to build several fully-structured prototypes of 3-D FSO spheres, which will constitute a lab-based prototype of a demonstrable FSO-MANET working at high speeds and longer communication distances. FSO is very attractive for power-scarce MANET applications such as sensor networks [52]. Though there have been initial attempts (including ours) to use FSO for MANETs [7, 32–34, 96, 99], an experimental lab demonstration of large-scale FSO-MANET or hybrid RF/FSO-MANET has not been done.

2.3 Effects of Directional Communication on Higher Layers

As discussed earlier, in comparison to RF physical communication characteristics, FSO has critical differences in terms of error behavior, power requirements and different types of hidden node problems. The implications of these physical FSO characteristics on higher layers of the networking stack have been studied in recent years. The majority of the FSO research in higher layers has been on topology construction and maintenance for optical wireless backbone networks [60, 62, 68]. Some work

considered dynamic configuration [61], node discovery [75], and hierarchical secure routing [76,77] in FSO sensor networks. However, no deep investigation of issues and challenges that will be imposed on MANETs by FSO has been performed. In this sense, our work is the first to explore FSO-MANET research issues relating to routing and data link layers.

A key FSO characteristic that can be leveraged at higher layers is its *directionality* in communication. Though the concept is similar to RF directional antennas, FSO can provide much more accurate estimations of transmission angle by means of its directionality. Previous work (including ours) showed that directionality in communication can be effectively used in localization [14,26], multi-access control [27,43], and routing [19,28,42,44,88]. In addition to directionality, our proposed FSO nodes introduce highly-intermittent disconnectivity pattern (i.e. aligned-misaligned pattern) which affects transport performance [13]. Also, the establishment of an FSO communication link implies that the space between the communicating nodes is Euclidian, which can be leveraged to better design routing and localization protocols. We explore the implications and potential benefits of these properties of directional communication within the context of FSO-MANETs in Chapter 6.

R. Choudhury *et al.* explains a simple MAC protocol for directional antennas in [27]. In their research report on directional transmission schemes that is adopted from IEEE 802.11 design, they use a node design that is able to use both omnidirectional and directional transmission modes. A node is able to steer the antenna to point to a desired angle. For the *Simple Directional MAC (DMAC)* approach, they assume that if a node is idle (i.e., there is no ongoing transmission or reception), the node is in omni-directional state. They also implemented RTS and CTS signaling in directional mode. Similar to the Network Allocation Vector (NAV) in 802.11, a directional

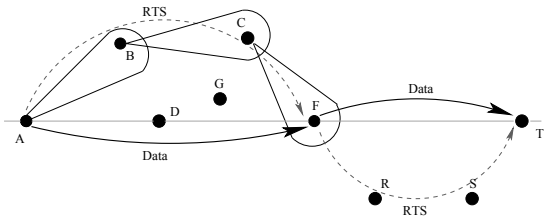

Figure 2.7: Multi-Hop RTS [27]

version is introduced (DNAV) to keep track of allocation of the time domain and *space domain with a local sense of direction*. Hence, a node looks up entries from this table whenever it needs to send an RTS to a specific direction. Later, the backoff phase starts. Also, nodes update this table upon receiving an RTS or CTS. However, the hidden terminal problem in 802.11 reveals itself in two new forms:

- Asymmetric Gain: Since the gain of a directional and omnidirectional antenna under the same power is typically different (i.e., directional gain is greater), sender and receiver nodes with transmit and receive gain of G^d (directional gain) and G^o (omnidirectional gain) respectively, may be out of each other's range, but may be within range if they both transmit and receive with gain G^d.

- Unheard RTS/CTS: A node that participates in an ongoing transmission (nodes A and B) will not hear (Figure 2.7) RTS/CTS frames (exchanged with C and D) since its antenna is directed to a specific point. Upon completion of its transmission, any of the two nodes (A and B) pose a potential interference danger to the nodes that are around them (C and D) and that started their transmission while previous nodes were communicating.

The authors of [27] propose a multi-hop RTS based algorithm (MMAC) to

better exploit the greater gain of directional antennas. The protocol is built up on DMAC. Consider a scenario in which A wants to communicate with F, but since they both have directional antennas with greater gain, they want to establish a link in one hop. The first thing A does is to send an RTS directly to F. F may or may not hear this RTS and most probably will not. A then sends a *multi-hop RTS* destined to F to request F to point its antenna in A's direction through the multi-hop route A-B-C-F. This RTS is treated as a high priority packet by forwarding nodes and it is not subjected to queueing delay. Then A expects a CTS directly from F. Thus, A can indeed communicate with T. The authors ran simulations of different scenarios to observe the average performance of explained protocols, finding that both protocols perform better than IEEE 802.11, with a dependence on network topology and traffic pattern. Their work also provides a motivation for us to better investigate and exploit spatial reuse in our spherical multi-element antenna design. Note that their design exploits the upper layers to route the multi-hop RTS. Also, their design of directional antennas is not capable of utilizing multiple antennas at the same time. Hence, a simple broadcast is achieved by using the antennas sequentially to achieve 360 degree coverage. In our design, multiple transceivers are *intended* to communicate at the same time, yielding simplicity in broadcast operations. Also, this sequential process of transmitters sending out frames will cause operation to span a window of time instead of being instantaneous and will cause different frames to be timestamped with different values.

In the context of effects of directional antennas on upper layers, Choudhury *et al.* evaluate the performance of DSR (Dynamic Source Routing) using directional antennas [28]. They identify issues that emerge from executing DSR (originally designed for omnidirectional antennas) over directional antennas. Specifically, they ob-

serve that route request (RREQ) floods of DSR are subject to degraded performance due to directional transmission and do not cover as much space as omnidirectional transmission. This makes route reply (RREP) take a longer amount of time. They also observed that using directional antennas may not be suitable when the network is dense or linear because of increased interference. However, an improvement in performance may be encouraging for networks with sparse and random topologies. Note that both simulations are conducted using Constant Bit Rate (CBR) on top of User Datagram Protocol (UDP); they do not present any results using to Transport Control Protocol (TCP). Additionally, the performance boosts that they found are only available using a specific network topology and traffic pattern.

2.4 Localization in MANETs

The problem of node localization has been studied in various contexts: using ranging techniques [39, 50, 94], bearing techniques [74], and their combinations of [14, 26]. In this section, we position our work in the related literature that focuses on directional and energy-efficient methods for node localization.

2.4.1 Range-Only Techniques

Range-based methods require at least 3 nodes (4 in a 3 dimensional setting) with location information to enable localization of a fourth node with varying degrees of quality. The major limitation of range-only methods is that they require high density deployment of nodes to achieve high localization coverage. SpotON [50] and Calamari [94] systems build on the assumption of a simple path propagation model with known parameters for RF (via measuring the signal strength) whereas this does not hold

in practical environments where multi path propagation is the norm, especially in in-door settings. Such systems have a 10% error in ranging even after an intense calibration process. Another ranging method is via measuring time-of-flight of an ultrasound or acoustic signal, which provide high accuracy in short ranges (a few meters).

The robotics and image processing communities have been working on the localization problem using landmark detection techniques and laser range finders [20,56,84]. However, those methodologies are irrelevant in MANET localization either because of power consumption concerns or lack of a camera.

Saravese *et al.* present an approach that is resilient to ranging errors in [87]. However, their list of constraints also confirm the fact that a high node density is required in order to achieve sound results of localization extent. Moreover, they propose a refinement phase based on confidence metrics that is employed after a node is able to triangulate. In such a refinement process, nodes that are closer to the anchor nodes have higher priority. This way of prioritization provided more insight in our research. We investigated different ways of prioritizing available localization information that is available from different nodes.

Whitehouse *et al.* presented Calamari which is their test bed for estimating the system parameters of an ad hoc localization system in [94]. Their design involves signal strength and acoustic time of flight measurement and extract the distance between two nodes using the difference between the speed of light and the speed of sound. The number of required message exchanges increase with the hop distance. The two main components in the system, i.e., radio transmitter and acoustic sensing device, although cheap and low-power-consuming, vary highly in accuracy. Hence, their work is mainly focused on eliminating accuracy problems.

2.4.2 Orientation-Only Techniques

Niculescu *et al.* argue that setting up infrastructures for localization only, such as beaconing mechanisms, would not be cost-effective for mobile systems in [74] and they consider angle of arrival detection devices such as an antenna array or a set of ultrasound devices to aid in both positioning and orientation. However, their simulations cover only static scenarios and their assumption is that the approach can be easily applied to *limited-mobile* systems. Their findings agree with ours as they indicate that localization errors are amplified as the number of hops from anchor nodes is increased and they try to avoid using ill-formed triangles while triangulation phase. Again, their usage of extra hardware is a disadvantage when compared with our approach.

2.4.3 Hybrid Techniques

Akella *et al.* proposed a hybrid technique in [14] that uses optical wireless (FSO) to further relax the requirement of node density to only one. The most important advantage of hybrid techniques is they do not require a high node density. Hence, they can achieve high localization extent without high messaging overhead or high node density. Although our work overlaps at the point that both approaches use FSO for its directionality, they need ranging measurements as well. Their work stands out to point that even 3D localization can be achieved without high node density.

Chintalapudi *et al.* lays out two highly desirable properties of ad hoc localization systems in [26]:

- unplanned placement of anchors since some environments may not permit precise placement of anchor nodes,

- ad hoc localization systems should be able to functions with good performance using an order of magnitude fewer anchors than nodes.

The second argument is an important way of distinguishing the family of localization schemes in terms of performance. Moreover, their conclusion of ranging-only techniques requiring node densities (an average of 11-12 immediate neighbors to achieve 90% localization with 5% accuracy) well beyond the density required for network connectivity implies that the bearing or sectoring techniques (i.e., techniques that require directionality) reduce this overwhelming requirement of node density significantly.

Even though the results that they present are promising and stand as a viable alternative to ranging only localization schemes, there is one shortcoming of their approach. It is unknown if accurate bearing (or even sectoring) estimation devices can be built at the form factors and energy levels of sensor networks. Our approach to the problem does not require an additional device and it uses the naturally available directionality information.

Akcan *et al.* present a GPS-free localization algorithm that can be used in mobile ad-hoc networks in [12] since GPS signals may not be available in enclosed environments. However, their assumptions and hardware requirements (compass and motion actuator) exceed the capabilities of a typical MANET node, especially when compared to our approach that does not require any additional hardware.

Langendoen *et al.* perform a fairly comprehensive comparison of three different localization algorithms: ad-hoc positioning, robust positioning and N-hop multileteration in [59]. They point out three common phases of distributed localization algorithms: determine node-anchor distances, compute node positions and iteratively refine the results. Their conclusion is that no, while no single algorithm outperforms the others significantly, there are cases where each may be preferable based on the

requirements of the application.

Hightower *et al.* summarizes different approaches to the problem of node localization in [47]. From early solutions like proximity sensors [24, 58, 78, 82, 93] to scene analysis techniques [20, 56, 84] that are often employed in robotics community and to triangulation [3, 50, 56, 82, 84]. Their work contributes to classification and survey of available methodologies for localization. They also point out different concerns in the localization process such as privacy. The two basic approaches are: node itself calculating its own location using the information broadcast by external infrastructure and the infrastructure calculating a node's location and informing the node. Their work also contributes to proper justification of localization mechanisms since accuracy does not always increase linearly with the amount of cost. In the context of all the above literature on node localization, although our contribution to the solution of localization does not initiate a new branch, it certainly stands out because of the usage of intrinsically available directionality information without requiring any additional hardware.

Our proposition provides high localization extent with as little as only 2 GPS-enabled nodes with acceptable accuracy through the use of narrow transceivers when the 2-connectedness requirement is satisfied. Unlike the infrastructures used in [24, 82], the anchor nodes used in our simulations do not have extra communication or energy capabilities. Despite the conclusion of localization error being insensitive to the amount of anchor nodes in the network found in [59], our findings reveal that localization accuracy can be increased via denser deployment of GPS-enabled nodes which gives flexibility to post-deployment tuning. As flat (ill-formed) triangles were an issue for the lateration step in [73], we also watch for attempting to intersect parallel 3-D lines or collinearity and avoid the situation by not accepting the second

information set that makes an angle less than a threshold value (e.g., 0.005*PI) with any of the previously accepted information sets. Also, we employ a similar sanity check that checks if the estimated location lies inside the line-of-sight of all of the transmitters. If not, we reject the estimate and fall back to the second best couple for a secondary estimation.

2.5 Buffer Allocation and Management in Multi-Element Structures

Free-space-optical mobile ad-hoc networking differs fundamentally in its link availability characteristics in the sense that an ordinary physical link based on radio frequency does not experience frequent disconnections due to mobility. In a typical RF link, the physical propagation medium can get disrupted by weather obstacles such as rain, or sensing can experience poor performance due to multipath propagation. Although the physical link can fade because of the nature of the medium, it does not show a frequent disconnection pattern since the RF signal propagates omni-directionally. This phenomena of *intermittent connectivity* is a new problem in networking and was not present before because of the usage of single-antenna systems. Even in multi antenna and MIMO systems, the problem does not reveal itself since only the infrastructure (access points) is equipped with such antenna structures. Moreover, to be able to appreciate the size of the problem, the nodes with multi-element antennas should gain mobility. Hence, a typical single-element RF antenna or MIMO system consisting of only a few communication components will not show degraded performance because of the above reasons.

The most influential factor behind the requirement of buffering in a FSO

MANET is mobility. The challenge of mobility is present and creates an equally serious performance degradation in Delay Tolerant Networks (DTN) as well. In a DTN, nodes rarely get connected to a neighbor and constantly experience packet drops due to existence of a down link somewhere along the route to destination.

The nature of the problems in FSO and DTN are different. Although the drops are caused by some form of mobility in both cases, in FSO the next hop may still be inside the reachable perimeter but may not be aligned. In DTN, since a DTN is considered in the RF context, the next hop is out of the reachable perimeter. Moreover, a multi-element FSO system should be able to quickly recognize the relative mobility of a next hop and direct a logical flow to the appropriate transceiver without requiring to buffer the frames furthermore. Hence, one can draw possible scenarios for FSO of a *misalignment* that have possible solutions and have no counterparts in a DTN *disconnection*.

In [30], Mooi *et al.* points the ferries: nodes that store, carry and forward packets in a DTN and name this scheme Message Ferrying. They address the disconnection problem in DTNs by allocating buffers in ferry nodes and other nodes in a max-min-fair fashion. They also incorporate this buffer allocation technique into the routing and present buffer efficient routing scheme (BERS) to achieve better session throughput and lower latency.

Because of the store-carry-forward mechanism that is commonly used in DTNs, typical buffers that operate using algorithms like drop-tail does not provide optimal buffer usage. Additionally, the physical channel can get used poorly due to replicated transmissions to increase delivery probability. Krina *et al.* propose a statistically sound mechanism that collects historical data of node encounters in a distributed manner and determines the drops and channel allocations using the encounter-based

message dissemination theory in [55].

As the above representative works show, the specific scheme of buffering, the discipline of resource allocation (especially memory) is determined by a set of inputs from the network itself. It may either be a limited scheme that determines which packets to drop in a static fashion or a much more dynamic scheme that takes the core cause of disconnection, mobility and its variants into account while determining how to allocate its resources. Both of the approaches and most of the work that can be classified in between falls short to be effectively employed in FSO because of the difference in the very nature of the intermittency problem. The time scale of disconnection and reconnection in FSO is much shorter than the time scale in DTN. Hence, buffered packets have a much shorter life time than the ones in DTN. The network layer handles the task of buffering in DTN, whereas in FSO, although different solutions would result varying throughput numbers, the buffering must be handled below the networking layer (MAC or physical layer). In FSO, the most important responsibility is on auto-alignment circuit and algorithm to quickly hand-off logical flows to the appropriate transceiver (or transceiver group) and eliminate most of the possible packet drops without further buffering just by detecting relative mobility of a neighbor.

2.6 Summary

In this chapter, we provided a summary of relevant major research efforts in the literature, their common use cases, problems, and solutions in those fields. We presented representative papers in the fields of terrestrial last mile and indoor applications where FSO has been popularly deployed. We covered hybrid applications of FSO

and RF as well as free-space-optical interconnects in the literature. We also covered how mobile FSO has been provisioned in the past and provided insight on how researchers have coped with directionality and sectored communication instead of omnidirectional communication. We provided a survey on localization techniques for MANETs: range-only, orientation-only, and hybrid techniques. Lastly, we covered cross-layer buffering usage in the literature.

Chapter 3

Packet-Based Simulation for Multi-Transceiver Optical Communication

In this chapter, we present the details of the free-space-optical communication technology, propagation model used in our simulations and interface alignment [95].

3.1 FSO Propagation Model

The important difference between a fiber-optical and free-space-optical link is the lack of a reliable medium for the propagation of light. This poses an important challenge for FSO since the medium can change significantly over time. To tolerate adverse effects of water vapor, carbon dioxide, ozone and etc. the designer of a FSO system must be aware of of losses in the system. We will describe dominant system characteristics of the FSO to derive such system losses. For the sake of simplicity. we

neglect any optical losses since we do not use any optical lenses in our design.

3.1.1 Geometrical Loss

Geometrical loss accounts for the losses that occur due to the divergence of the optical beam (Figure 3.1). The result of divergence is that some or most of the beam is not collected at the receiving side. The loss can be roughly sketched as the area of receiver relative to the area of the beam at the receiver. We can accurately assume that the cone formed by the beam is in the shape of a linear rectangle. If we measure the diameters in cm, the distance in km and the divergence in $mrad$, the formula becomes as follows [99]:

$$\frac{A_R}{A_B} = \Big(\frac{D_R}{D_T + 100 * d * \theta}\Big)^2 \tag{3.1}$$

Abbreviated parameters are as follows:

Parameter Descriptions	
A_R	Area of the receiver
A_B	Area of the beam
D_R	Diameter of the receiver at receiver
D_T	Diameter of the transmitter
d	Separation of transmitter and receiver
θ	Divergence angle

3.1.2 Atmospheric Loss

The atmosphere causes signal degradation and attenuation in a free-space system link in several ways, including absorption, scattering (mainly modeled as Mie scattering),

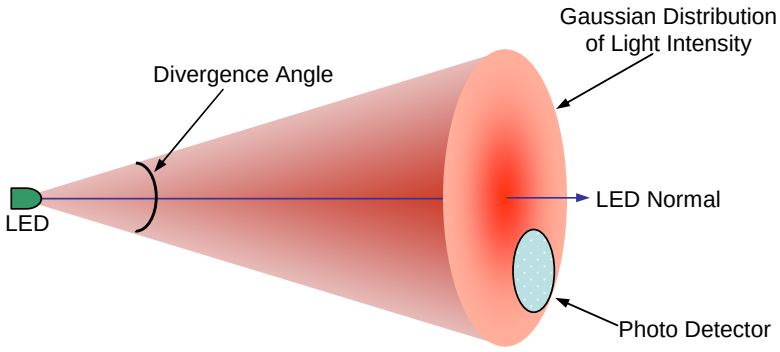

Figure 3.1: Light intensity profile of an optical beam.

and scintillation. All these effects vary in time and basically depend on the condition of the weather. The atmospheric attenuation A_L consists of absorption and scattering of the laser light photons by the different aerosols and gaseous molecules in the atmosphere. The power loss due to atmospheric propagation is given by Bragg's Law [95] as:

$$A_L = 10\log(e^{-\sigma R}) \tag{3.2}$$

where σ is the attenuation coefficient consisting of atmospheric absorption and scattering. Mie scattering occurs because of the particles that are about the size of beam wavelength. Therefore, in the near infrared wavelength range, fog, haze, and pollution caused by the aerosols are the major contributors to the Mie scattering effect. There are also scattering models, but for the wavelengths used for FSO communication, Mie scattering dominates the other losses and it is given by [90, 95]:

$$\sigma = \frac{3.91}{V}\left(\frac{\lambda}{550}\right)^{-q}. \tag{3.3}$$

In the above formulation of σ, V is the atmospheric visibility in kilometers, q is the size distribution of the scattering particles whose value is dependent on the

visibility:

$$q = \begin{cases} 1.6 & V \geq 50\text{km} \\ 1.3 & 6\text{km} \leq V < 50\text{km} \\ 0.583V^{1/3} & V < 6\text{km} \end{cases} \tag{3.4}$$

The above losses and receiver sensitivity threshold must be taken into account for calculation of the link margin.

3.2 NS-2 Simulation Models for Multi-Element FSO Structures

3.2.1 Interface Alignment Implementation in NS-2

Our interface alignment implementation gradually evolved. This section focuses on the initial implementation and later improvements.

Initial Alignment Implementation and Enhancements

This first implementation was placed in NS to cover the urgent needs of researchers. The code that determined alignment of two interfaces was placed in *channel*. Hence, the channel was kept responsible for determining the network interfaces receives the packet that is handed to *channel* (Figure 3.2).

The logical flow was as follows (only details that are relevant to alignment are included, leaving everything else excluded for simplicity reasons) :

1. A packet is given from MAC (i.e., *mac-802_11.cc*) to *wireless-phy*
2. *wireless-phy* hands the packet to *channel*

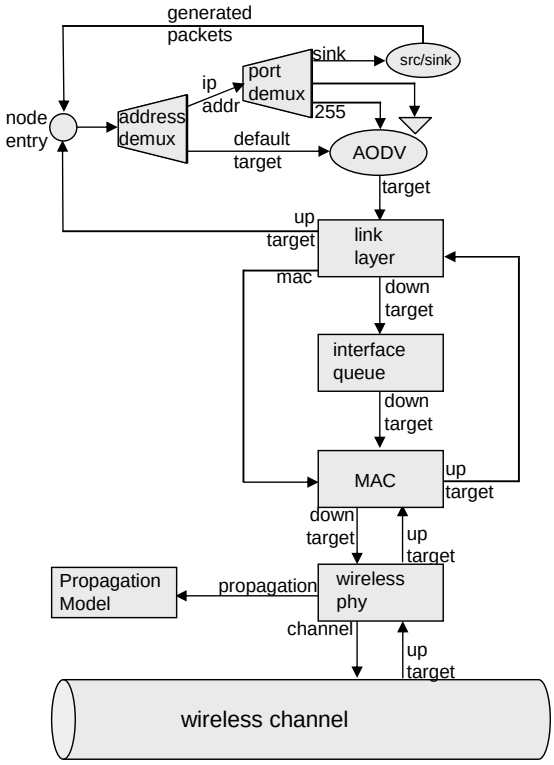

Figure 3.2: Internal design of a wireless node in NS-2. [5]

3. *channel* extracts the meta data information, that was put in the packet headers to determine the divergence angle, specific position and normal of the sending transceiver.

4. *channel* goes through every node in the network, to find out if the sender transceiver can see the candidate node based on the center of the node, and if one of the transceivers on the candidate node can see the sender node.

5. If the two given nodes can see each other, *channel* schedules a reception for each transceiver in the candidate node. Hence, each transceiver receives a copy of the packet and delivers it to the upper layers.

As the first enhancement, we changed the above procedure such that; *channel* goes through every transceiver in the network to find out if the sender transceiver and the candidate transceiver can *see* each other, i.e., if they are in one another's line of sight. Note that this way of determining alignment based on the position of transceivers is more accurate since the center of the node and coordinates of a transceiver can be considerably apart from each other based on the diameter of the node. For small nodes, this does not pose a problem but for nodes with 10 cm or bigger diameter, this affects the alignment accuracy. If the two given transceivers can see each other, *channel* schedules a reception: the receiving transceiver is the candidate transceiver that was just examined and the packet is the packet handed to *channel*.

This procedure was executed every time a packet is given to the channel. Note that, although it is not impossible to design the auto-alignment circuit such that two transceivers exchange search signals every time a packet is going to be sent, it does not adhere to the initial design of the auto-alignment circuit. The basic principle in the

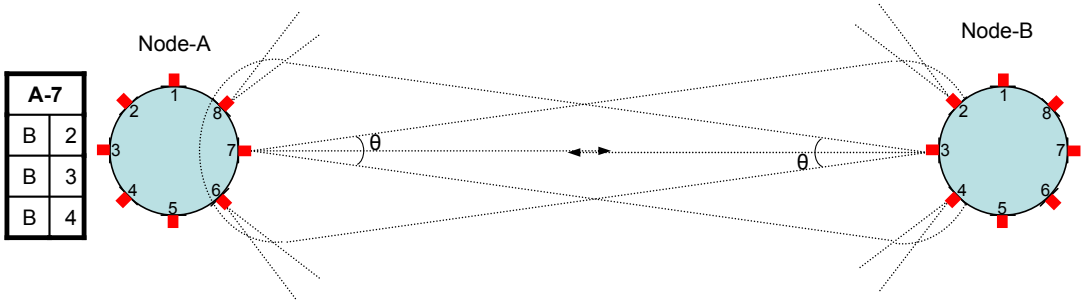

Figure 3.3: Multi-element antenna design in 2D view and sample alignment table kept in interface 7 of node A.

design of the auto-alignment circuit is that search signals are sent from a transceiver periodically every second, so that, according to the received responses, a transceiver can keep track of its aligned neighbors.

Note that the alignment is conservatively determined mutually. Thus, for two interfaces to be considered as *aligned*, both must see each other; if one of them sees the other, then the alignment is not considered as established. Although partial alignment would be a perfectly acceptable improvement, we made our design decisions conservatively.

Timer-Based Alignment Implementation

According to the principal idea in auto-alignment circuitry, we decided to implement the interface alignment procedure periodically instead of every time a packet is sent. As the second enhancement, we introduced a MAC level timer. This timer goes off with a predetermined (roughly, 0.5 sec) frequency and calculates the alignments in the network. Since every interface has its own MAC layer, it also has an alignment timer (code name *AlingmentTimer*). Practically, the resulting design is that every transceiver determines its aligned neighbor and keeps a table that has an entry for

each aligned transceiver.

As illustrated in Figure 3.3, interface 7 on node A, named *A-7*, has an alignment table and its entries are *B-2, B-3* and *B-4*. Identically, every transceiver in the network keeps a similar table to keep track of its aligned neighboring transceivers. In this design, whenever a packet is being sent, the channel determines alignments based on this alignment table. The channel checks the entries of alignment table to ensure that the nodes reside in each other's alignment list. Next, the channel conducts a secondary check to see if the two interfaces are still aligned using their current location and orientation. If they are still aligned, the channel delivers the packet to the receiving transceiver. If they are not aligned, the channel quietly purges the packet. This model is not only computationally more relaxing, but is also more realistic from the auto-alignment circuit's point of view.

3.2.2 Alignment Scenarios and Mobile Node Design

The directionality of FSO antennas causes the alignment and misalignment pattern to repeat frequently in mobile scenarios. Consider a scenario with two nodes: Node-A and Node-B (Figure 3.4). While Node-A stays stationary, Node-B moves with an arc route from Position-1 to Position-3 as illustrated. In this scenario, the two nodes loose their alignment while Node-B is in intermediate states, i.e., between positions 1 and 2 and between 2 and 3.

Choosing the divergence angle and number of transceivers in the node are two important parameters that effect intermittency of the connection between two nodes. Such a choice should optimize a number of metrics: reduce the interference area that is created by two adjacent transceivers and increase overall coverage area. Also, putting more transceivers is good for spatial reuse, but adversely affects network throughput

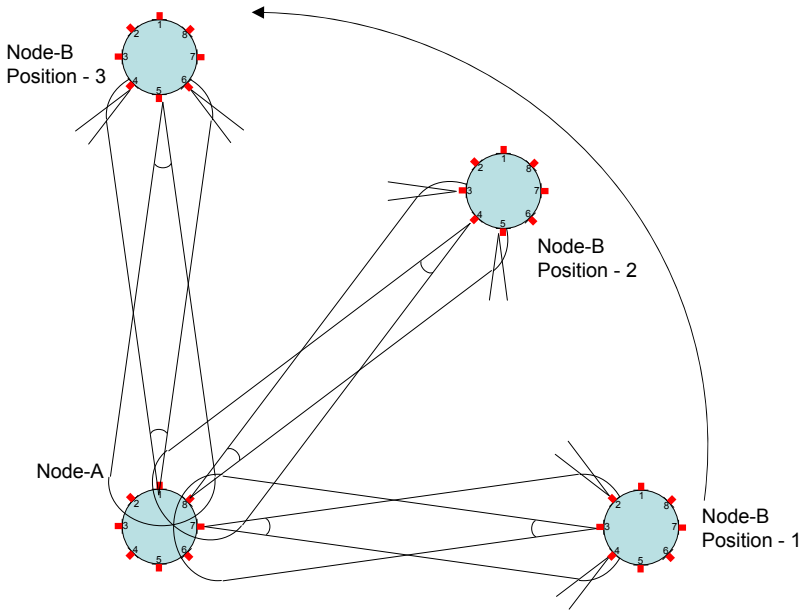

Figure 3.4: Sample alignment scenario for two mobile nodes.

in mobile cases. Those system parameters and their implications are examined in depth by Yuksel *et al.* in [99]. We adhere to the designs proposed by Yuksel *et al.* and base our simulations on those indoor and outdoor designs (Tables 3 and 4 in [99]).

3.2.3 Auto-Alignment Circuitry

Yuksel *et al.* designed alignment circuitry to remedy the problem of hand-off [99]. Note that as two nodes are mobile with respect to each other, they will loose and re-gaining their alignments with each other. The specific transceivers used for communication in both nodes should be changed as the nodes move. Auto-alignment circuitry, contrary to mechanical steering mechanism, delivers quick and automatic hand-off of logical flows among different transceivers.

Alignment is detected in a two-phased fashion [13], whenever the light intensity drops under a predefined threshold, the search phase begins to re-establish the align-

ment. In the event of misalignment, the transceiver first sends a pilot search signal (e.g., 1010110), which is commonly known among all nodes in the network. If the transceiver receives the same input as the search signal, then it determines that LOS is available and the alignment is established. Once LOS alignment is established the structure selects this transceiver as the one that needs to send data and the second phase is entered. The key idea is that two nearby spheres, which lost alignment due to mobility, will eventually receive the search signals upon existence of a new LOS.

In the mobility scenario that we illustrated in Figure 3.4, auto-alignment circuitry in Node-A for instance, will successfully switch from *interface 7* to *8* and finally to *1* as Node-B changes its position from *Position-1* to *Position-2* and *Position-3*; thus *handing-off* the logical stream to a different physical channel, i.e., transceiver. Ideally, this selection of specific transceiver to carry a logical flow (e.g., an FTP session) and the switching between different transceivers should be transparent to the upper layers.

3.3 Validation Simulations

To show that our FSO simulation modules comply with the theoretical propagation model, we have done several simulation experiments. Our experiments involved two transceivers positioned in different ways with respect to each other. We observed received power, error probability and bit error rate in packet transmissions while varying important parameters like the separation between the two transceivers, visibility and noise.

Table 3.1: Table of default values common to each simulation set in our experiments.

Parameter Name	**Default Value**
Visibility	6 km
Number of interfaces	8
Transmission range and separation between nodes	30 m
Divergence angle	1 rad
Photo detector diameter	5 cm
LED diameter	0.5 cm
Per-bit error probability	10^{-6}
Noise	1.1428e-12 Watt
Capture threshold	1.559e-11 Watt
Receive threshold	3.652e-10 Watt

3.3.1 Effect of Separation

Complying with the theoretical framework, our results reveal that the received power follows Lambert's law [95] from the transmitter itself and normal of the transmitter as depicted in Figure 3.5. The original transmission power for this scenario is calculated for 0.1 meter. We increased the separation between transmitter and receiver antennas from 0.01 meter to 100 meters in our simulations (Figure 3.5). Figure 3.6 shows the Gaussian distribution of the received light intensity clearly as the receiver is moved away from transmitter's normal line by focusing on the last 10 meters of Figure 3.5.

Distance also affects the theoretical error probability and simulated packet error since the received power decreases significantly. We sampled the theoretical error with separation between antennas ranging from 10 meters to 4000 meters. Figure 3.7 shows that the theoretical error probability increases significantly as the receiver is moved away from the transmitter while keeping the transmission power fixed. Similarly, the simulated packet error shown in Figure 3.8, follows the theoretical error

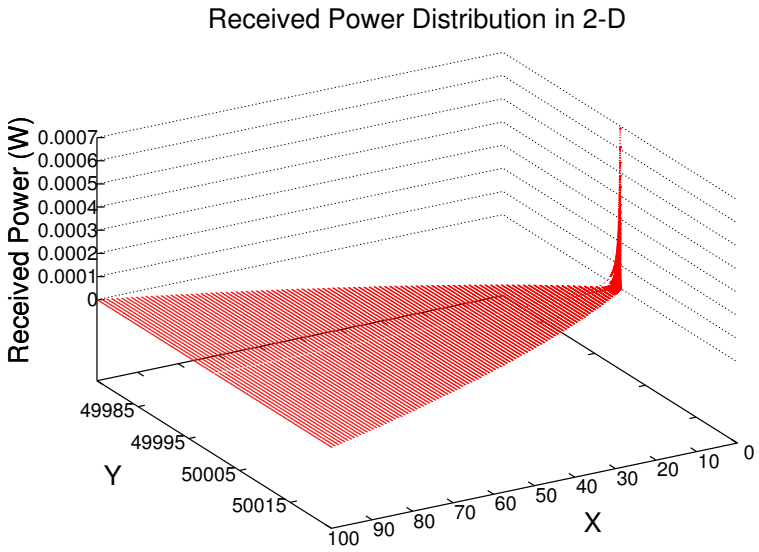

Figure 3.5: Received power in the field of view of a 1 rad light source.

probability.

3.3.2 Effect of Visibility

Low visibility in the medium makes the light experience more deviation from its intended direction by hitting aerosols in the air. This causes the received light intensity to drop which in turn causes more bit errors. Hence, increasing visibility decreases the theoretical error probability and the simulated packet error. For this simulation scenario, the power is calculated for 100 meters with 6 km visibility and kept the same for all the simulations. Separation between antennas is 100 meters. We increased visibility from 0.037 km to 0.041275 km. In Figure 3.9, we show that the visibility in the medium affects the theoretical bit error probability and the simulated packet error significantly. From the figure, we can see that if visibility is set to a value from 0 to 0.037 km, the system experiences a high level of error but recovers after 0.04 km.

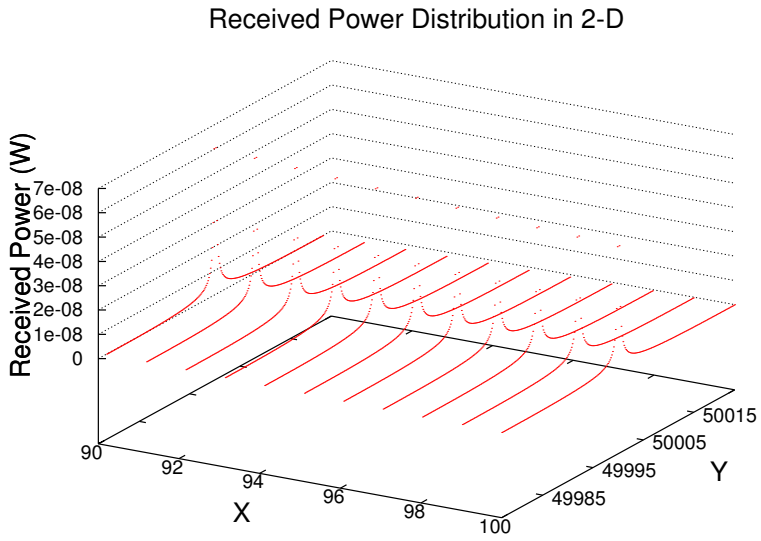

Figure 3.6: Received power between 90 and 100 meter ranges.

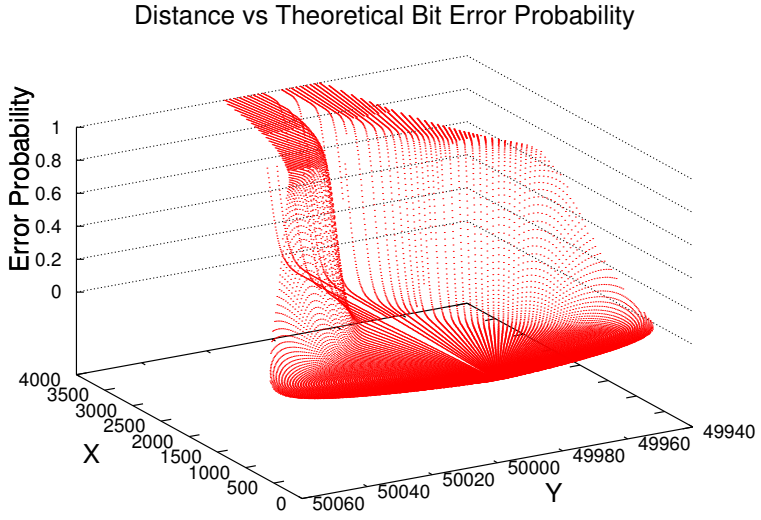

Figure 3.7: Probability of error increases as a receiver is moved away from the transmitter.

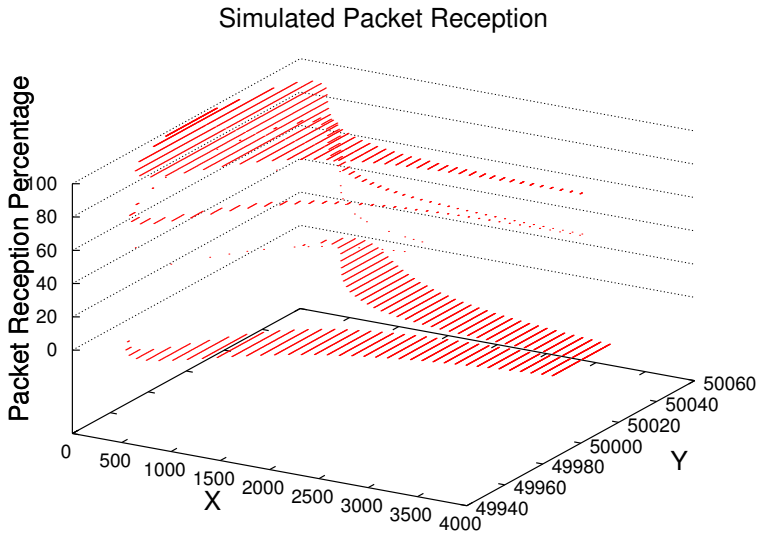

Figure 3.8: Percentage of successfully delivered packets decreases as the receiver is moved away from the light source. Used transport agent is UDP.

3.3.3 Effect of Noise and Interference

We found that noise has an important impact on theoretical bit error probability and simulated packet error since it is harder for the receiver to operate at a low signal-to-noise ratio. We used a transmission power that reaches 100 meters with a noise level of 1.1428e-12 Watt for all of our simulations in this scenario. We increased the noise in the medium from 3.0e-5 W to 2.01e-4 W and found that both the theoretical error probability and simulated packet error are increased considerably as depicted in Figure 3.10.

3.4 Summary

In this chapter, we presented our contribution to NS-2 for simulating free-space-optical links as we have demonstrated in [63, 64]. We took visibility in the medium,

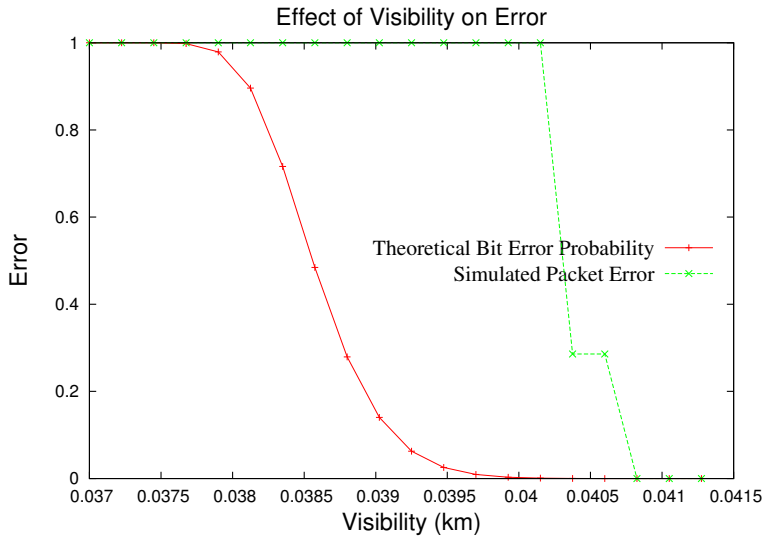

Figure 3.9: Probability of error decreases as the visibility in the medium is increased. Percentage of delivered packets follows a similar but coarser grained behavior.

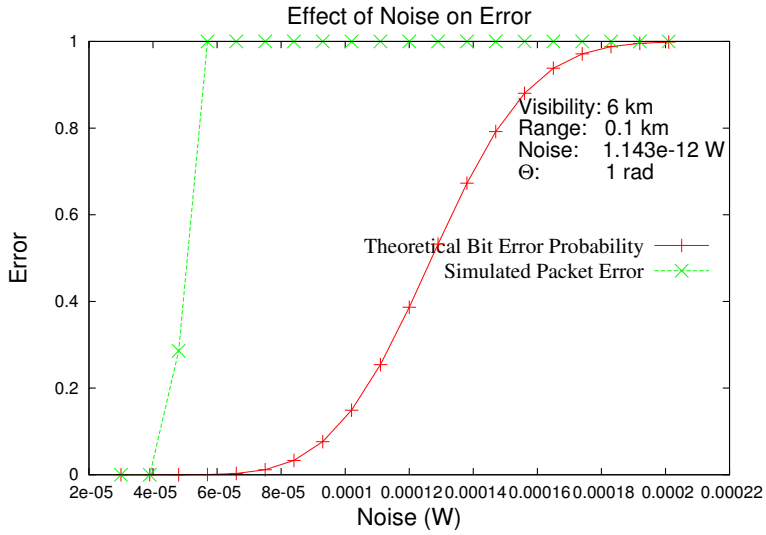

Figure 3.10: Theoretical error probability and simulated packet error increase as the noise is increased.

divergence angles of transmitters, field of view of photo-detectors, and surface areas of transceiver devices into account while implementing our enhancements. We provided results of our efforts that comply with theoretical models, showing a drop in the received power, theoretical error probability and simulated packet error with an increase in separation, medium visibility, and noise.

Chapter 4

Effects of Multi-Element FSO Structures on Higher Layers

In this chapter, we examine a subset of the research problems raised by using such multi-element FSO structures in MANETs and proposals to remedy such issues. We specifically investigate the issues raised by directionality in combination with mobility, and their implications on TCP and overall network throughput. We present a thorough simulation study that covers all the important system parameters. In this chapter, we extend the study to MANET scenarios involving many of such multi-transceiver nodes, and investigate achievable throughput gains in comparison to a pure RF-based MANET.

We perform extensive simulation experiments to investigate end-to-end throughput performance over an FSO-MANET using multi-element spherical FSO nodes. We compare FSO performance to RF under the same conditions. Particularly, we aim to answer the following research questions:

- How robust can the multi-element spherical FSO nodes be against *mobility*?

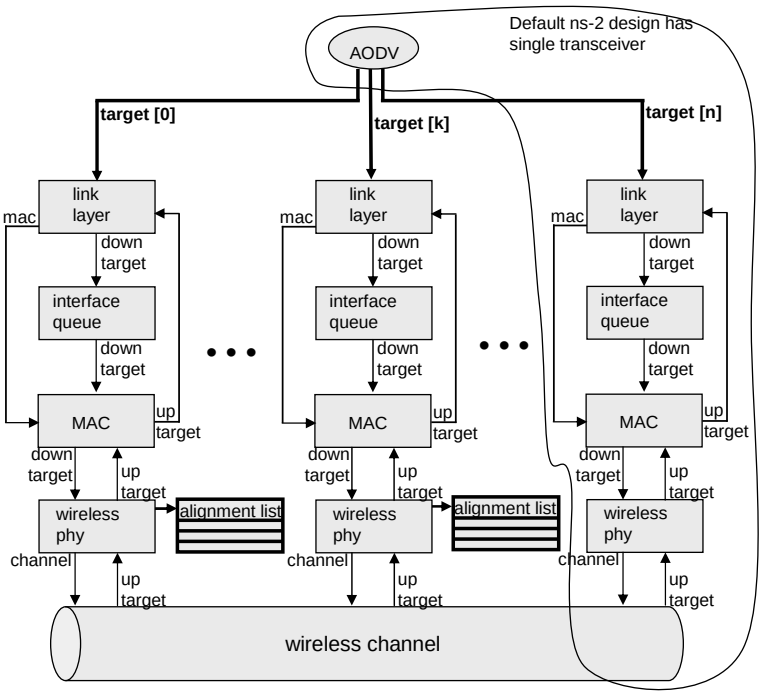

Figure 4.1: FSO node structure with a separate stack for each optical transceiver.

- How important are the effects of node design (e.g., number of transceivers per node) and transceiver characteristics (e.g., divergence angle) on the throughput?
- Can the FSO nodes deliver acceptable throughput in a typical *indoor* environment?
- Can the FSO nodes deliver acceptable throughput in an *outdoor* city environment where several obstacles exist?

4.1 Simulation Environment Setup

Our simulations consist of 49 nodes (each with 8 transceivers) organized as a 7 by 7 grid initially before they start moving. Every node opens FTP file transfer sessions

Parameter Name	**Default Value**
Number of nodes	49
Number of flows	49x48
Visibility	6 km
Number of interfaces	8
Mobility	1 m/s
Simulation time	3000 s
Transmission range and separation between nodes	30 m
Area	210 m by 210 m
Node radius	20 cm
Divergence angle	0.5 rad
Photo detector diameter	5 cm
LED diameter	0.5 cm

Table 4.1: Table of default parameter values common to each simulation set in our experiments.

on top of TCP to every other node in the network, which makes 49x48 flows in total. All the nodes are mobile doing 1 meter per second except for the lounge simulations in Section 4.7 where nodes are stationary. We used an area of 210x210 meters and visibility of the medium was 6 kilometers. We ran the simulations for 3000 seconds and repeated each simulation for 5 iterations. We show the average throughput plots with 95% confidence intervals.

Table 4.1 shows the *default* parameters we feed to our simulation experiments. The FSO node structures are circular in shape, except the lounge scenario in Section 4.7 where the nodes are spherical. Transceivers are placed on the nodal shape with a deterministic separation, i.e., the distance among any two neighbor transceivers is the same. The node structure has a radius of 20 cm. The LEDs have 0.5 cm and PDs have 5 cm radius.

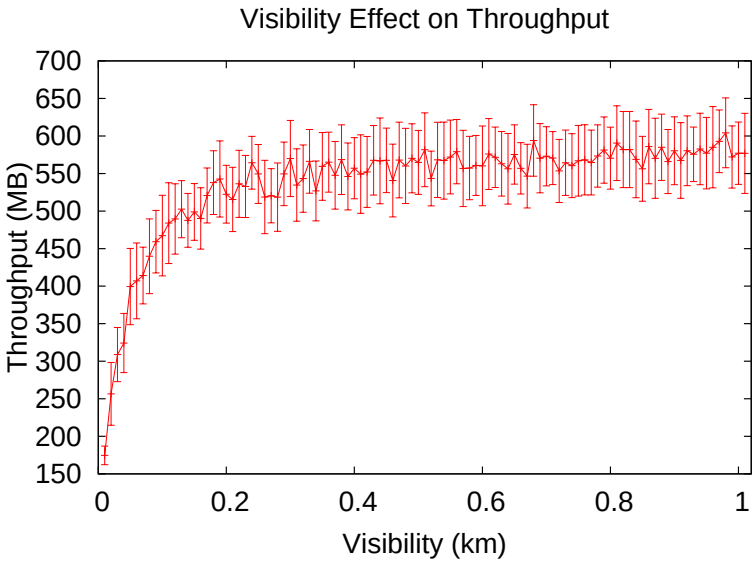

Figure 4.2: Visibility Effect.

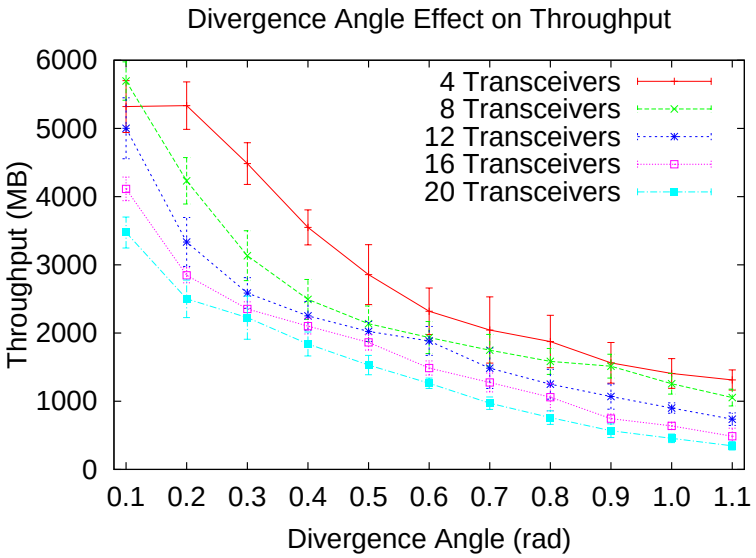

Figure 4.3: Divergence Angle Effect.

4.2 Visibility

FSO communication has been known for its intolerance to adverse weather. In traditional point-to-point applications of FSO, especially fog has been considered as a serious threat to the reliability of the communication. To quantify how aerosols affect the overall network throughput, we simulated our network scenarios under different visibility conditions. We varied the visibility in the medium from 10 m to 1 km. We depict our findings in Figure 4.1 which shows the clear trend of increasing throughput as the visibility conditions become better.

4.3 Divergence Angle

We investigated how divergence angle of transceivers affects the network throughput. We used different number of transceivers with varying divergence angles. The number of transceivers changes from 4 up to 20 and we increase the divergence angle from 0.1 radian to 1.1 radians. The only different parameter in this scenario from the default setup given in Table 4.1 is that the mobility of the nodes is 0.01 m/s. One must note that, as we increase the divergence angle of transceivers the coverage area of a node starts to resemble to that of RF. If the divergence angle is further increased, adjacent beams on a node start to overlap and cause crosstalk and interference. This is why we see a decrease in the overall network throughput in Figure 4.1.

4.4 Mobility

A rather intriguing question is how FSO-MANETs would perform in a mobile setting. We investigate the extent of packet drops caused by mobility and compare

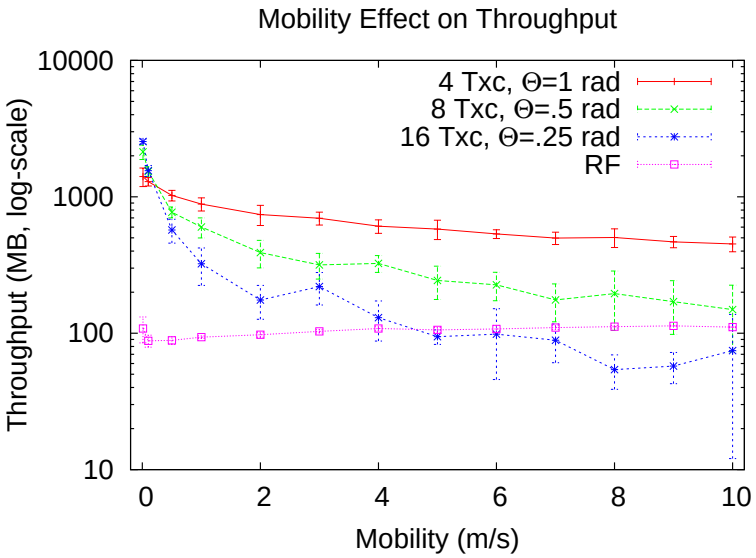

Figure 4.4: Mobility Effect.

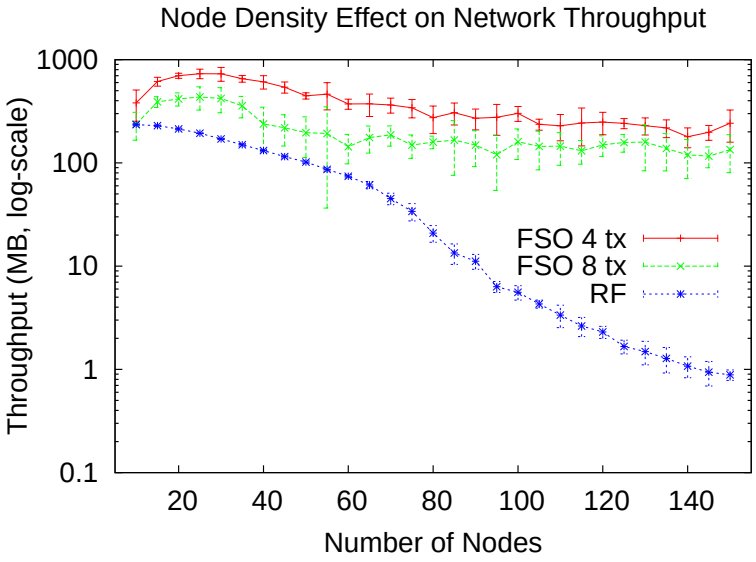

Figure 4.5: Network-wide throughput.

FSO-MANETs with similarly designed RF-based networks. To answer this question, we simulated a network of FSO nodes with 4 transceivers, each with 1 radian of divergence angle and other networks of FSO nodes with 8 and 16 transceivers with further decreasing divergence angles. Figure 4.3 shows the results of these experiments. The first observation is that while RF stays almost the same with respect to mobility, FSO throughput decreases dramatically due to the directional nature of the transceivers. Secondly, at low mobility rates, node designs with more transceivers achieve better throughput due to greater spatial reuse. Moreover, node designs with more transceivers and narrower angles tend to get affected more seriously by mobility. We conclude that 4-transceiver design performs the best at high mobility rates since it is the closest one to RF in terms of coverage and wide field of view. From the given results, we conclude that networks of multi-transceiver directional FSO nodes exhibit a pattern of *intermittent connectivity*. This frequent alignment/misalignment of the communicating transceivers affects TCP seriously. A solution to this problem is to introduce buffers to reduce packet drops in the event of a misalignment as a future direction. Such buffering techniques can be cross-layer in that they should be able to mitigate the loss of layer 2 frames by storing them in layer 2 and/or layer 3 buffer(s). Each layer 3 buffer is either shared by all the transceivers of the node or dedicated to a particular layer 3 flow.

4.5 Node Density

One of the main motivations behind our work is the reduction in per-node throughput of RF-based MANETs when the network experiences a large increase in the number of actively communicating nodes. RF per-node throughput scales with $\sqrt{n}$ as number of

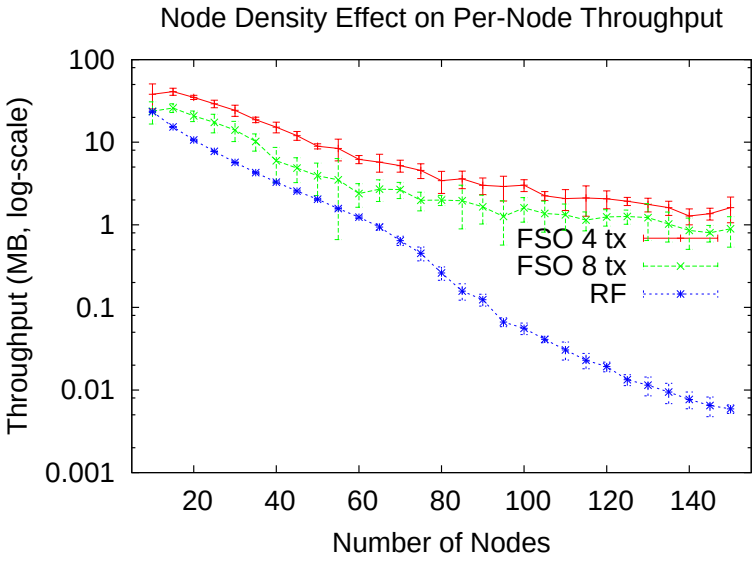

Figure 4.6: Per-node throughput.

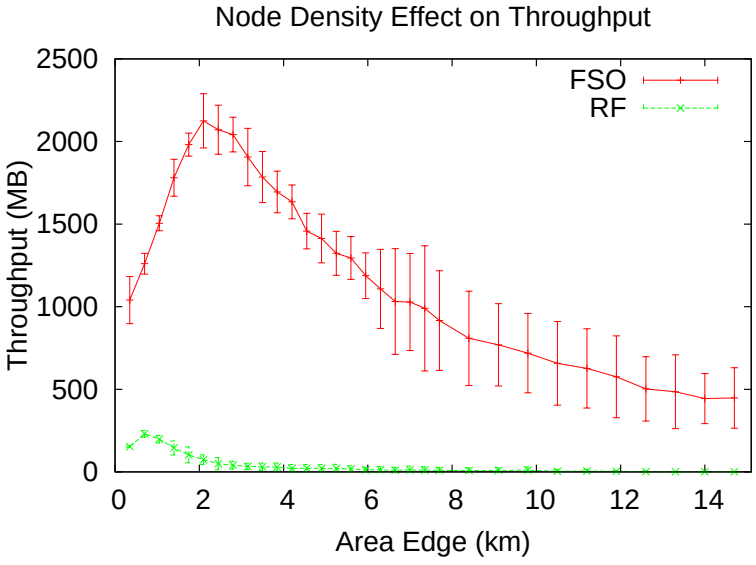

Figure 4.7: Enlarging Simulation Area.

nodes (n) grows [45] since RF spectrum becomes saturated and interference dominates the throughput behavior because of the omnidirectional RF propagation. Hence, we conducted node density experiments in which we increase the number of nodes from 10 to 150 in a confined area of 50x50 meters.

First, we increase the number of nodes in the confined area while keeping area size and the other parameters such as transmission range fixed at 8 m (refer to the discussion in Section 3.3 for power degradation behavior) the same. Figures 4.3 and 4.4 show the overall network throughput and per-node throughput. We conclude that the drop in RF throughput is much more significant than the drop in FSO throughput in both scenarios, again, because of spatial reuse and decreased interference.

Second, we increase the area size and keep the number of nodes and all the other parameters (e.g., transmission range is 30 m) the same. Figure 4.4 shows the network throughput as one edge of the area is increasing. The network throughput first increases as the node density is decreasing. This shows that the initial node density is too high for the 30 m transmission range and there is significant interference. Later, as the node density gets even smaller, the network throughput starts to decrease as 30 m becomes insufficient to cover the average node separation.

4.6 Re-alignment Timer

We conducted another set of simulations to find out the effect of re-alignment timer on throughput and failure. We repeated the experiments for 20 iterations with different random seeds and we depicted 95% confidence intervals. In Figure 4.5 and 4.5, we show how overall network throughput and failure are affected with this phenomenon, respectively. Our conclusion is that especially the failures are not dramat-

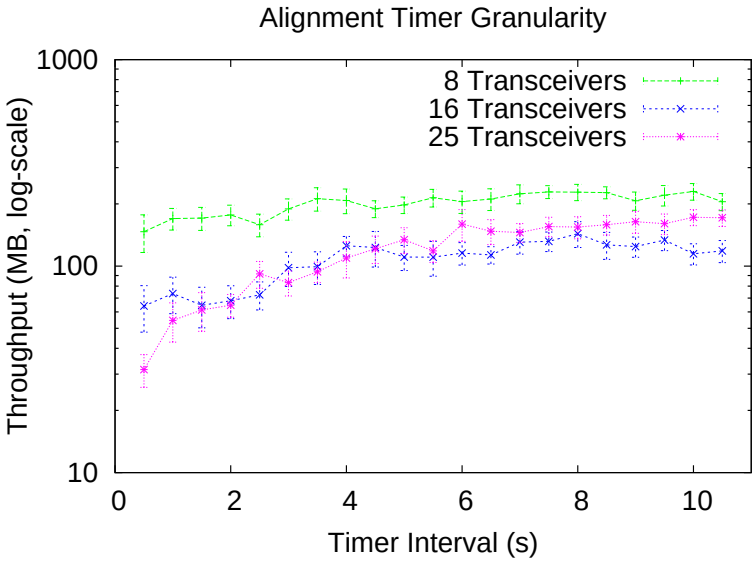

Figure 4.8: Alignment timer effect.

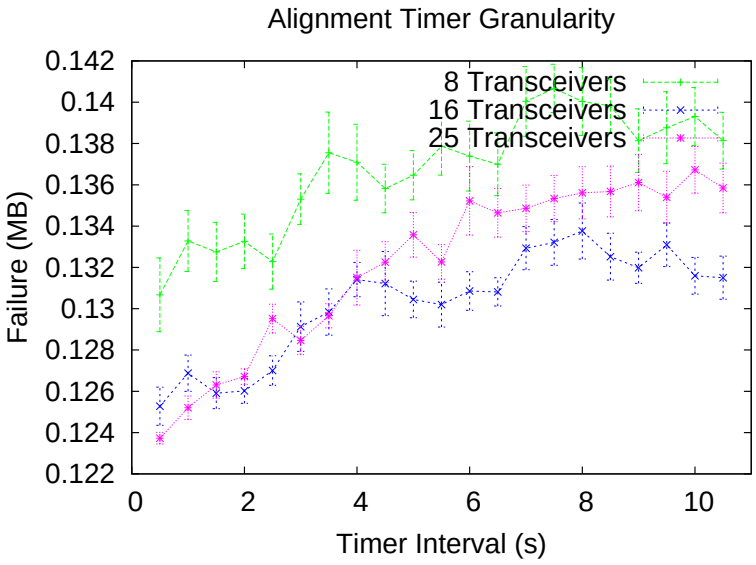

Figure 4.9: Alignment timer effect in log-scale.

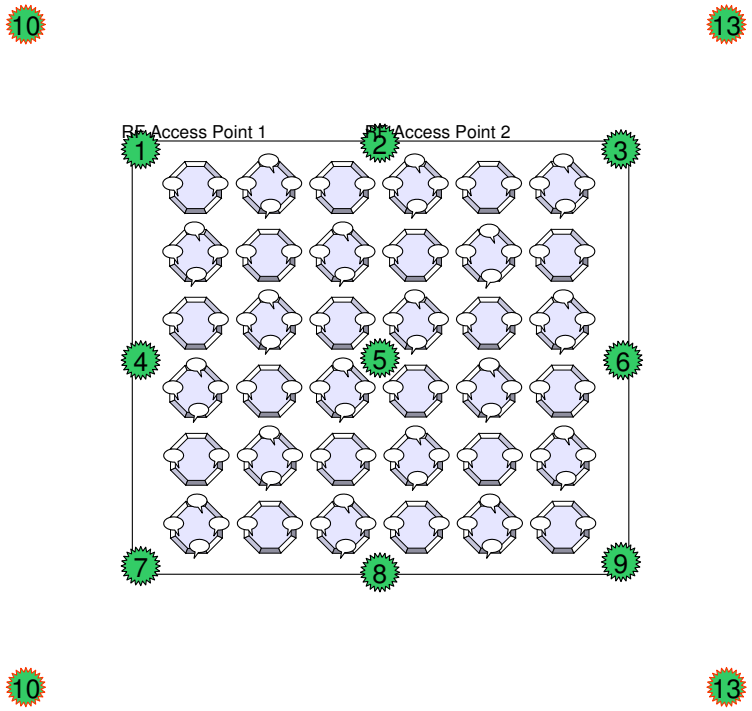

Figure 4.10: A dense lounge setting with multiple RF wireless devices to demonstrate the substantially decreasing per node throughput problem in RF.

ically affected with larger timer intervals. This is an important finding to reduce the re-alignment overhead.

4.7 Obstacle Scenarios in Lounge and City Environments

We extended our simulation effort to find out how FSO behaves in possible applications in indoor and outdoor environments. For indoors, we considered a lounge setting where there is a dense presence of nodes on top of tables that are 10 m apart. We placed either 2 or 4 spherical nodes on 16 tables which makes 48 nodes each

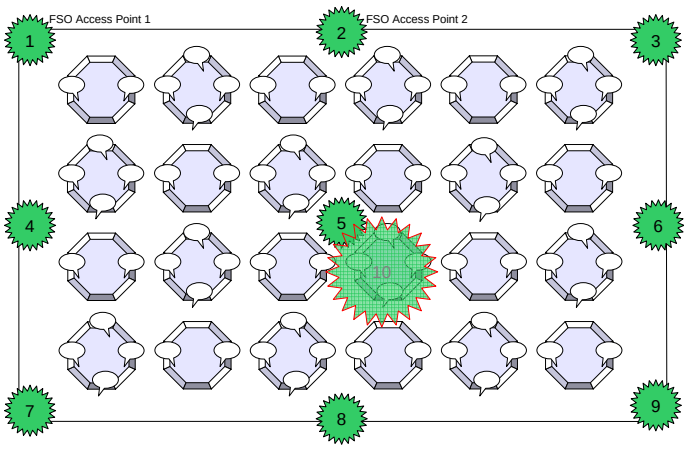

Figure 4.11: A two story lounge with FSO nodes communicating with another backend node in the second floor.

with 18 transceivers. We placed access point FSO nodes with 26 transceivers at arbitrary locations shown in Figure 4.6 including one in a second floor where all the FTP traffic is to and from this node through 9 access points. Similarly, Figure 4.6 shows the upper left quarter of the network establishing FTP sessions to and from node 10 through access point 1. The remaining quarters of the network have similar FTP sessions with their corresponding remote nodes where traffic needs to be relayed by an access point node. We observe a significant difference in throughput as shown in Figure 4.12 in lounge settings due to difference in propagation nature of RF and FSO.

For outdoor, we put 25 (in a 5 by 5 setting) buildings with 10 meters of separation from each other. Between each building, there are 2 people and 1 car. Our re-alignment algorithm takes the obstacles into account so that if a building is blocking two communicating devices, they have to find other intermediate nodes that will carry their traffic. We also modified the default NS-2 random way-point mobility generator to acknowledge existing obstacles. We did not penalize RF transmissions

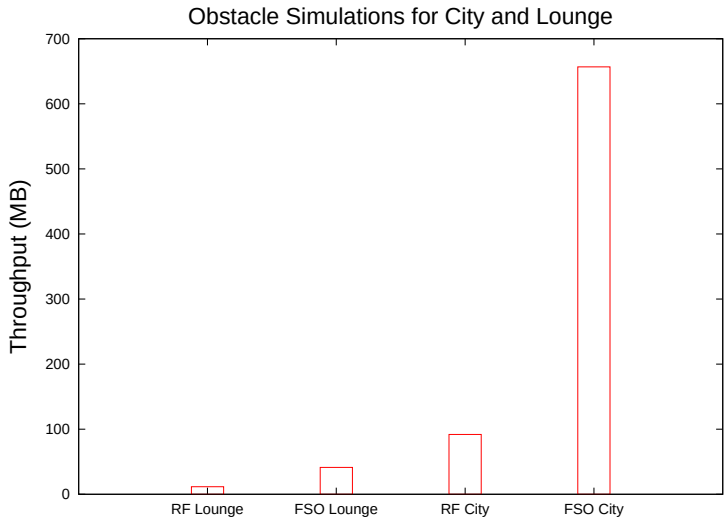

Figure 4.12: Throughput comparisons for in-door and out-door deployment of RF and FSO.

going through those obstacles since RF signal can get through obstacles although the signal strength drops. Observe that FSO's spatial reuse makes a significant difference compared to RF simulation results even though this is an outdoor scenario (Figure 4.12). Note that we observe such results since obstacles are blocking the communication only temporarily because of node mobility.

4.8 Summary

In this chapter, we presented our contribution to the NS-2 network simulator, mainly on the FSO propagation model, multi-transceiver directional FSO structures, and obstacle-avoiding mobility generation as we first introduced in [21, 65, 71]. We assessed the effects of multiple system parameters on the overall network throughput. FSO-MANETs are fundamentally different than RF-based MANETs because of the highly-directional FSO communication in combination with mobility. We conclude

that our simulations of FSO networks deployed in lounge and downtown city environments show clear advantages over RF deployments. We introduce cross-layer buffering schemes in the next chapter to remedy the disruptions caused by intermittent connectivity.

Chapter 5

Buffering Techniques for Multi-Element Communication Structures

Chapter 4 revealed an important phenomenon, i.e., high intermittent connectivity, that emerges only when a large number highly-directional transceivers are used at each node in a mobile wireless network. The intermittent connectivity patterns arising from highly directional transceivers need special treatment, since existing networking protocols and technologies are designed with the assumption that there exists an underlying link that is always connected. Such an issue does not emerge in today's wireless networks where a few (typically 3 to 5) directional RF antennas are used for each coverage cell [81]. To the best of our knowledge, the intermittent connectivity pattern is currently specific to free-space-optical mobile ad-hoc networks since directional RF antennas generate much larger communication lobes [81]. However, we envision that as directional RF antennas become more precise and more focused

with smaller divergence angles, researchers will experience similar problems in bridging the gap between existing protocols and an underlying communication paradigm where connectivity is highly intermittent. Additionally, we anticipate that, as the boundaries between delay-tolerant networking (DTN) and conventional networks disappear, buffering techniques relevant in DTN area will be introduced for similar buffer management issues, especially considering directional communication possibility for DTNs because of power consumption benefits.

In this chapter, we propose two buffering schemes: *node-wide* and *per-flow* buffering to achieve better throughput in mobile settings where intermittence of the underlying wireless links is the norm. The common point to both of these buffering schemes is that they keep an otherwise-would-be-dropped packet during the misalignment period of two communicating nodes till an alignment is re-established through the same or a different pair of transceivers. We discuss the aforementioned buffering schemes in Section 5.1 and 5.2 in detail and provide differences in their behavior. Section 5.3 gives the performance results of major simulation settings and compares the two buffering mechanisms with non-buffered performance results. We conclude our findings in Section 5.4.

5.1 Node-Wide Buffering

Node-wide buffering mechanism, whose algorithm is given in Algorithm 5.1, uses a single buffer for all the transceivers in the node. This buffer is a simple drop-tail memory space that holds packets if the next hop of the packet is not aligned.

Consider a packet going through the layers of the node stack depicted in Figure 5.1. First, the routing agent (i.e., AODV) will select the outgoing interface to the

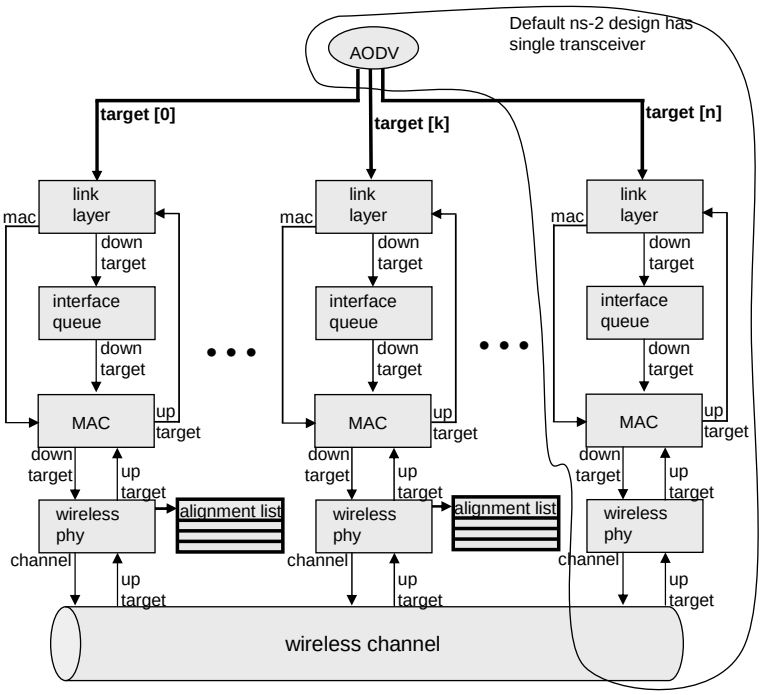

Figure 5.1: FSO node structure with a separate stack for each optical transceiver.

best of its knowledge. Since the routing agent operates at a much coarser time scale than realignment periods, it is possible that the alignment to the next hop node no longer exists when the packet is handed from the routing agent to the queue of the interface. Upon reception of a packet, the queue checks the alignment list of the interface to see if the next hop of the packet is still aligned. If the next hop is aligned, the packet gets queued at that outgoing interface. If the next hop is not aligned, the packet will be handed to a dispatching function to see if any of the interfaces of the node are aligned with the next hop. If an appropriate interface is found, the packet will be delivered to the correct link layer object. If no interface is found, the packet will be buffered in the node-wide buffer. If the node-wide buffer is already at its full capacity, then the packet will be dropped.

In the event of realignment, we go through all the queues in the node and try

to place the packets to the correct outgoing queue. If the packet's next hop is not aligned through any transceiver, the packet is put to node-wide buffer. Additionally, we also consider each packet in the buffer and try to deliver it to the appropriate link layer object if one of the interfaces become aligned with the next hop of a packet in the buffer.

5.2 Per-Flow Buffering

In the per-flow buffering mechanism, we keep a buffer for each next hop node as explained in Algorithm 5.2. After the routing agent hands the packet to the link layer, the queue forwards the packet to a per-flow buffer according to the next hop address field of the packet. It does not check if this interface is aligned with the next hop of the packet or not. The interface then explicitly checks if the MAC is idle. If the MAC state is idle, the interface retrieves a packet to its queue from one of the buffers whose next hop is aligned with this interface and that packet is handed to the MAC.

Additionally, whenever the MAC becomes idle again, it notifies the interface about its idle state and that again causes the interface to retrieve a packet to its queue from one of the per-flow buffers whose next hop nodes are known to be aligned with this interface. We time-stamp the packet retrieval times from each per-flow buffer. When MAC requests a packet, we have a number of per-flow buffers to retrieve a packet from, considering that the interface is aligned with multiple nodes. Among those candidate per-flow buffers, we select the one that has the oldest packet retrieval time. By doing so, we ensure that all of the flows experience a more fair scheduling. Note that we dedicate buffers according to the next hop address of the packets, not

Quantity	Abbreviation
Number of Buffers	n
Number of Interfaces	k
Max Node-Wide Buffer Size	t
Queue Size	q
Max Per-Flow Buffer Size	p

Table 5.1: Abbreviations for quantities of buffering components.

Action	Node-Wide Buffer	Per-Flow Buffer
Enqueue	k (redirection)	n (packet checkout)
Buffer	Constant	n (find target buffer)
Queue Resume	Constant	n
Realignment	k*q + t (deliver the queues and buffer)	Not Applicable
Fathom Timer	Not Applicable	n*p

Table 5.2: Complexity of each major step in buffering.

the destination addresses. Also, we acknowledge that the original behavior of the FIFO queue is no longer preserved since packets belonging to the same flow will be queued based on their arrival but packets from different flows will be multiplexed while being sent out.

Table 5.2 provides the complexity of each step involved in the transmission process of a packet. With the help of Table 5.1, we see that per-flow buffering scheme's computational complexity can easily hinder its responsiveness and agility when it has a large number of next-hop neighbors, and thus per-flow buffers. A typical example of this is when the nodes are moving with a low mobility and hence, have a larger number of per-flow buffers.

Finally, we implemented a timer mechanism to discard the packets in stale buffers. Such a timer makes room for the new flows by periodically discarding all the packets in a buffer if it has not been accessed during the last timer period. Since the

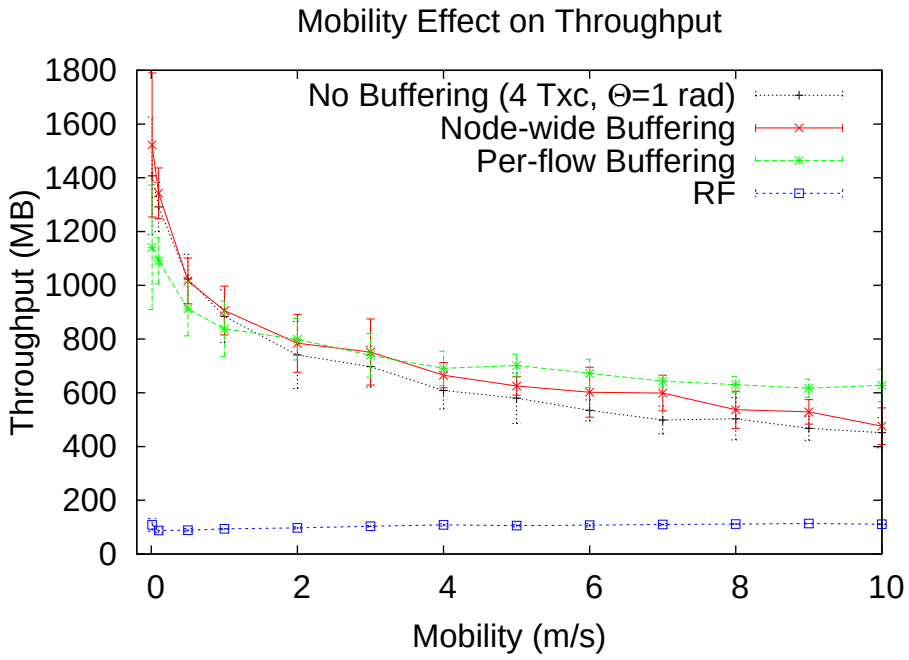

Figure 5.2: Mobility results for 4 transceiver node design.

timer period is as long as multiple re-alignment intervals, discarding stale buffers is safe because the next hop is declared unreachable after multiple re-alignment trials.

5.3 Buffering Performance Results

After implementing all the necessary buffering extensions for both schemes, we re-ran major simulation scenarios that we have discussed in Chapter 4. To lay out the simulation setup: we had 49 nodes with 8 transceivers. Each transceiver had a divergence angle of 0.5 rad. The default mobility of the nodes is 1 m/s and transmission range and the node separation is 30 m. Nodes move according to a random way point algorithm in an area of 210 m by 210 m. In each simulation set, we modify a default parameter and observe its effect on overall network throughput. We repeat

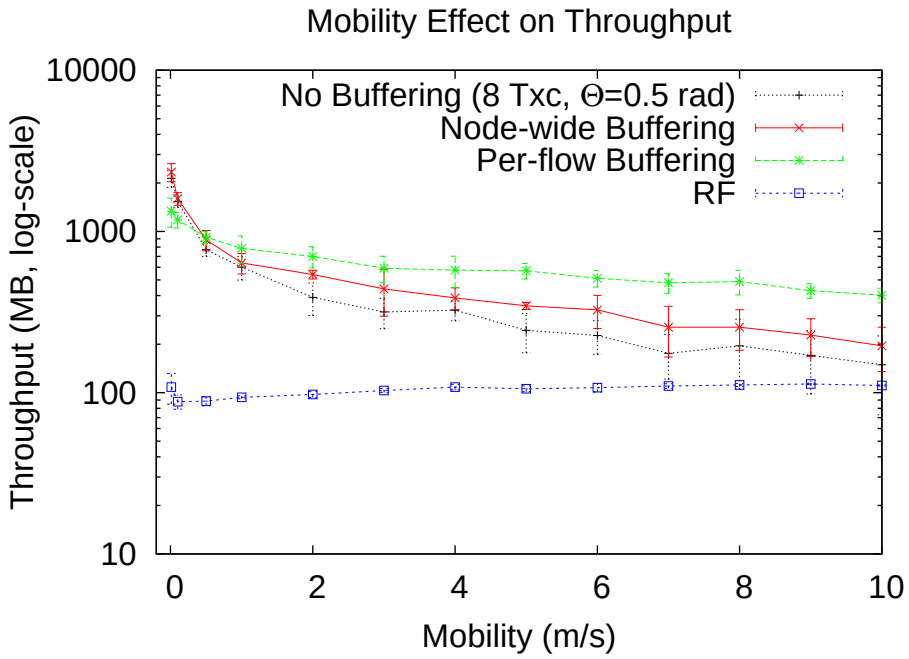

Figure 5.3: Mobility results for 8 transceiver node design.

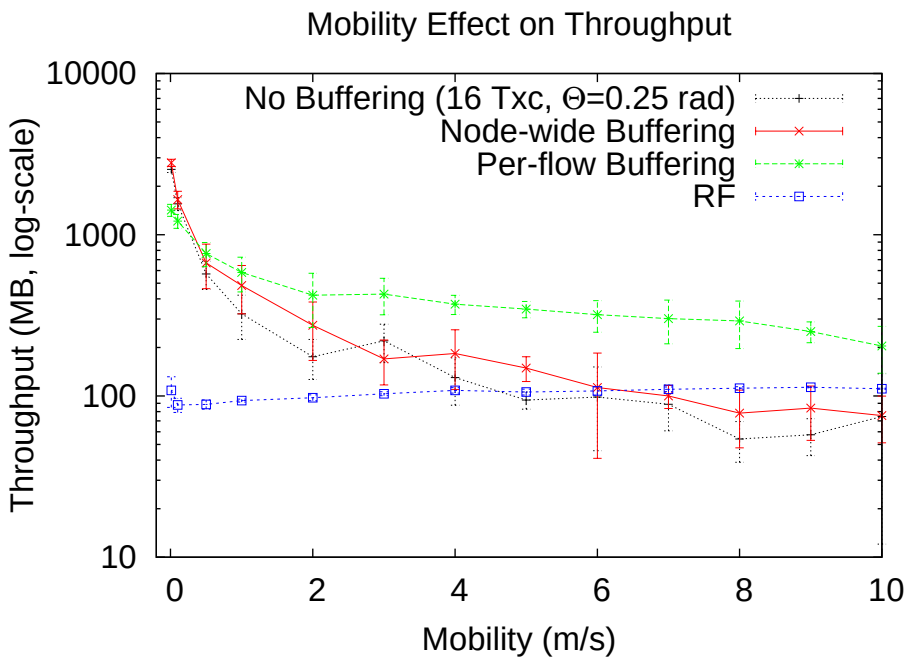

Figure 5.4: Mobility results for 16 transceiver node design.

each simulation 5 times and plot with 95% confidence intervals.

The most important of the simulations is the mobility simulations which have a critical role in judging the effectiveness of our approach since our aim is to enable high mobility in FSO-MANETs via these buffering schemes. We have considered three node designs for mobility scenarios. In Figures 5.2, 5.3, and 5.4, we show the results in a network that consists of FSO nodes with 4, 8, and 16 interfaces, respectively. We gradually increase the average speed of each node in the network and plot the overall network throughput. We observed that the per-flow buffering performs poorly compared to non-buffered case and node-wide buffering at low speeds due to the overhead caused by per-flow buffering and its implications on other layers. Moreover, at high speeds and at nodes with larger number of transceivers, per-flow buffering scheme out-performs node-wide buffering due to its much more fine-grained scheduling of the packets and larger buffer space.

Figure 5.4 clearly shows that the per-flow buffering mechanism is superior to both the node-wide and non-buffered cases. Both node-wide buffering and default no buffering approaches deteriorate under the RF throughput line at high speeds while per-flow mechanism steadily provides better results. We conclude that even though our graphs suggest using the node-wide buffering approach for low mobility, per-flow buffering provides the best possible results for high-speed settings and node designs with large number of transceivers.

The second important set of simulations is node density scenarios. We have previously concluded that per-node RF throughput reaches its limit as we add more nodes to the network. We have also shown that FSO performs much better due its spatial reuse in Chapter 4. In Figures 5.5 and 5.6, we provide the results for the overall network throughput and per-node throughput for a network of FSO nodes with

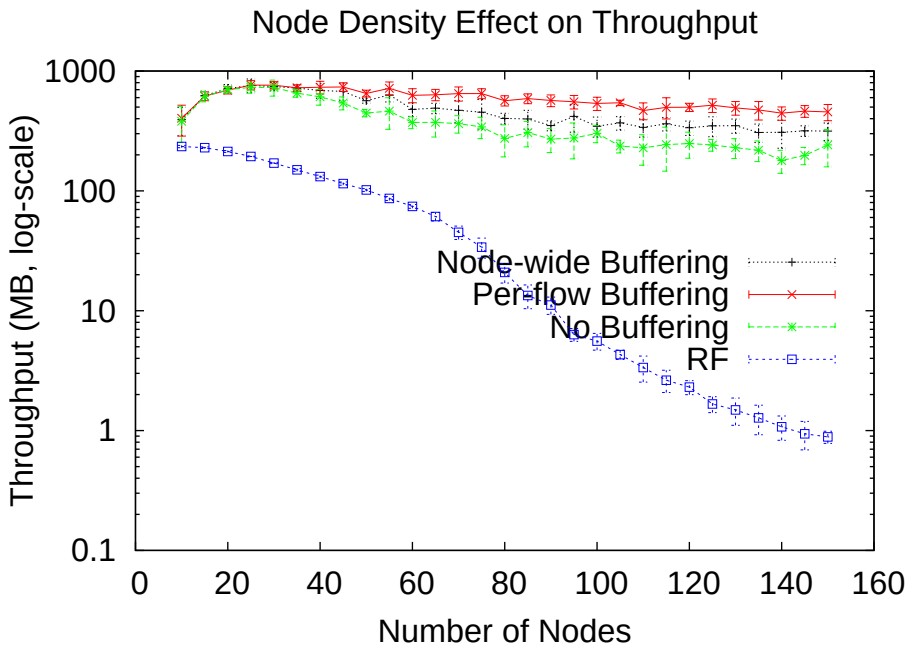

Figure 5.5: Node density results in which the number of nodes are increased (4 transceivers).

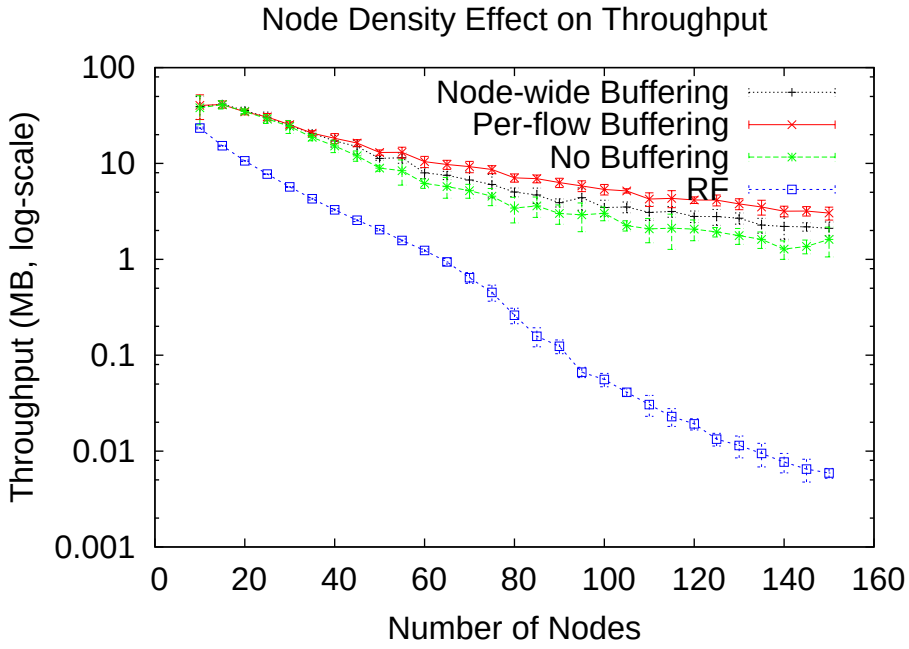

Figure 5.6: Node density results showing per-node throughput (4 transceivers).

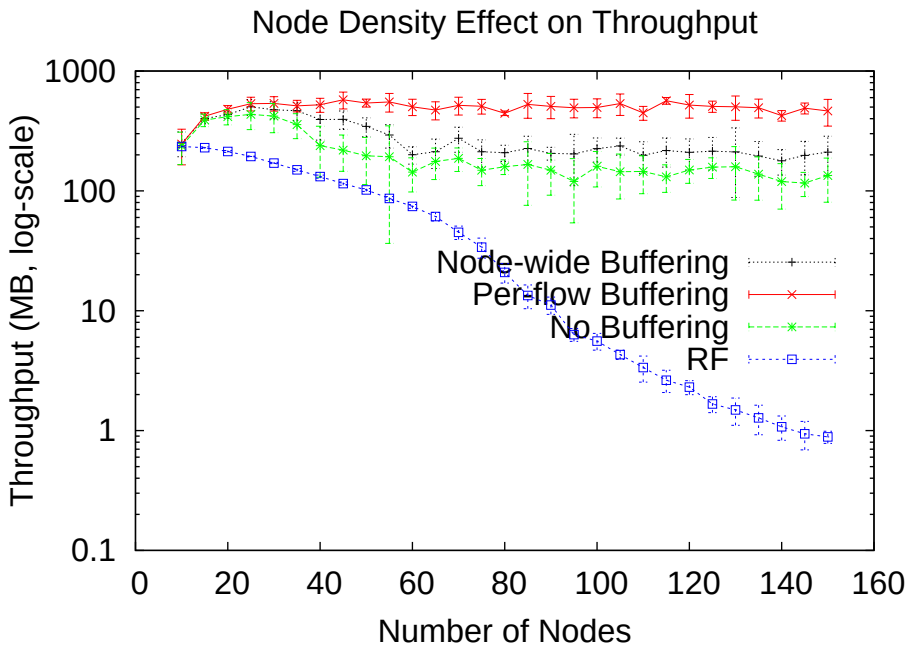

Figure 5.7: Node density results in which the number of nodes are increased (8 transceivers)

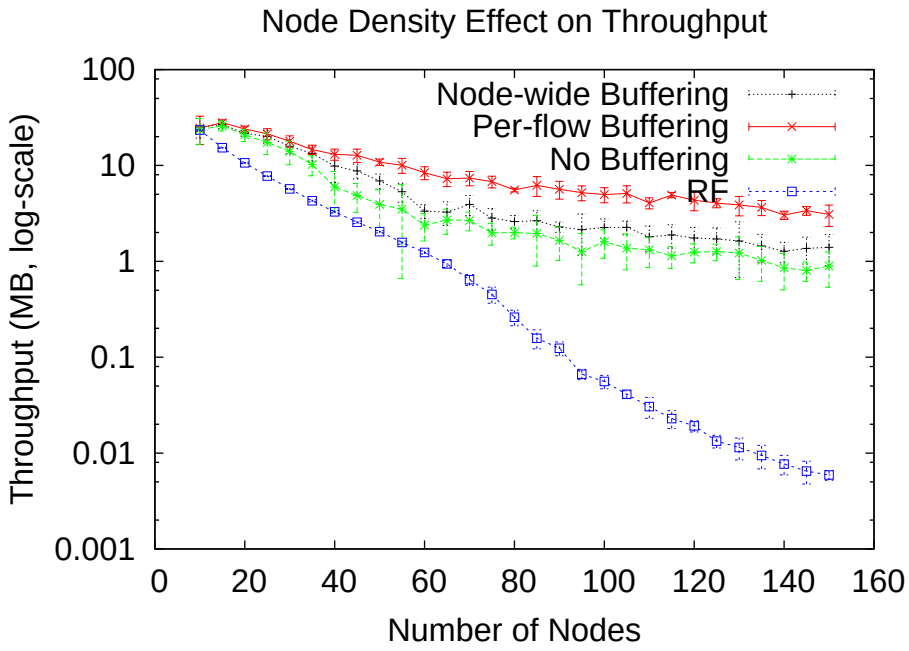

Figure 5.8: Node density results showing per-node throughput (8 transceivers).

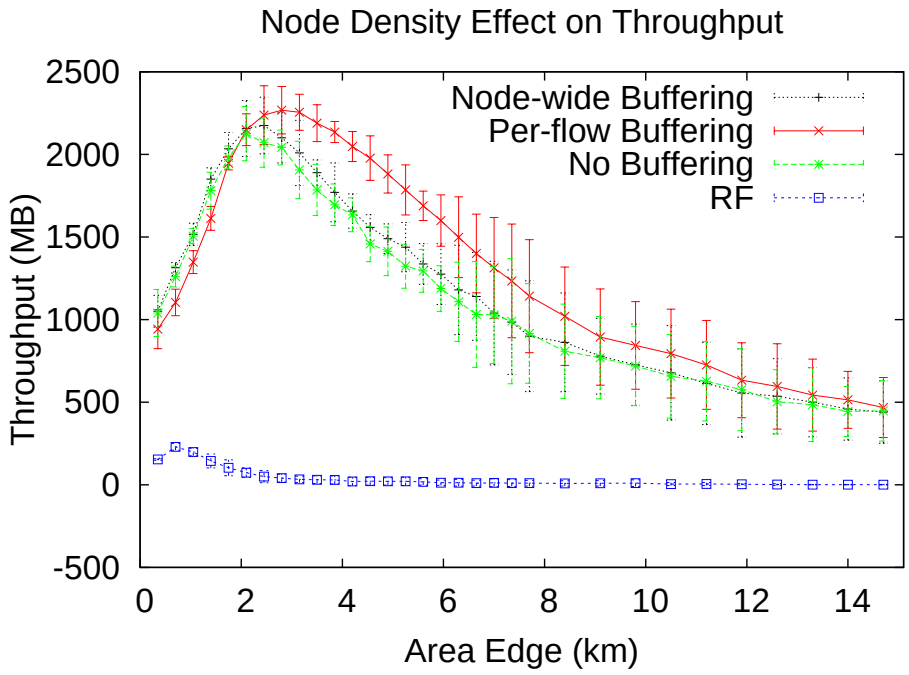

Figure 5.9: Node density results for fixed power and enlarged area configuration.

4 transceivers. We also show the 8 transceiver case in Figures 5.7 and 5.8. In all of these 4 graphs, we see a constant increase in overall network throughput when either of the two buffering mechanisms is used. Additionally, per-flow buffering provides better throughput results compared to node-wide buffering and this fact is depicted more clearly when we increase the number of transceivers. In Figure 5.9, we depict the results of a scenario where the transmission power of the transceivers are kept the same and the area is made larger. We observe that, at first the area was very small for the network, and as we make the are larger, the overall throughput increases. After the peak point, the throughput starts to drop due to insufficient power and reduced coverage. Here, we observe in Figures 5.5, 5.6, 5.9, 5.7, and 5.8 that with buffering, the difference between RF and FSO per-node end to end throughput enlarges.

Additionally, we show that the visibility case shows a steady increase in through-

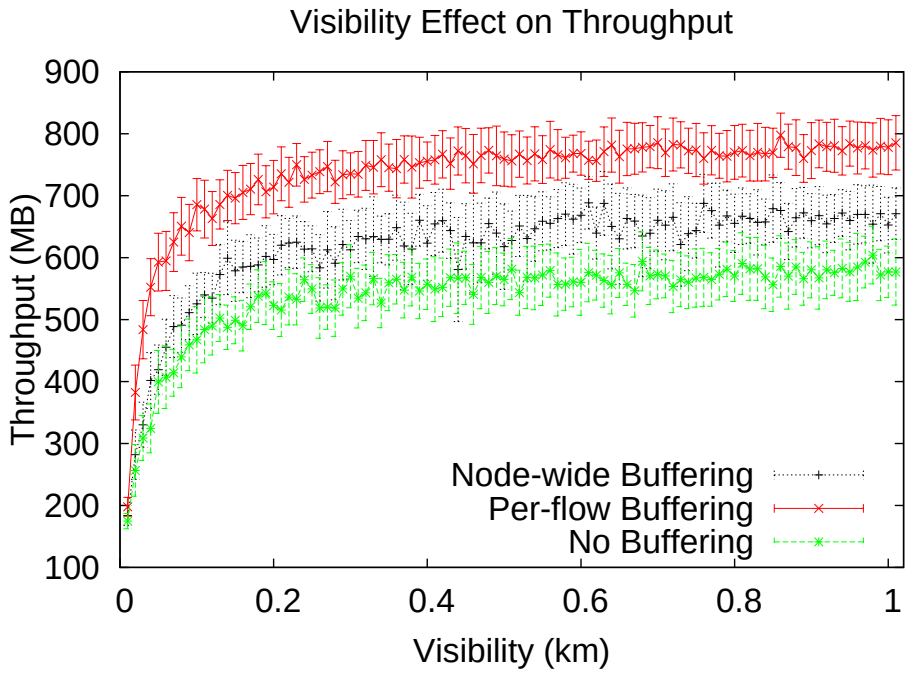

Figure 5.10: Visibility simulations.

put from buffering as well (Figure 5.10). We observe that this particular speed of 1 meter per second differentiates the two buffering schemes nicely and shows that per-flow outperforms the node-wide scheme once more.

5.4 Summary

In this chapter, we have provided insight into the two buffering schemes to remedy the problem of reduced throughput in multi-transceiver free-space-optical mobile ad-hoc networks due to high intermittence of the optical wireless link. We discussed their design in detail and identified their differences. We have provided their throughput results for increasing mobility and number of transceivers. We conclude that the per-flow buffering provides better network-wide throughput than the node-wide buffering

mechanism. We leave scheduling fairness issues as future work, expecting interesting designs to emerge for node designs with an extremely large number of transceivers with highly focused beams.

Algorithm 5.1 Node-wide Buffering

```
1: DEFINE LINK LAYER ROUTINE:
2: UPON Reception Of Packets At Link Layer:
3: if This interface is aligned with the next hop of the packet then
4:     Enqueue the packet in the interface queue
5: else
6:     DISPATCH the packet
7: end if

8: DEFINE REALIGNMENT HANDLER ROUTINE:
9: UPON The Event Of Realignment:
10: for all Interfaces of the node do
11:     for all Packets in the interface queue do
12:         if The interface is not aligned with the next hop of the packet then
13:             DISPATCH the packet
14:         end if
15:     end for
16: end for
17: for all Packets in the node-wide buffer do
18:     for all Interfaces of the node do
19:         if The interface became aligned with the next hop of the packet then
20:             Deliver the packet to the corresponding link layer
21:         end if
22:     end for
23: end for

24: DEFINE DISPATCH ROUTINE:
25: for all Interfaces of the node do
26:     if The interface is aligned with the next hop of the packet then
27:         Deliver the packet to the corresponding link layer
28:         EXIT ROUTINE
29:     end if
30: end for
31: BUFFER the packet

32: DEFINE BUFFER ROUTINE:
33: if Node-wide buffer is full then
34:     Drop the packet
35: else
36:     Put packet at the end of the buffer
37: end if
```

Algorithm 5.2 Per-flow Buffering

```
1: DEFINE LINK LAYER ROUTINE:
2: UPON Reception Of Packets At Link Layer:
3: BUFFER the packet according to its next hop address
4: if MAC is idle then
5:     FETCH a packet for this interface and deliver it to MAC
6: end if

7: DEFINE FETCH ROUTINE:
8: for all Per-flow buffers in the node do
9:     if Buffer's next hop node is aligned with this interface then
10:        Place the buffer at the end of the node's list of per-flow buffers
11:        RETURN a packet from the buffer
12:    end if
13: end for

14: DEFINE IDLE MAC HANDLER ROUTINE:
15: UPON MAC becoming idle:
16: FETCH a packet for this interface and deliver it to MAC

17: DEFINE BUFFER ROUTINE:
18: if Buffer space is full then
19:    Drop the packet
20: else
21:    for all Per-flow buffers in the node do
22:        if Buffer's next hop and packet's next hop are the same then
23:            Place the packet into the buffer
24:            EXIT ROUTINE
25:        end if
26:    end for
27:    Create a new buffer
28:    Place the packet into the buffer
29: end if
```

Chapter 6

Localization for FSO-MANETs

In this chapter, we explore the possibility of using directionality of free-space-optical communications for solving the 3-D localization problem in ad-hoc networking environments. Range-based localization methods have limitations due to two main reasons. They require at least three other localized neighbors which in turn requires the node density to be significantly higher than the node density to assure connectedness. Alternatively, they require a high-accuracy power-intensive ranging device such as a sonar or laser range finder whose form factor and power capabilities exceed those of a typical ad-hoc node. Our approach exploits the readily available directionality information provided by a physical layer using *optical wireless* and uses a limited number of GPS-enabled nodes, requiring a very low node density (2-connectedness, independent of the dimension of space) and no ranging technique. We investigate the extent and accuracy of localization with respect to (i) varying node designs such as nodes with a higher number of transceivers with better directionality and (ii) density of GPS-enabled and ordinary nodes as well as messaging overhead per re-localization. We conclude that although denser deployments are desirable for higher accuracy, our

method still works well with sparse networks with little message overhead and as few as two anchor nodes.

Providing contextual location information for the application-level data is a vital enhancement for ad-hoc networks. Localization capabilities are also important for network-level functionalities such as routing. Geographical routing protocols such as GPSR [53] are known to reduce the forwarding table sizes substantially, but need to know the location of nodes for successful ID-to-location mapping. Despite the strong need for localization, the task of localizing an ad-hoc node given its power capabilities, mobility, and other network parameters (e.g., node density, anchor density) is not trivial. The traditional approach of sensing the signal strength from 3 neighbors and triangulating using the derived distances requires at least 3 localized neighbors and is not accurate due to the multi-path loss in RF propagation. The issue becomes even more severe if the problem is considered in 3-D space where it takes 4 nodes to triangulate and even more samples preferably from different neighbors for calibration and better accuracy [26]. Sonar and laser range finder devices are not suitable for the power capabilities and form factors of ad-hoc nodes and explicit bearing devices are space consuming. Alternatively, we propose to use the *directionality that is inherent in FSO communication* which does not impose any additional hardware requirements. In our approach, a node can calculate its location given that it has 2 neighbors that know their own location, and advertise their location and interface normals in the packets that they transmit. Our method is lightweight in comparison to range-based methods since it *only requires 2 localized neighbors* and it *does not involve a complex tuning phase*.

We considered FSO as a complementary communication mechanism to aid in increasing the overall network throughput in [21]. Previous studies revealed that

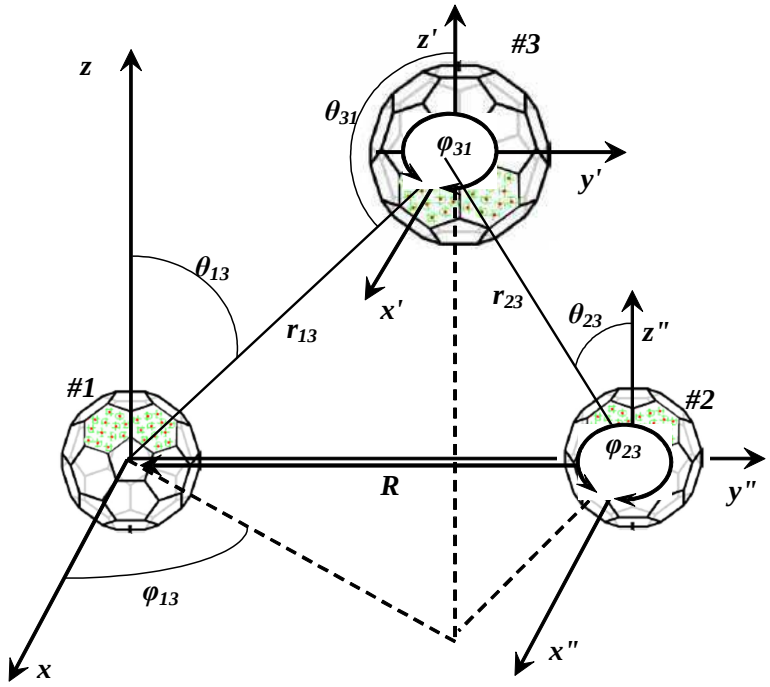

Figure 6.1: A third node triangulating using the advertised normals received from two other localized or GPS-enabled nodes.

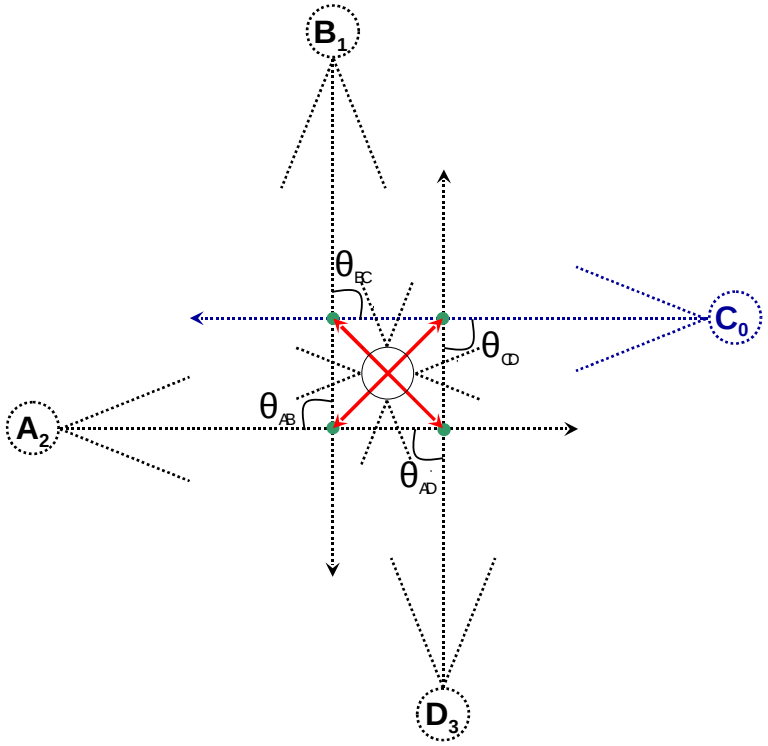

Figure 6.2: A simplified triangulation in 2D using two GPS-enabled nodes and error in default LOS model.

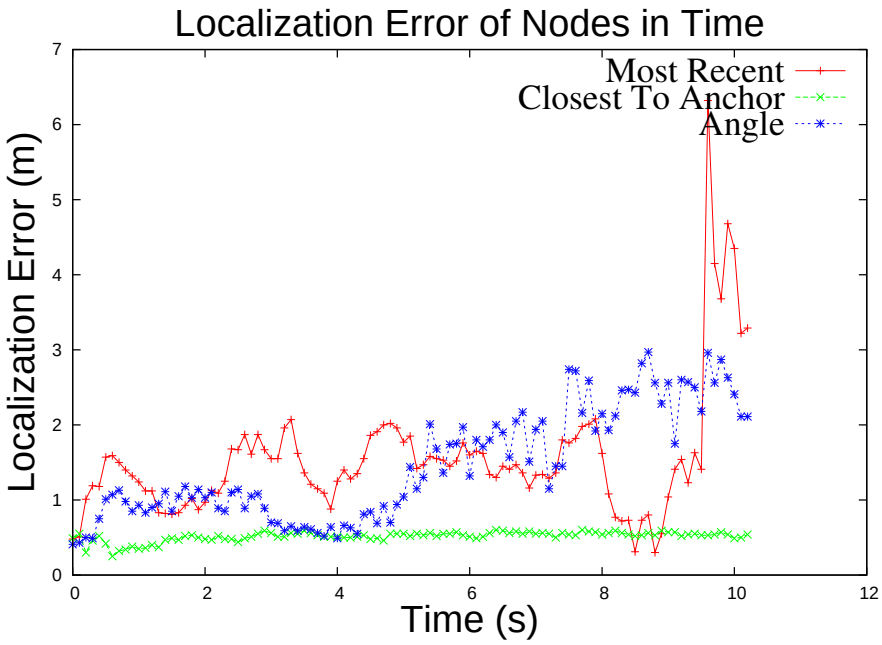

Figure 6.3: Localization errors are being amplified during the simulation when two latest received information sets are used for triangulation.

FSO-only mobile ad hoc networks are viable and line-of-sight issues can be remedied significantly using *auto-alignment* circuitry and protocol [10, 64, 65, 99]. Even though FSO communication technologies provide a substantial amount of potential since it is quite efficient to run triangulation algorithms using *direction of reception* (i.e., angle of arrival) they have not been used to solve the ad-hoc localization problem. We use directionality of FSO beams to identify the angle of arrival (Figure 6.1). By using *advertised normals* in packet headers, we can then calculate the relative angular orientation of neighbors with respect to each other. Since a node can receive packets containing advertised normal information from more than 2 neighbors, we need to choose which information sets to use while triangulating. We suggest and compare three different heuristics to make this selection.

The key characteristics of our FSO-based solution are:

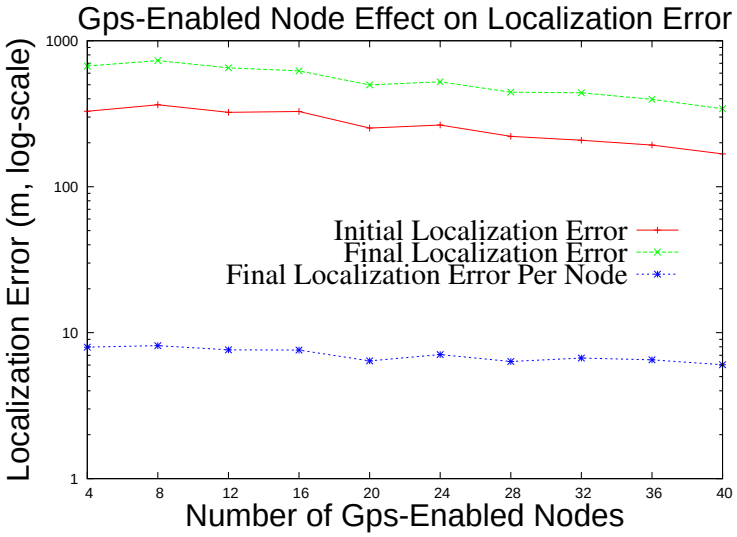

Figure 6.4: GPS-enabled node effect on localization error.

- capability of localization in 3-D,
- much less power consumption in comparison to techniques requiring RF hardware,
- only two localized neighbors are needed, which reduces the node density requirements, and
- fast heuristics to select a subset of neighbors to use for localization.

A key characteristic of our solution is to use *optical-only techniques* to achieve localization. Our method requires much less power availability than RF-based methods and is particularly useful for ad hoc networking settings where line-of-sight exists among low-power nodes. Our scheme provides high localization extent with as little as only 2 localized or GPS-enabled nodes with acceptable accuracy through the use of narrow transceivers when the 2-connectedness requirement is satisfied.

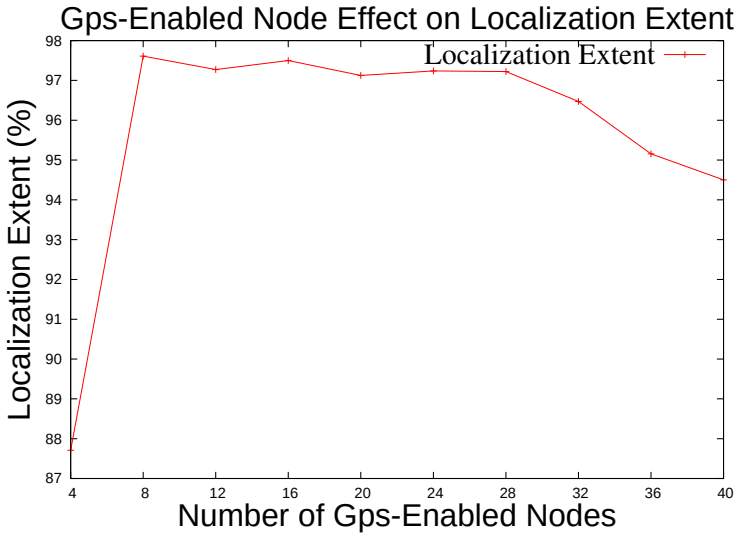

Figure 6.5: GPS-enabled node effect on localization extent.

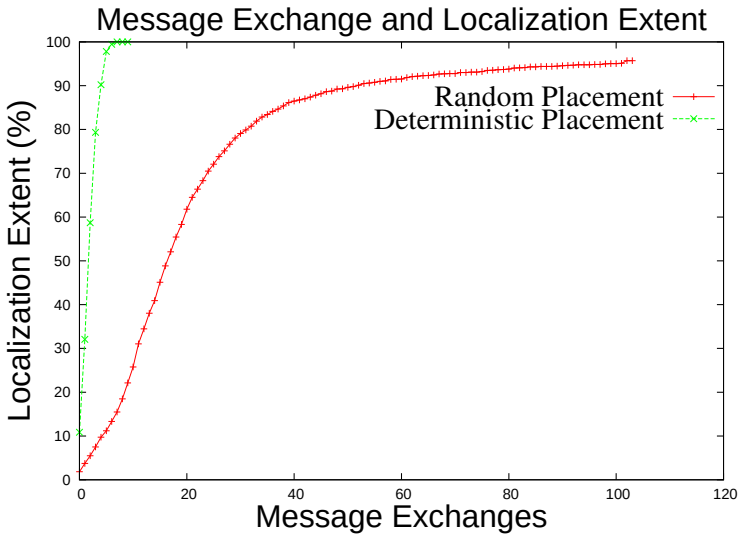

Figure 6.6: Localization extent with respect to message exchange for 200 nodes.

Algorithm 6.1 Relative Localization

```
1: UPON Reception Of Packets With Localization Header:
2: if This Node Has At Least 2 Neighbors' Advertised Normals AND It Is Not A
   GPS-Enabled Node then
3:     if Using Most Recent Sets To Triangulate then
4:         FIND 2 Latest Received Localization Packets
5:     end if
6:     if Using Angular Priority then
7:         FIND 2 Localization Packets That Make An Angle Closest To 90°
8:     end if
9:     if Using Localization Rank then
10:        FIND 2 Localization Packets With Minimum Ranks
11:    end if
12:    CALCULATE Closest-Point-Of-Approach Of The 2 Rays
13:    UPDATE This Node's Location
14:    UPDATE This Node's Localization Rank
15:    UPDATE This Node's State Flag As "Triangulated"
16:    START Stamping Outgoing Packets
17: end if
```

6.1 System Model

The 2 types of nodes are: anchor nodes with GPS devices and ordinary nodes that do not know their locations initially. The *localization rank* of a node is the hop distance of that node from the nearest anchor node. Network nodes with a GPS device send control packets including their location and direction information so that the immediate neighbors without a GPS device can use the transferred information to find their own locations. These control packets convey the *advertised normals*, which include sender node's ID, if sender has a GPS device, if sender has previously triangulated, hop distance of sender from the nearest anchor node (localization rank), if the sender node has previously triangulated, and transmit antenna's global location and its direction (normal). The receiver of such a packet stores this information in a table (mapping from node ID to localization information) with the arrival time of

the packet as presented in Algorithm 6.1.

One can derive simple algebraic equations based on Figure 6.1:

$$r_{31} = \frac{R}{\sin\theta_{31}(\tan\varphi_{31} + \tan\varphi_{32})}\sqrt{1+\tan^2\varphi_{31}} \tag{6.1}$$

$$r_{32} = \frac{R}{\sin\theta_{32}(\tan\varphi_{31} + \tan\varphi_{32})}\sqrt{1+\tan^2\varphi_{32}} \tag{6.2}$$

$$X_3 = X_1 + r_{13}\sin\theta_{13}\cos\varphi_{13}$$

$$Y_3 = Y_1 + r_{13}\sin\theta_{13}\sin\varphi_{13}$$

$$Z_3 = Z_1 + r_{13}\cos\theta_{13} \tag{6.3}$$

that give the location of a third node. The distance between two GPS-enabled nodes is R (Nodes 1 and 2). From this distance and θ and φ angles that are derived from the transmitter normal advertisements in packet headers, we can calculate r_{31} and r_{32} (Equations 6.1 and 6.2). Lastly, we need to conduct simple vector additions to find the coordinates of Node 1.

As depicted in Figure 6, node C has rank 0 indicated as a subscript. When a node without a GPS device triangulates, its rank is the maximum of the ranks of sender nodes plus 1. Hence if a node is next to 2 GPS-enabled nodes of rank 0 and it triangulates using the information that it received from these two nodes, it will have rank 1. Such a ranking mechanism helps us prioritize the available information while triangulating. Intuitively, if we consider a network with uniform geographical distribution of nodes and anchor nodes placed at the center, nodes that are in the skirt of the network will have the highest ranks. Moreover, nodes with higher ranks are subject to larger localization errors.

A node is "ill-connected" when the number of directly reachable neighbors is less than 2. Hence, we require a node to be in transmission proximity of at least 2 direct neighbors even though it may not be able to transmit and receive from those neighbors because of line-of-sight issues. Thus, upon starting to place ordinary nodes without GPS devices, we place the anchor nodes at arbitrary locations. For example, if the number of GPS-enabled nodes on the X axis is 2 and on the Y axis is 3, we divide the X edge of the determined area into 3 and the Y edge into 4 equal lengths and place one anchor node at the end of each X-Y edge with another corresponding anchor node placed on the same point with a given Z value. Hence a pair of GPS-enabled nodes are placed on top of each other with some distance in Z axis. We acknowledge that such a requirement on the placement of anchor nodes can limit the applicability of our approach. However, one can come up with placement methodologies that relax such strict placement requirements and ensure that a subset of surrounding non-anchor nodes have 2 connections to separate GPS-enabled nodes.

While placing non-anchor nodes, we consider a candidate location drawn from 3 uniform randoms for X, Y, and Z coordinates. We check if there are at least 2 nodes within the communication range of the candidate location. If so, we accept the candidate location and move to the next node. If we assume that there is only one pair of GPS-enabled nodes in the network, the rest of the nodes form a sphere-like cluster in 3-D space. Moreover, when we increase the number of GPS-enabled node pairs to 2, we introduce the possibility of creating two disconnected clusters and enable the nodes to be placed in a larger volume, which in turn may decrease the localization extent in the network because of the line-of-sight issues involved. The only strict requirement while placing anchor nodes is that they are *placed as pairs* on top of each other, which ensures that a third node that is able to see both nodes can

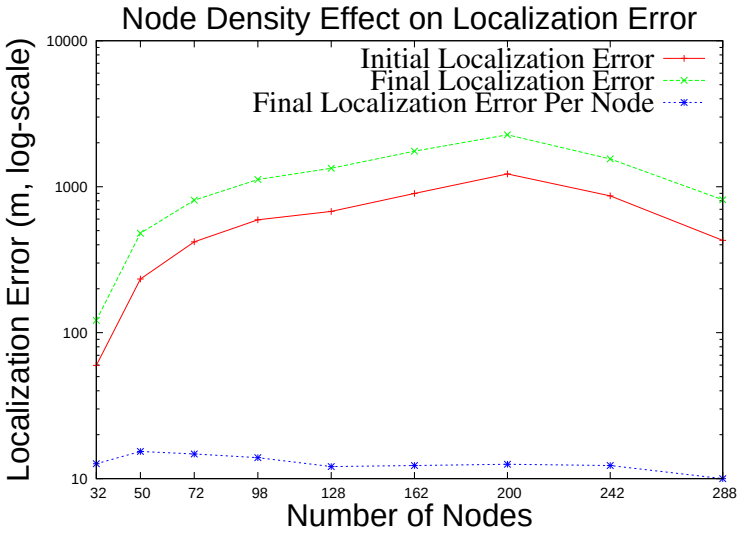

Figure 6.7: Node density effect on localization error.

localize itself.

6.2 Heuristics

In our study, we found that it is possible to employ a number of *simple heuristics* while deciding which two information sets to use for triangulation from a given number of information sets. Possible number of different ways to localize is $\binom{n}{2}$ where n is the number of information sets available to a given node.

6.2.1 Stale Info Gets Forgotten

Possibly the simplest heuristic is to use the information that became available the latest. Assuming a node can use 4 different localization information sets as depicted in Figure 6, the triangulating node will select the latest two arrivals. Observe that the localization error is amplified throughout the network with this heuristic. Since each

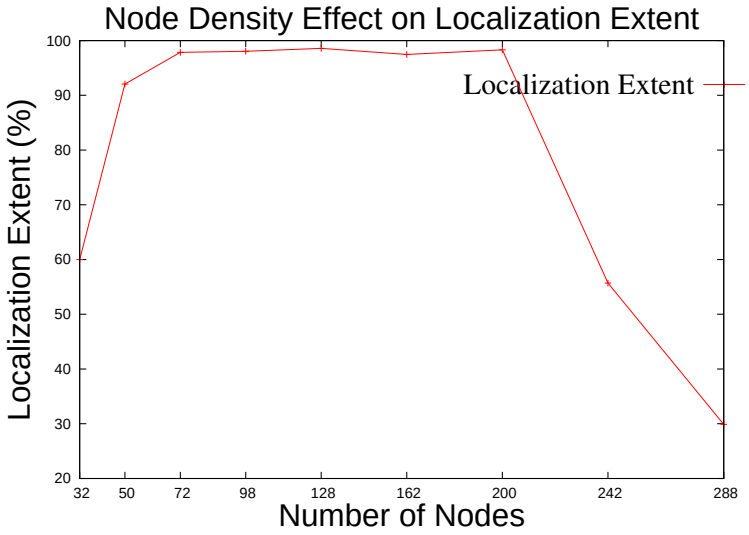

Figure 6.8: Node density effect on localization extent.

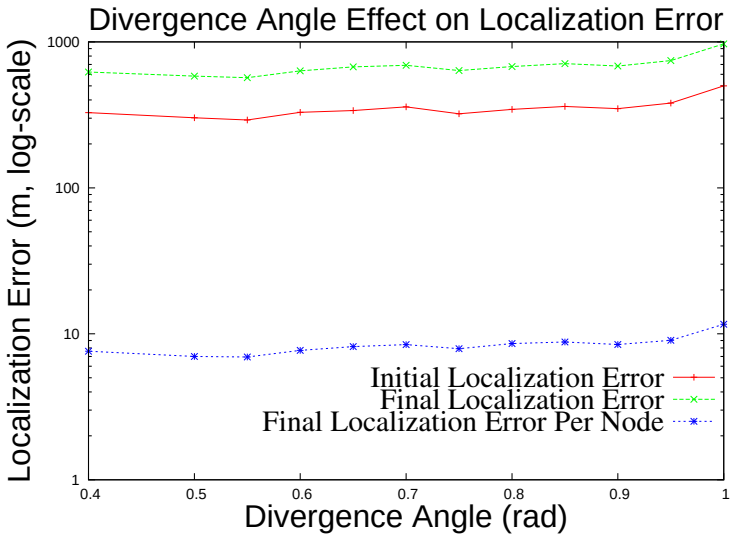

Figure 6.9: Divergence angle effect.

node re-triangulates as it receives a packet using the most up-to-date information, a node will consider the latest information no matter how far the sender node is to the closest anchor. Hence, even though more accurate information is available, the choice results in increased localization errors as can be seen in Figure 6. We found that the best triangulation result is obtained at the first attempt since the received localization information sets have been propagating from anchor nodes towards the nodes with higher ranks at the skirts of the network.

6.2.2 The Lower Rank Preference

In this heuristic, we first assign a "localization rank" of 0 to a GPS-enabled node. When a node triangulates using localization information obtained from two neighbors, it attains the localization rank of maximum of the two neighbors plus 1. If we assume that the network has only one pair of GPS-enabled nodes and the distribution of the nodes forms a sphere-like shape in 3-D, the nodes that are closer to the core where the two anchor nodes reside will have lower localization ranks and the outer skirts of the network will have larger localization ranks. This indicates that they are more distant from the core in number of hops. Hence, when a node is about to decide the pair of neighbors for triangulation, it may choose them such that the summation of the two ranks is minimized. This heuristic ensures that neighbors that are closest to anchor nodes are selected for triangulation. Figure 6 shows the nodes' ranks as subscripts. Assuming the node in the middle is triangulating, it will select the information sets that came from C_0 and B_1 since they have the lowest ranks.

6.2.3 Angular Prioritization

One of the hard cases to triangulate using only directionality information is node collinearity, that is when the triangulating node lies on the straight line that passes through the both two anchor nodes. Results become more accurate when the two nodes are chosen to attain a 90° angle between each other. Throughout our experiments we found that one major factor that increased localization error was ill-formed (flat) triangles that were the result of unwisely chosen candidate information sets. A natural way to remedy the problem is to impose a lower bound of $0.005 * \pi$ on the angle between the two nodes and favor those sets making an angle close to 90° for orthogonality. Figure 6 shows the angles made by all 4 nodes: θ_{BC}, θ_{AB}, θ_{AD} and θ_{AD}. Assuming θ_{BC} is closest to 90°, the triangulating node will choose information sets sent by node B and node C for triangulation.

6.3 Performance Evaluation

We looked at a number of metrics while justifying the performance of our approach. The first metric is initial localization error. Initial localization error indicates the *aggregate absolute difference* between calculated location and the actual location of all nodes in the network. This metric is calculated for a node when it localizes itself for the first time. Nodes in the network continue to re-localize themselves as they receive more packets. We stop the simulation when all the nodes are localized or when the simulation time reaches 10 seconds, whichever happens first. Since the simulated network is stationary, 10 seconds is enough as an upper bound for simulation duration. We calculate the final localization error using the last calculated location of each triangulated node before the simulation ends. Another metric that needs to be

considered is the final localization error averaged by the number of all the localized nodes.

6.3.1 Comparison of Heuristics

We ran simulations of 100 nodes with 14 interfaces on each for 10 iterations using each heuristic. Each interface had a divergence angle of 600 mrad (-34°). There were 4 pairs of GPS-enabled nodes and all nodes were placed on the 3-D volume randomly. We found that selecting the latest information set gives the worst results since the error is neither predictable nor close to the desired level. Angular prioritization also gives large localization errors but is still better than selecting the latest information sets and is relatively stable. Among the 3 heuristics, the one based on localization ranking resulted in the lowest localization error per-node as depicted in Figure 6. Hence, throughout the rest of the simulation sets, we used this ranking based heuristic to determine which 2 sets to use for triangulation.

6.3.2 Node Density

Our second simulation set is designed to determine the effect of node density in the network on localization extent. For this experiment we increased the number of nodes from 32 to 288. There are 26 interfaces with 400 mrad of divergence angle on each node. There are 16 anchor nodes in the network and all of the ordinary nodes are placed randomly on a 3-D terrain. We ran the simulation setup for 5 iterations and averaged the results. As depicted in Figure 6.1, we found that as we increase the node density the localization extent first increases, but later drops as more neighbors start falling into their blind regions and start becoming obstacles to each other. A

similar trend is observed in localization error as seen in Figure 6.1. However, the final per-node localization error improves steadily with more neighbors.

6.3.3 Anchor Density

In Figure 6 and Figure 6, one can see that in a simulation of 100 nodes, when the number of GPS-enabled nodes is increased from 4 to 40 both *aggregate* and *per-node* localization errors decrease. An important observation is that the localization extent makes a significant jump from 2 pairs to 4 pairs. However, increases beyond that point reduce the localization extent. We conclude that the scattering effect of the random node placement algorithm increases the volume over which nodes are distributed, which in turn makes the LOS a more significant problem.

6.3.4 Divergence Angle

Figure 6.1 shows the how divergence angle affects the overall and per-node localization error. As we increase the divergence angle, the accuracy of the default-normal estimates drops and the localization error is consequently increased. We conclude that designing multi-element optical antennas with more transceivers not only increases throughput [21], but also increases the accuracy of localization.

6.3.5 Message Overhead and Localization Extent

A key practical metric is how long it takes the whole network to localize. In this set of simulations, we investigated the localization extent after each message exchange. We used 200 nodes each with 26 transceivers using 400 mrad divergence angle. There were 8 GPS-enabled nodes and we ran the simulations for 10 iterations. We ran two

separate simulation setups for this scenario. In the first setup we placed the nodes on a 10x10x2 perfect grid and in the second setup, we placed all the nodes randomly. As depicted in Figure 6, we saw that node placement on the terrain is a significant factor in extent of localization and message exchange overhead. The setup with deterministic placement reaches over 90% localization extent in 10 message exchanges. However, the setup with randomly placed nodes reaches 90% after 90 message exchanges and 80% after 33 message exchanges.

6.4 Summary

In this chapter, we proposed a novel approach to the problem of node localization in stationary ad-hoc networking context via multi-element free-space-optical antennas as we have published in [66]. We used readily available directionality information to perform a simple triangulation. Our approach has low processing needs and does not need a complex tuning phase, or extra hardware. We conclude that optical wireless is attractive both because of its high throughput and because of its easy to exploit directionality benefits that help solving the localization problem.

Chapter 7

Prototype Implementation and Experiments

In this chapter[1], we present a prototype implementation of multi-transceiver electronically-steered communication structures. Our prototype uses a simple LOS detection and establishment protocol and assigns logical data streams to appropriate physical links. We show that by using multiple directional transceivers we can maintain optical wireless links with minimal disruptions that are caused by relative mobility of communicating nodes.

Figure 7 shows the general concept of a spherical surface being covered with FSO transceivers. Our design of optical antenna is based on two principles; (i) *spatial reuse and angular diversity* via directional transceivers tessellated on the surface of the spherical node and (ii) an *alignment protocol* that establishes alignment of two transceivers in line-of-sight of each other. Unlike the traditional mechanical steering mechanisms to manage LOS alignment, our alignment protocol can be implemented

[1]This chapter was prepared in collaboration with Mr. Abdullah Sevincer.

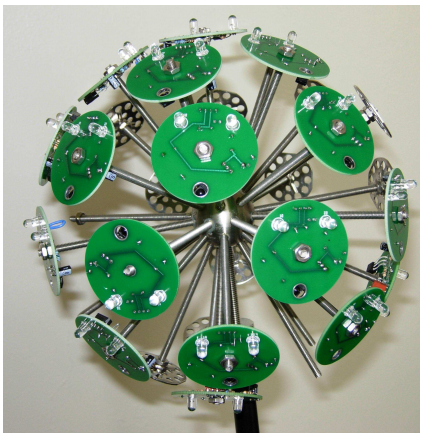

Figure 7.1: Picture of prototype optical antenna.

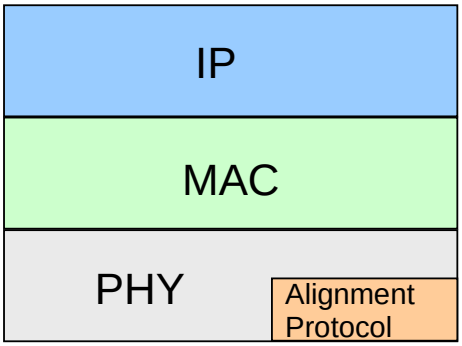

Figure 7.2: Default placement of alignment protocol in protocol stack.

by simple electronics, which we call "electronic steering". Essentially, we use a simplified 3-way handshake protocol to establish alignment between transceivers in LOS of each other. Such an alignment protocol delivers quick and automatic hand off of data flows among different transceivers while achieving a virtually omni-directional propagation and spatial reuse at the same time [13, 99].

The main purpose of the alignment protocol is to make the alignment process seamless to the higher layers of the protocol stack. Figure 7 shows this basic architecture which makes FSO links appear like any other RF link to the higher layers. It

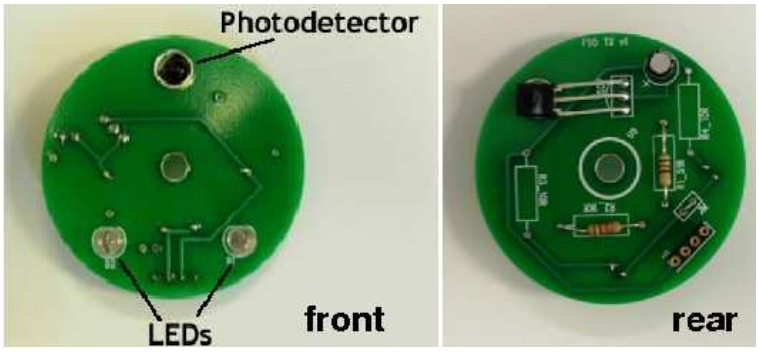

Figure 7.3: Transceiver circuit front and rear view.

is possible to let higher layers know about the dynamics of the alignment protocol to optimize communication performance for multiple transceivers of the spherical FSO nodes. However, we focus on the proof-of-concept design in Figure 7.

7.1 Prototype Blueprints

By employing commercially available off-the-shelf electronic components, we designed and built a prototype consisting of two main parts: the transceiver circuit and the controller circuit. The transceiver circuit has a circular shape which includes both emitting diode and photodiode on itself, as shown in Figure 7.3. The controller circuit contains a microcontroller which is responsible for alignment detection, data transfer and data restoration. The controller circuit also includes the microcontroller and transistor which is responsible for driving emitting diodes at desired modulation frequency and line transceiver which is responsible to convert TTL logic levels to RS232 in order to communicate with a laptop computer.

7.1.1 Transceiver Circuit

The transceiver circuit contains 2 LEDs, one photodetector and a simple biasing circuit. The picture of the front side and back side are shown in Figure 7.3. We used two LEDs to boost the emitted optical power and thereby provide an effective communication range. GaA1As double heterojunction LEDs with peak emission wavelength of 870 nm named TSFF5210 [9] were selected for transmission. TSFF5210 is a high speed infrared emitting diode which has high modulation bandwidth of 23 MHz with extra high radiant power and radiant intensity while maintaining low forward voltage as well as being suitable for high pulse current operation. The angle of half intensity is ± 10 for this LED which makes it suitable for desired node positions. The signal that is sent from the microcontroller is modulated by PIC12f615 at 455 kHz and sent to the LEDs. The TSOP7000 series [9] is used for receiving modulated signals. TSOP7000 is a miniaturized receiver for infrared remote control and IR data transmission. A PIN diode and preamplifier are assembled on a lead frame and the epoxy package is designed as an IR filter. The demodulated signal can directly be decoded by a microcontroller. The circuit of the TSOP7000 is designed so that the disturbance signals are identified and unwanted output pulses due to noise or disturbances are avoided. A bandpass filter, an automatic gain control and an integrator stage are used to suppress such disturbances. The distinguishing marks between the data signal and the disturbance are the carrier frequency, burst length and the envelope duty cycle. The data signal should fulfill the following conditions:

- The carrier frequency should be close to 455 kHz.
- The burst length should be at least $22\mu s$ (10 cycles of the carrier signal) and shorter than $500\mu s$.

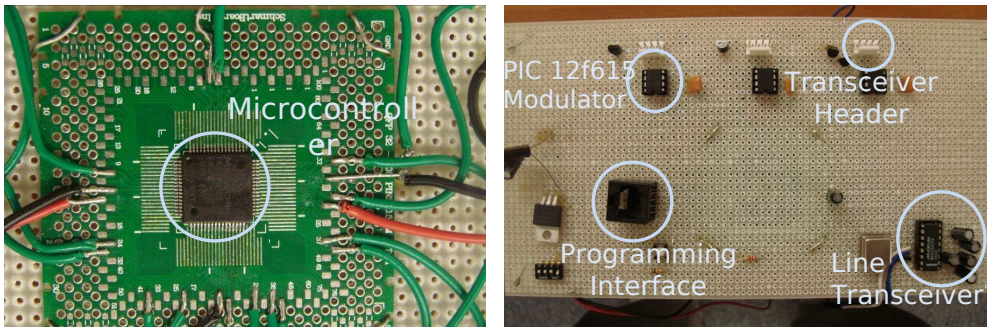

Figure 7.4: Controller circuit front and rear view.

- The separation time between two consecutive bursts should be at least $26\mu s$.
- If the data bursts are longer than $500\mu s$ then the envelope duty cycle is limited to 25% .
- The duty cycle of the carrier signal frequency of 455 kHz may be between 50% ($1.1\mu s$ pulses) and 10% ($0.2\mu s$ pulses). The lower duty cycle may help to save battery power.

TSOP7000 can communicate up to 19200 bits/sec and this is the bottleneck for the prototype's data rate. We used serial communication to transmit data between nodes with speeds up to 460800 bits/sec. Different types of photo-detectors can be used to increase data bandwidth.

7.1.2 Controller Circuit

Transmission units that carry the sent and received data are controlled by a microcontroller that runs the alignment protocol to decide whether an alignment is established or not. It also detects if an alignment goes down and it buffers data that will be sent once the alignment is re-established. We used the PIC24FJ128GA106 16 bit micro-

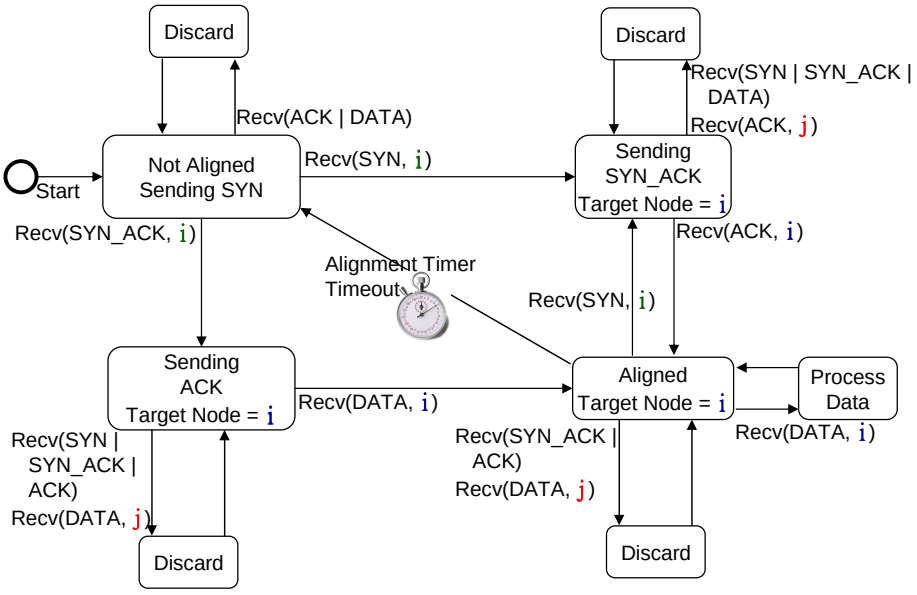

Figure 7.5: State diagram of alignment algorithm.

controller [8] for implementing the alignment algorithm. The controller circuit shown in Figure 7.1.1 is responsible for searching for possible alignments and simultaneous data transmission through multiple transceivers.

Because each prototype FSO structure has 3 transceivers connected to it and we use RS-232 communication, there must be 4 serial ports on the microcontroller. Software serial ports can be implemented on a microcontroller's digital input and output pins. However, this approach lacks internal buffers on digital input and output pins. Our alignment and data transmission algorithm needs buffering when the frames are received and transmitted and requires a microcontroller with built-in serial ports. The PIC24FJ128GA106 carries 4 built-in bidirectional serial ports onboard.

7.1.3 Alignment Protocol

The essence of our LOS alignment protocol is to exchange small frames between neighboring FSO nodes and identify the transceivers that are in each other's line-of-sight. The protocol aims to establish a *bi-directional* optical wireless link and hence uses a simple three-way handshake messaging method for full assurance of the alignment (Figure 7.5). Our alignment protocol uses a small frame of 4 bytes. Hence a frame does not keep the physical channel busy for too long. A frame starts with a FRAME_START byte, indicating the start of channel usage by another transceiver. SENDER_ID and RECEIVER_ID fields follow the frame indicator. Both bytes are node IDs instead of transceiver IDs. Last byte is the FRAME_TYPE byte that indicates the intention of the sender of this frame. In a frame of type DATA, the fifth byte is the length of the payload. Hence, the payload length is variable.

There are 4 different types of frames: SYN, SYN_ACK, ACK and DATA. The re-alignment algorithm starts by sending SYN frames through a particular transceiver. Lets assume A.1 on node A. The algorithm keeps sending this initial signal periodically until it receives a SYN_ACK answer to its SYN or it receives a SYN originated from a transceiver on a different node than itself: B.1 on node B. If it receives a SYN, it replies with a SYN_ACK. If it receives a SYN_ACK, it replies with an ACK. For simplicity, let us follow the case in which that A.1 sends a SYN, B.1 replies with SYN_ACK and A.1 replies with an ACK. When A.1 sends out its first ACK frame it changes internal state to ALIGNED with node B and same is true for B when it receives the ACK. At this point, B and A starts exchanging DATA frames. We did not implement an ACK mechanism for DATA frames to keep the protocol simple.

After 2 seconds the alignment timer goes off and changes the state of the interface to SENDING_SYN which starts the alignment process again. This simple

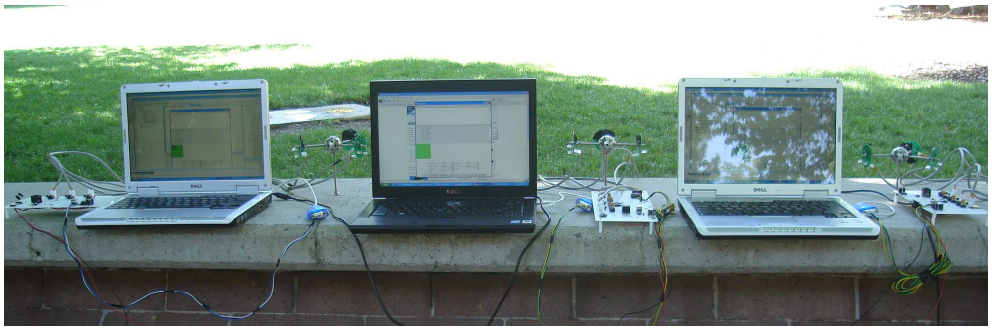

Figure 7.6: Experiment setup: 3 laptops (collinear placement), each with a 3-transceiver optical antenna.

alignment process, although exchanges a very small number of frames, will disrupt the carried flow and cause drops. The algorithm has been successful in establishing the alignment at the first trial, that is with exchange of only 3 frames.

Although the alignment protocol is fairly straightforward and similar to the RTS-CTS-DATA-ACK sequence found in RF MAC implementations, it plays a vital role in detecting available extra physical layer communication channels and it is the key components that makes intermittency of FSO links seamless to the upper layers as shown in Figure 7. By implementing a physical layer LOS alignment protocol it also becomes possible to realize solutions such as buffering of "physical layer frames" to make the FSO communication's intermittency seamless to upper layers.

7.2 Experiments

7.2.1 Proof-of-Concept Experiments

We implemented a simple FSO transceiver and alignment circuit prototype. The design consists of 3 FSO transceivers connected to a circuit board with a microcon-

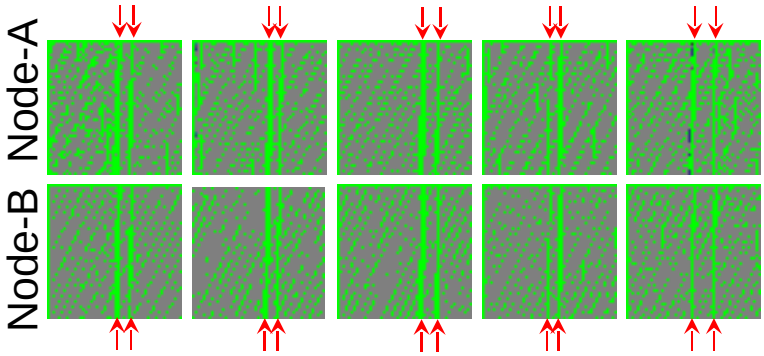

Figure 7.7: Throughput screen shots of a prototype experiment where transmitting node is mobile. Straight green lines show the drops due to the transmitting node's mobility. Red arrows indicate loss of alignment (and data) due to mobility. Once the mobile node returns to its place, data phase is restored and transmission continues. (Green spots show data loss)

troller. The microcontroller connects to a laptop computer (A) through RS-232 serial port. This microcontroller implements the alignment algorithm: it routinely probes for new alignments. This simple prototype is duplicated for 2 other laptop computers. labeled B and C, so that we can establish file transfers among the three nodes (Figure 7.1.3 and 7.1.3).

Our goal in this initial design is to test the feasibility of an LOS alignment algorithm, and demonstrate that *despite a major change in physical network topology, data phase can be effectively restored upon re-establishment of alignments*. To illustrate these goals, we present 6 experiments. Except for the last two experiments each experiment lasted 10 seconds and was repeated 10 times for more reliable results. In each experiment, we transfer an image file. We transfer every pixel of the file in one data frame. Hence, a typical data frame consists of 5 bytes: x and y of the pixel and red, green and blue values. The first 3 experiments do not involve mobility.

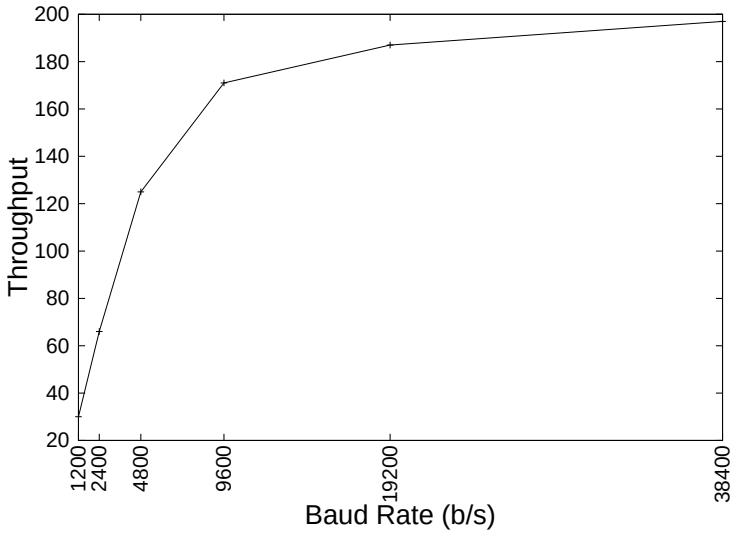

Figure 7.8: Throughput behavior as baud rate varies.

Baud Rate Experiment

In this experiment the transmission is bi-directional. Node-A and Node-B are placed 1 meter apart. The aim is to observe the number of frames that can be sent per second as the baud rate varies. Here we define throughput as number of frames that can be sent in each second. We increased the baud rate from 1200 bits/sec to 38400 bits/sec. As shown in Figure 7.2.1, we observed that the number of frames that are successfully sent increases as the baud rate is increased. We observed that transmission becomes impossible when the baud rate goes beyond 38400 bits/sec. Thus, 38400 bits/sec baud rate is the upper bound for our transceivers. We used 19200 baud rate level for next experiments.

Payload Size Experiment

Similar to the previous experiment, Node-A and Node-B are placed 1 meter apart. The transmission is again bi-directional. The aim is to observe the effect of payload

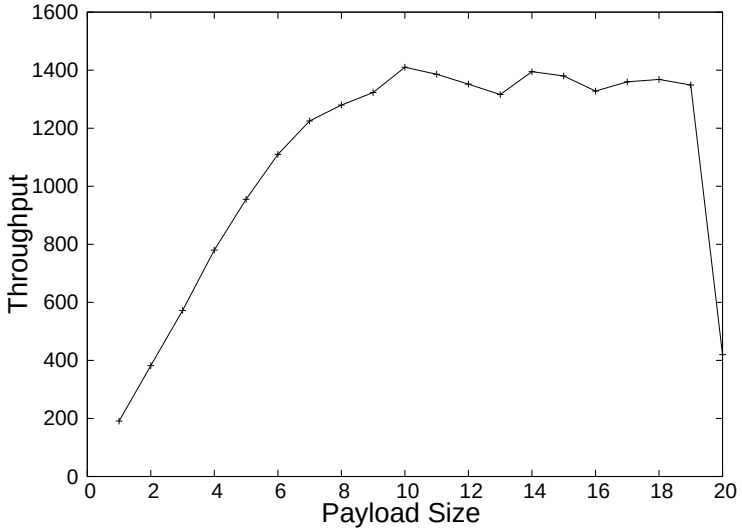

Figure 7.9: Payload size effect on throughput.

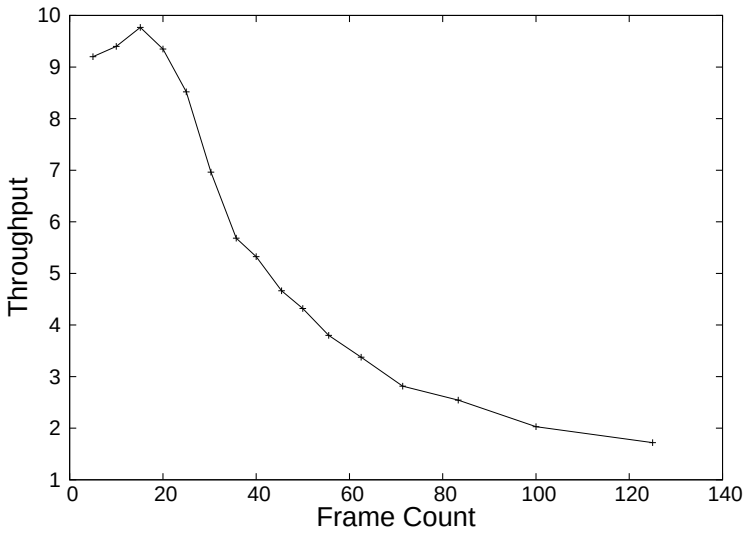

Figure 7.10: Frame count effect on channel usage.

size on frame count that is being sent per seconds and achievable throughput that can be achieved. Here we define throughput as the number of bytes that can be sent in ten seconds. We can formulate our throughput as:

$$Throughput = PayloadSize * FrameCount$$

Payload size has a negative effect on frame count in that frame count decreases when payload size is increased. Figure 7.2.1 shows that we achieve maximum throughput when payload size is 15 and frame count is 93. We increased payload size until we reached the maximum throughput. We observed that the increased payload size has a negative effect on the frame count and it makes throughput decrease beyond a maximum value.

Frame Count Experiment

In this experiment we increased frame count that is sent in each alignment interval and observed its effects on channel usage. We can formulate our channel usage as:

$$ChannelUsage = 100 * ChannelCapacity/Throughput$$

Here the capacity is the number of frames that is sent in 10 seconds and throughput is the number of bytes that is received in 10 seconds. We found that (Figure 7.2.1) channel usage increases until it reaches its maximum value, and then decreases until channel saturates due to the change in frame count that is being sent in each second. We achieved the maximum channel usage of 97.68% when the number of frames being sent was 15. The channel saturates when throughput is 215 frames in ten seconds.

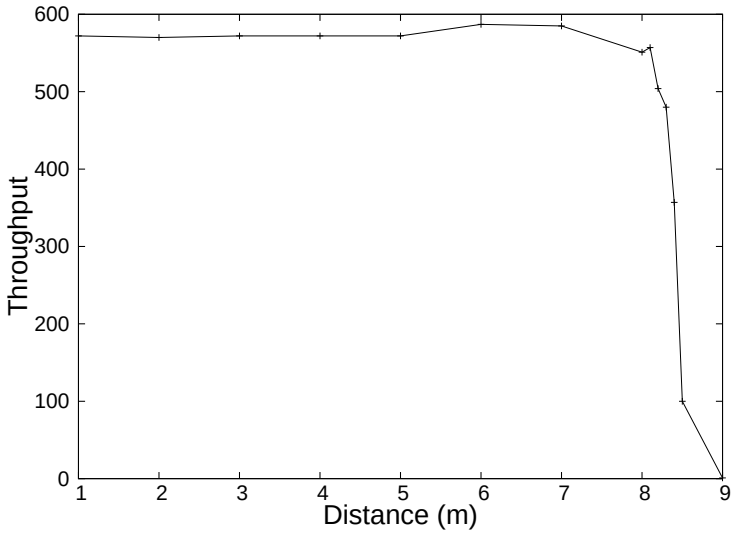

Figure 7.11: Distance effect on throughput.

Distance Experiment

In this experiment we observed throughput behavior as the communication distance varies. We again placed two nodes 1 meter apart for the initial condition and then increased the distance between the two nodes. We observed that throughput does not change until the transmission distance becomes critical for transceivers. As shown in Figure 7.2.1, we found that the critical point is 8 meters. We continued increasing the distance and we found that 9 meters is the maximum separation for transceivers to communicate. Thus our critical interval is between 8 and 9 meters.

Stationary Experiments

The stationary experiment is fairly simple: Node-A sends an image file (126 by 126 pixels) to Node-B. The transmission is unidirectional. We found that since the alignment between 2 nodes is re-established every 2 seconds, the nodes experience 10% data loss. This experiment reveals a simple improvement: we can delay/cancel re-

alignments as long as a data flow is live and totally remove the 10% overhead.

The second experiment is done between two nodes: Node-A and Node-B. In this case, both nodes send an image file of 126x126 pixels to each other. Node-A was able to receive 14136 of 15876 pixels. Node-B experienced a similar throughput: 13904 pixels.

The third experiment is conducted using 3 nodes. We placed 3 nodes in a ring topology and started file transfers from Node-A to Node-B and from Node-B to Node-C and from Node-C to Node-A. In this experiment, *every node was able to utilize 2 out of its 3 transceivers at the same time*, which clearly demonstrates the potential of spatial reuse. At the end of the transmissions, Node-A received 12950 pixels, Node-B received 9395 pixels and Node-C received 12755 pixels.

Mobility Experiment

In this experiment, we placed Node-A and Node-B 2 meters apart while Node-C was placed midway between them. Hence, Node-C was able to connect to A and B. While, Node-A and Node-B could not communicate when Node C was in between. We transferred an image file of 49 by 49 pixels from Node-C to the other two nodes. The transmission went on without significant disruption until the transmission reached the half of the file. We moved Node-C 1 meter away perpendicular to the line between nodes A and B, and waited for 10 seconds. Ten seconds later, we placed Node-C in its original location. Another 10 seconds later, we removed it again, then returned it after another 10 seconds. We observed that these 10-second disruptions have a marked effect on the file transfer as can be clearly seen on all 5 iterations of this experiment in Figure 7.1.3. We saw that Node-C was able to successfully restore the data transmission every time after loosing its alignments.

7.3 Summary

We demonstrated a prototype of multi-transceiver spherical FSO node which can successfully hand off multiple data flows between optoelectronic transceivers as we have published in [10]. We conclude that FSO communication systems can be embroidered with such auto-alignment mechanisms and cross-layer buffering schemes in order to overcome the inherent challenges of FSO directionality. Those mechanisms make FSO an attractive solution for dense use cases as in a lounge as well as mobile inner-city settings.

Chapter 8

Conclusions

Free-space-optical communication via multi-element antennas has potential for use as a next generation wireless communication technology because of its high speed modulation capability where RF networks suffer from a vanishing end-to-end throughput due to interference. Our research revealed through both an extensive simulation study and a proof-of-concept prototype that free-space-optical mobile ad-hoc networks are possible. Additionally, FSO can perform multiple times better than RF because of a multi-element optical antenna design that exploits spatial reuse of directional FSO beams.

We presented our contribution on simulating FSO propagation model, multi-transceiver directional FSO structures, and obstacle-avoiding mobility generation. We assessed the effects of multiple system parameters on the overall network throughput. We observed that intermittent connectivity pattern of FSO nodes cause the transport-level end-to-end throughput to drop severely. FSO-MANETs are fundamentally different than RF-based MANETs because of the highly-directional FSO communication in combination with mobility. We conclude that our simulations of

FSO networks deployed in lounge and downtown city environments show clear advantage over RF deployments.

We remedied this problem of degrading end-to-end per-node throughput by proposing cross-layer buffers. We have provided insight on the two buffering schemes to handle the problem of reduced throughput in multi-transceiver free-space-optical mobile ad-hoc networks. We discussed their design in detail and identified their differences. We have provided their throughput results for increasing mobility and number of transceivers. We conclude that the per-flow buffering provides better network-wide throughput than the node-wide buffering mechanism. We leave the fairness of the buffer scheduling issues as future work, expecting interesting designs to emerge for nodes with extremely large number of transceivers with highly focused beams.

Additionally, we presented a derived use case for the directionality of FSO. We found that directionality of FSO can be used as an aid to routing by enabling relative ad-hoc localization. We proposed a novel approach to the problem of node localization in stationary ad-hoc networking context via multi-element free-space-optical antennas. We used readily available directionality information to perform a simple triangulation with only two localized neighbors. Our approach has low processing needs and does not need a complex tuning phase or extra hardware. We conclude that optical wireless is attractive because of both its high throughput and easy to exploit directionality benefits that helps us solve the ad-hoc localization problem.

We demonstrated a prototype multi-transceiver spherical FSO node which can successfully hand off multiple simultaneous data flows between optoelectronic transceivers. We conclude that FSO communication systems can be equipped with such auto-alignment mechanisms and cross-layer buffering schemes in order to overcome

the inherent challenges of FSO directionality but still exploit the spatial reuse for larger aggregate throughput. Those mechanisms make FSO an attractive solution for dense deployment use cases such as a lounge as well as mobile inner-city settings.

Lastly, the RF and FSO technologies are in fact complementary. In a hybrid environment where nodes accommodate both RF and FSO capabilities and a suitable network stack that can take advantage of both technologies, RF can overcome FSO's coverage issues while FSO can meet high-bandwidth requirements of the network.

8.1 Future Work

Our work provides a basis for evaluation of performance characteristics of multi-transceiver free-space-optical mobile ad-hoc networks. We have conducted an extensive set of simulations to compare FSO-MANETs with RF-MANETs. We have always taken the omni-directional RF communication as the basis while concluding the results of our simulation comparisons. However, an important question that researchers shall tackle is: How does FSO-MANETs compare to directional RF-MANETs? Compared to FSO device sizes, directional RF components still have form factor issues that limit their dense packaging; and hence, result in limited spatial reuse. On the other hand, directional RF still has the advantage of penetrating through soft obstacles. Directional RF antennas and complex beam forming methodologies are becoming mainstream research topics as well. Hence, we expect the comparison of two directional communication technologies to draw attention.

Additionally, we expect the performance analysis studies to focus on concrete use cases such as vehicular networks or emergency rescue applications rather than the generalized application domain of mobile ad-hoc networks. We expect FSO-

based pedestrian, vehicular, and aerial networks to eventually emerge. We expect the researchers to conduct connectivity and throughput simulation experiments and implement prototypes of such applications since each scenario will differ in their tolerance to disconnection.

The current state of our prototype implementation is only able to provide slow transmission speeds. We expect it deliver significantly larger throughput using an increased number of transceivers, each with a higher transmission speed. Hence, the increased number of transceivers will not only provide a higher throughput but better localization accuracy as well. There will be a need for smart transceiver selection algorithms when the multi-transceiver designs reach 100s of transceivers on each node. This line of work will benefit from orientation-only and hybrid (ranging and orientation) localization mechanisms to model the mobility behavior of the neighbor nodes.

Additionally, we expect more complicated buffering mechanisms to emerge. Such buffering mechanism will be closely related with smart transceiver selection algorithms. Researchers will model the mobility behavior of the neighbor nodes and use appropriate buffers accordingly. We also expect to observe buffer allocation and management algorithms to focus on end-to-end fairness and this line of research to find applications in delay tolerant networking.

Finally, since LEDs are not only used for communication but also for solid state lighting, we expect the two requirements to be satisfied using only one apparatus: a high number of densely packaged FSO transceivers. Since such a system would still have connectivity issues caused by obstacles in the medium, we expect to see RF's integration in such a system, resulting in a hybrid design.

Bibliography

[1] Cotco, Cotco Ultra Bright Ingaalp Red-orange Led, Model number LO564TRO4-B0G. http://www.digchip.com/datasheets/parts/datasheet/275/LO564TRO4-B0G.php.

[2] Lightpointe Inc. http://www.lightpointe.com.

[3] Pinpoint. http://www.rft.com/pinpoint.aspx.

[4] Terescope Series. http://www.mrv.com/wireless/.

[5] The Network Simulator. http://www.isi.edu/nsnam/ns/.

[6] Toward an all-optical Internet. Lightwave, November 1998.

[7] The Future: Bringing Down Barriers to Wireless Communications. http://www.mitre.org/news/the_edge/fall_05/cady.html, 2005.

[8] Microchip technology inc., 2009. http:/www.microchip.com/.

[9] Vishay-manufacturer of discrete semiconductors and passive components, 2009. http://www.vishay.com/.

[10] A. Sevincer, M. Bilgi, M. Yuksel, and N. Pala. Prototyping multi-transceiver free-space-optical communication structures. In *Proceedings of IEEE International Conference on Communications*, May 2009.

[11] S. Acampora. A broadband wireless access network based on mesh-connected free-space optical links. *IEEE Personal Communications*, 6:62–65, October 1999.

[12] H. Akcan, V. Kriakov, H. Brönnimann, and A. Delis. Gps-free node localization in mobile wireless sensor networks. In *MobiDE '06: Proceedings of the 5th ACM international workshop on Data engineering for wireless and mobile access*, pages 35–42, New York, NY, USA, 2006. ACM.

[13] J. Akella, C. Liu, D. Partyka, M. Yuksel, S. Kalyanaraman, and P. Dutta. Building blocks for mobile free-space-optical networks. In *Proceedings of IFIP/IEEE International Conference on Wireless and Optical Communications Networks (WOCN)*, pages 164–168, Dubai, United Arab Emirates, March 2005.

[14] J. Akella, M. Yuksel, and S. Kalyanaraman. A relative ad-hoc localization scheme using optical wireless. In *Proceedings of IEEE/Create-Net/ICST International Conference on Communication System Software and Middleware (COMSWARE)*, 2007.

[15] J. W. Armstrong, C. Yeh, and K. E. Wilson. Earth-to-deep-space optical communications system with adaptive tilt and scintillation correction by use of near-earth relay mirrors. *OSA Optics Letters*, 23(14):1087–1089, July 1998.

[16] S. Arnon. Effects of atmospheric turbulence and building sway on optical wireless-communication systems. *OSA Optics Letters*, 28(2):129–131, January 2003.

[17] S. Arnon and N. S. Kopeika. Performance limitations of free-space optical communication satellite networks due to vibrations-analog case. *SPIE Optical Engineering*, 36(1):175–182, January 1997.

[18] S. Arnon and N. S. Kopeika. Performance limitations of free-space optical communication satellite networks due to vibrations-digital case. *SPIE Optical Engineering*, 36(1):175–182, January 1997.

[19] B. Cheng and M. Yuksel and S. Kalyanaraman. Orthogonal Routing Protocol for Wireless Mesh Networks. In *Proceedings of IEEE International Conference on Network Protocols (ICNP)*, Santa Barbara, CA, November 2006.

[20] P. Bahl. RADAR: an in-building RF-based user location and tracking system. In *Proceedings of Conference on Computer Communications (INFOCOM)*, 2000.

[21] M. Bilgi and M. Yuksel. Multi-element free-space-optical spherical structures with intermittent connectivity patterns. In *Proceedings of IEEE INFOCOM Student Workshop*, 2008.

[22] E. Bisaillon, D. F. Brosseau, T. Yamamoto, M. Mony, E. Bernier, D. Goodwill, D. V. Plant, and A. G. Kirk. Free-space optical link with spatial redundancy for misalignment tolerance. *IEEE Photonics Technology Letters*, 14:242–244, February 2002.

[23] G. C. Boisset. Design and construction of an active alignment demonstrator for a free-space optical interconnect. *IEEE Photonics Technology Letters*, 7:676–678, June 1999.

[24] N. Bulusu. GPS-less low cost outdoor localization for very small devices. *IEEE Personal Communications Magazine, Special Issue on Smart Spaces and Environments*, October 2000.

[25] V. W. S. Chan. Optical space communications: a key building block for wide area space networks. *IEEE Lasers and Electro-Optics Society*, 1:41–42, 1999.

[26] K. Chintalapudi. Ad hoc localization using ranging and sectoring. In *Proceedings of IEEE INFOCOM*, Hong Kong, China, March 2004.

[27] R. R. Choudhury. Using directional antennas for medium access control in ad hoc networks. In *Proceedings of ACM MOBICOM*, September 2002.

[28] R. R. Choudhury. Impact of directional antennas on ad hoc routing. In *Proceedings of the International Conference on Personal Wireless Communication (PWC)*, Venice, September 2003.

[29] C. Chuah. Capacity of multi-antenna array systems in indoor wireless environment. In *Proc. of IEEE Global Commun. Conf.*, Sydney, Australia, nov 1998.

[30] M. C. Chuah and W.-B. Ma. Integrated buffer and route management in a dtn with message ferry. In *Military Communications Conference, 2006. MILCOM 2006. IEEE*, pages 1–7, Oct. 2006.

[31] D. C. O'Brien, et al. High-speed integrated transceivers for optical wireless. *IEEE Communications Magazine*, 41:58–62, March 2003.

[32] C. Davis, Z. Haas, and S. Milner. On how to circumvent the manet scalability curse. In *Proceedings of IEEE MILCOM*, 2006.

[33] J. Derenick. *Multi-Robot Systems: From Swarms to Intelligent Automata, Alan C. Schultz and Lynne E. Parker (eds.)*, chapter Hybrid Free-space Optics/Radio Frequency (FSO/RF) Networks for Mobile Robot Teams. Springer, 2005.

[34] J. Derenick. On the deployment of a hybrid fso/rf mobile ad-hoc network. In *IEEE/RSJ International Conference on Intelligent Robots and Systems*, 2005.

[35] P. Djahani. Analysis of infrared wireless links employing multibeam transmitters and imaging diversity receivers. *IEEE Transactions on Communications*, 48:2077–2088, December 2000.

[36] F. Shubert. Light-Emitting-Diodes-dot-org. `http://www.lightemittingdiodes.org`.

[37] G. E. F. Faulkner. A cellular optical wireless system demonstrator. In *IEEE Colloquium on Optical Wireless Communications*, pages 12/1–12/6, 1999.

[38] R. M. Gagliardi. *Optical Communications*. John Wiley and Sons, 1976.

[39] L. Girod and D. Estrin. Robust range estimation using acoustic and multimodal sensing. volume 3, pages 1312–1320 vol.3, 2001.

[40] S. Gokhale. Deployment of fiber optic networks through underground sewers in north america. *J. Transp. Engrg.*, 132(8):672–682, August 2006.

[41] D. J. Goodwill. Free space optical interconnect at 1.25 gb/s/channel using adaptive alignment. In *Optical Fiber Communication Conference and the International Conference on Integrated Optics and Optical Fiber Communication (OFC/IOOC)*, pages 259–261, 1999.

[42] H. Gossain. A cross-layer approach for designing directional routing protocol in manets. In *Proceedings of IEEE Wireless Communications and Networking Conference (WCNC)*, March 2005.

[43] H. Gossain. Mda: An efficient directional mac scheme for wireless ad hoc networks. In *Proceedings of IEEE GLOBECOM*, 2005.

[44] H. Gossain. Drp: An efficient directional routing protocol for mobile ad hoc networks. *IEEE Transactions on Parallel and Distributed Systems*, 17(12):1438–1541, 2006.

[45] P. Gupta and P. Kumar. The capacity of wireless networks. *IEEE Transactions on Information Theory*, 46(2):388–404, March 2000.

[46] D. J. T. Heatley, D. R. Wisely, I. Neild, and P. Cochrane. Optical wireless: The story so far. *IEEE Communications*, 36:472–74, December 1998.

[47] J. Hightower. Location systems for ubiquitous computing. *IEEE Computer*, 34(8):57–66, aug 2001.

[48] K. Ho. Methods for crosstalk measurement and reduction in dense wdm systems. *IEEE/OSA Journal of Lightwave Technology*, 14(6):1127–1135, 1996.

[49] D. K. Hunter and I. Andonovic. Approaches to optical internet packet switching. *IEEE Communications Magazine*, 38(9):116–122, 2000.

[50] Jeffrey Hightower; Chris Vakili; Gaetano Borriello and Roy Want. Design and Calibration of the SpotON Ad-Hoc Location Sensing System.

[51] J. M. Kahn. Wireless infrared communications. In *Proceedings of the IEEE*, pages 265–298, February 1997.

[52] J. M. Kahn. Next century challenges: mobile networking for smart dust. In *Proceedings of MOBICOM 1999*, pages 271–278, 1999.

[53] B. Karp. GPSR: Greedy perimeter stateless routing for wireless networks. In *Proceedings of ACM/IEEE MobiCom 2000*, August 2000.

[54] D. Kedar. Backscattering-induced crosstalk in wdm optical wireless communication. *IEEE/OSA Journal of Lightwave Technology*, 23(6):2023–2030, 2005.

[55] A. Krifa, C. Barakat, and T. Spyropoulos. An optimal joint scheduling and drop policy for delay tolerant networks. In *World of Wireless, Mobile and Multimedia Networks, 2008. WoWMoM 2008. 2008 International Symposium on a*, pages 1–6, June 2008.

[56] J. Krumm, S. Harris, B. Meyers, B. Brumitt, M. Hale, and S. Shafer. Multi-camera multi-person tracking for easyliving. *Visual Surveillance, IEEE Workshop on*, 0:3, 2000.

[57] S. G. Lambert. *Laser Communications in Space*. Artech House, 1995.

[58] L. E. G. Lance Doherty, Kristofer S. J. Pister. Convex position estimation in wireless sensor networks. *Proceedings of the INFOCOM 1999*, 2001.

[59] K. Langendoen and N. Reijers. Distributed localization in wireless sensor networks: a quantitative comparison. *Comput. Netw.*, 43(4):499–518, 2003.

[60] F. Liu. Bootstrapping free-space optical networks. In *Proceedings of the IEEE International Parallel and Distributed Processing Symposium (IPDPS)*, 2005.

[61] J. Llorca. Reconfigurable optical wireless sensor networks. In *Proceedings of the SPIE Conference, Remote Sensing*, 2003.

[62] J. Llorca. Design and implementation of a complete bootstrapping model for free-space optical backbone networks. In *Proceedings of SPIE Optics and Photonics, Free-Space Laser Communications VI*, 2006.

[63] M. Bilgi, and M. Yuksel. Multi-transceiver simulation modules for free-space optical mobile ad hoc networks. In *Proceedings of SPIE Defense, Security and Sensing*, April 2010.

[64] M. Bilgi, and M. Yuksel. Packet-based simulation for optical wireless communication. In *Proceedings of IEEE Workshop on Local and Metropolitan Area Networks*. IEEE, 2010.

[65] M. Bilgi, and M. Yuksel. Throughput characteristics of free-space-optical mobile ad hoc networks. In *Proceedings of ACM International Conference on Modeling, Analysis and Simulation of Wireless and Mobile Systems*. Sheridian Publishing, October 2010.

[66] M. Bilgi and M. Yuksel and N. Pala. 3-d optical wireless localization. In *Proceedings of IEEE GLOBECOM 2010 Workshop on Optical Wireless Communications*, December 2010.

[67] B. Metcalfe. An all-optical internet is the vision of infoworld's internet plumber of 1999. InfoWorld, January 2000.

[68] S. D. Milner. Hybrid free space optical/rf networks for tactical operations. In *Proceedings of IEEE MILCOM*, 2004.

[69] A. R. Moral, P. Bonenfant, and M. Krishnaswamy. The optical internet: architectures and protocols for the global infrastructure of tomorrow. *IEEE Communications Magazine*, 39(7):152–159, 2001.

[70] A. J. C. Moreira. Optical interference produced by artificial light. *ACM/Springer Wireless Networks*, 3:131–140, 1997.

[71] B. Nakhkoob, M. Bilgi, M. Yuksel, and M. Hella. Multi-transceiver optical wireless spherical structures for manets. *IEEE Journal on Selected Areas of Communications*, 27(9), 2009.

[72] M. Naruse, S. Yamamoto, and M. Ishikawa. Real-time active alignment demonstration for free-space optical interconnections. *IEEE Photonics Technology Letters*, 13:1257–1259, November 2001.

[73] D. Niculescu. Ad-hoc positioning system (aps). In *Proceedings of GLOBECOM*, 2001.

[74] D. Niculescu. Ad hoc positioning system (aps) using aoa. In *INFOCOM 2003*, pages 1734–1743, Atlanta, GA, March 2003.

[75] U. N. Okorafor. Efficient routing protocols for a free space optical sensor network. In *Proceedings of the IEEE International Conference on Mobile Adhoc and Sensor Systems (MASS)*, 2005.

[76] U. N. Okorafor. Opsenet: A security enabled routing scheme for a system of optical sensor networks. In *Proceedings of the International Conference on BroadbandCommunications, Networks and Systems (BROADNETS)*, 2006.

[77] U. N. Okorafor. Security and energy considerations for routing in hierarchical optical sensor networks. In *Proceedings of the International Workshop on Wireless and Sensor Networks Security*, 2006.

[78] R. J. Orr and G. D. Abowd. The smart floor: a mechanism for natural user identification and tracking. In *CHI '00: CHI '00 extended abstracts on Human factors in computing systems*, pages 275–276, New York, NY, USA, 2000. ACM.

[79] A. Ozgur, O. Levesque, and D. Tse. Hierarchical cooperation achieves optimal capacity scaling in ad hoc networks. *IEEE Transactions on Information Theory*, 53(10):3549–3572, February 2007.

[80] G. Pang, T. Kwan, H. Liu, and C.-H. Chan. Optical wireless based on high brightness visible leds. In *IEEE Industry Applications Conference*, pages 1693–1699, 1999.

[81] K. Pedersen, P. Mogensen, and J. Ramiro-Moreno. Application and performance of downlink beamforming techniques in umts. *Communications Magazine, IEEE*, 41(10):134 – 143, Oct. 2003.

[82] N. Priyantha. The cricket compass for context-aware mobile applications. In *Proceedings of ACM MOBICOM*, 2001.

[83] C. Qiao. Optical burst switching (obs): A new paradigm for an optical internet. *Journal of High Speed Networks*, 8(1):69–84, 1999.

[84] F. Raab, E. Blood, T. Steiner, and H. Jones. Magnetic position and orientation tracking system. *Aerospace and Electronic Systems, IEEE Transactions on*, AES-15(5):709–718, Sept. 1979.

[85] R. Ramaswami. *Optical networks: A practical perspective*. Morgan Kaufmann Series In Networking, 1998.

[86] D. Raychaudhuri. New architectures and disruptive technologies for the future internet: The wireless, mobile and sensor network perspective. Technical Report GDD-05-04, NSF, 2005.

[87] C. Savarese, J. M. Rabaey, and K. Langendoen. Robust positioning algorithms for distributed ad-hoc wireless sensor networks. In *ATEC '02: Proceedings of the General Track of the annual conference on USENIX Annual Technical Conference*, pages 317–327, Berkeley, CA, USA, 2002. USENIX Association.

[88] M. Sekido. Directional nav indicators and orthogonal routing for smart antenna based ad hoc networks. In *Proceedings of IEEE International Conference on Distributed Computing Systems Workshops*, pages 871–877, 2005.

[89] H. Uno. Ask digital demodulation scheme for noise immune infrared data communication. *ACM/Springer Wireless Networks*, 3:121–129, 1997.

[90] H. C. Van de Hulst. *Light Scattering by Small Particles*. John Wiley and Sons, 1957.

[91] V. Vistas. Performance analysis of the advanced infrared (air) csma/ca mac protocol for wireless lans. *ACM/Springer Wireless Networks*, 9:495–507, February 2003.

[92] D. Wang and A. A. Abouzeid. Throughput capacity of hybrid radio-frequency and free-space-optical (rf/fso) multi-hop networks.

[93] R. Want, A. Hopper, V. Falcao, and J. Gibbons. The active badge location system. *ACM Trans. Inf. Syst.*, 10(1):91–102, 1992.

[94] K. Whitehouse and D. Culler. Calibration as parameter estimation in sensor networks. In *WSNA '02: Proceedings of the 1st ACM international workshop on Wireless sensor networks and applications*, pages 59–67, New York, NY, USA, 2002. ACM.

[95] H. Willebrand and B. S. Ghuman. *Free Space Optics*. Sams Pubs, 2001. 1st Edition.

[96] P. Yan. An initial study of mobile ad hoc networks with free space optical capabilities. In *Proceedings of IEEE Digital Avionics Systems Conference (DASC)*, 2005.

[97] Y. E. Yenice. Adaptive beam-size control scheme for ground-to-satellite optical communications. *SPIE Optical Engineering*, 38(11):1889–1895, November 1999.

[98] M. Yoo, C. Qiao, and S. Dixit. Optical burst switching for service differentiation in the next-generation optical internet. *IEEE Communications Magazine*, 39(2):98–104, 2001.

[99] M. Yuksel, J. Akella, S. Kalyanaraman, and P. Dutta. Free-space-optical mobile ad hoc networks: Auto-configurable building blocks. *ACM Springer Wireless Networks*, 15(3):295–312, April 2009.

[100] X. Zhu. Free-space optical communication through atmospheric turbulence channels. *IEEE Transactions on Communications*, 41:58–62, August 2002.